Studies of Bore Water Oxidation Using a Multi Electrode-Perforated Electrode flow Through Cell

A thesis submitted in partial fulfilment

of the requirements for the degree

of

Masters of Science

in Materials and Processing Engineering

at

The University of Waikato

by

Ronnie Kurian

KO TE TANGATA

THE UNIVERSITY OF
WAIKATO
Te Whare Wānanga o Waikato

2012

Abstract

Anoxic groundwaters in the Waikato region are naturally contaminated with iron and manganese at levels of 25.0 mg/L and 0.9 mg/L respectively and above. Often these contaminants can be removed by simple aeration and clarification and/or filtration. However when present with elevated levels of silica and/or organic matter, these waters, upon oxidation, can form highly stable brownish colloidal suspensions that are difficult to filter. Typical treatment methods for these waters usually involve expensive ion exchange to remove the metal ions in their reduced forms or chemical oxidation, using strong oxidising agents such as calcium hypochlorite, to precipitate the metals as their respective hydrous oxides. An improved multiple electrode perforated electrode flow through (ME-PEFT) cell has been developed for in-line electrochemical oxidation of these problem waters. In initial work, using low cost graphite anodes and with added sodium chloride (250 mg/L), 40% instant oxidation at 16 V was achieved. When dimensionally stabilised anodes (DSA) consisting of titanium metal coated with $TiO_2/RuO_2/IrO_2$ were used in a dual electrode pair ME-PEFT cell, 100% oxidation of the iron was obtained after a single pass through the cell using only the naturally available chloride (10 to 12 mg/L). Power consumption was 3.80 kWh/m^3.

The oxidised iron clarified readily yielding a clear solution containing less than 0.2 mg/L of iron and having a turbidity of 1.5 NTU after 5 hours settling time. Preliminary tests for an inline flotation clarifier have yielded promising results.

Acknowledgements

I am deeply indebted to my supervisor Assoc. Prof. Alan Langdon for his guidance, never ending encouragement and enthusiasm. I am grateful for your extraordinary kindness, patience, support and above all for imparting knowledge.

I would also like to thank Dr. Hilary Nath, my mentor, for his unending support and encouragement during the research.

I would like to express my sincere thanks to technical officers John Little, Wendy Jackson, Pat Gread, Amu Uperti, and Annie Barker at the Department of Chemistry, for their support from the very beginning of the research.

The Department of Engineering technical staff Stewart Finlay, Indar Singh, Luke van de Pas and the Engineering Workshop team for helping me with instruments, tools and fabrications.

Finally to my parents, this is what I have been up to for the past two years. Thank you for your unending love and affection. And to Shwetha, you’ve always stood beside me with love and motivation that has led me to where I am.

Table of Contents

Abstract ii

Acknowledgements iii

Table of Contents iv

List of Figures ix

List of Tables xii

Chapter 1: Introduction and Literature Review 1

- 1.1 General Introduction 1
- 1.2 Literature Review 4
  - 1.2.1 Waikato bore water 4
  - 1.2.2 Issues relating to iron and manganese in groundwater 5
  - 1.2.3 Colloidal chemistry 7
    - Stability of Colloidal Suspension 8
    - Electrical Double Layer 8
  - 1.2.4 Colloid chemistry of Waikato's problem bore waters 9
  - 1.2.5 Existing technologies for treating iron and manganese water 11
    - Air oxidation 11
    - Chemical oxidation 13
  - 1.2.6 The aqueous chemistry of chlorine 15
  - 1.2.7 Electrochemical chlorine generators 16
    - Divided and undivided cells for electrochemical chlorine generation 17
    - Electrolytic chlorination of drinking water 19
    - Electrolytic chlorination of wastewater 19
  - 1.2.8 The chlor alkali industry 20
    - Liquid Mercury Chlor-Alkali process (Divided cell) 20
    - Diaphragm and Membrane cell processes 21

Undivided cell hypochlorite generators 22

1.2.9 Electrode Materials 22

Graphite 23

Dimensionally Stabilized Anodes (DSA) 24

Boron Doped Diamond (BDD) 26

1.2.10 Factors affecting electrochemical efficiency 27

Gas bubbles in the inter electrode gap 27

Effect of Current Density on Cell efficiency 27

Effect of inter-electrode gap on current density 28

Effect of pH and Conductivity 29

1.2.11 Clarifier Design 30

Dissolved air flotation (DAF) 31

1.3 Previous work at the University of Waikato 31

1.3.1 Divided cell using porous anode 31

1.3.2 Online Chlorine generation using natural chloride in novel undivided cells 32

Breadbox cell 33

Flume cell 33

1.3.3 Micro-gap perforated electrode flow through (PEFT) cell 34

1.4 Objectives of the Present Study 35

1.5 Thesis Outline 36

Chapter 2: Material and Methods 37

2.1 Perforated electrode flow through cell (PEFT) 37

2.2 Development of the multi-electrode PEFT (ME-PEFT) cell 37

2.3 Electrode Materials 40

2.3.1 Anode Materials 40

2.3.2 Cathode Material 40

2.4 General procedure for electrolysis experiments 41

2.5 Analytical Methods 41

2.5.1 Ferrous ion Analysis 41

Preparation of 20 mg/L iron solution 42

2.5.2 Chlorine Analysis 42

2.5.3 Chloride Analysis 42

Preparation of the Colour Reagent for chloride analysis 43

Chapter 3: Evolution of the multi-electrode PEFT cell and DAF clarifier system……………………………………..…………………………44

3.1 Multi-electrode PEFT cell 44

3.2 DAF clarifier 47

Chapter 4: Multi-electrode PEFT (ME-PEFT) Cell Using Graphite Anodes 49

4.1 Trials of the ME-PEFT cell using synthetic bore water 49

4.1.1 Effect of increased number of electrode pairs..................................... 49

4.1.2 Effect of chloride concentration and current density 50

4.1.3 Effect of Perforation Configuration 52

4.2 Oxidation versus iron removal with staggered perforations. 53

4.3 Effect of chloride concentration with staggered perforations 54

4.4 Electrochemical chlorine generation using graphite anodes 55

4.5 Trials with bore water 57

4.6 Conclusion 58

Chapter 5: Multi-electrode system using dimensionally stabilised titanium anodes (DSAs)……………………………………………………………..59

5.1 Laboratory preparation of Ruthenium stabilised DSAs 59

5.2 Electrochemical chlorine generation using laboratory prepared DSAs 60

5.3 Electrochemical chlorine generation using commercial DSAs.................. 61

5.4 Rapid oxidation of Fe(II) in bore water using DSAs 62

5.3.1 Single Cell Electrolysis 62

5.3.2 Multiple Cell Electrolysis 63

5.5 Metal ion removal 64

5.6 Summary 65

Chapter 6: Clarification of oxidised bore water 66

6.1 Settling characteristics of oxidized bore water 66

6.1.1 Oxidation of bore water with a single electrode pair PEFT cell 66

6.1.2 Oxidation with a two electrode pair PEFT cell 67

6.1.3 The effect of chloride concentration on settling after oxidation of bore with a two electrode pair PEFT cell 68

6.1.4 Oxidation and settling of a synthetic iron water 69

6.2 Development of a DAF apparatus for oxidised bore water clarification.... 70

6.2.1 Preliminary design 70

6.2.2 Pressurised DAF system 71

6.2.3 Modified Pressurised DAF System 72

Chapter 7: Summary and Conclusion 74

7.1 The importance of rapid oxidation of iron and manganese......................... 74

7.2 Importance of the electrode material.. 74

7.3 Oxidised iron removal.. 75

7.4 Conclusions.. 75

7.5 Suggestions for future research.. 76

References.. 77

Appendices.. 83

Appendix A: Calibration curves... 83

A.1 Analysis of ferrous ion concentration in water using 1, 10 Phenanthrolein spectrophotometric method 83

A.2 Analysis of chloride ions concentration in water using Mercury (II) thiocyanate spectrophotometric method 83

Appendix B: Calculations 84

B.1 Chlorine Generation 84

B.2 Current Density 85

B.3 Power Consumption 86

B.4 Current efficiency 87

Appendix C: Chlorine generation data (Section 5.3).. 88

C.1 Chlorine generation using titanium ruthenium oxide and iridium oxide anode.. 88

List of Figures

Figure 1. 1 Waikato Region geology and wells drilled since 1989 4
Figure 1. 2 Left: Wells drilled with resource consent Right: Total number of wells drilled in Waikato Region.. 5
Figure 1. 3 Median concentration of total dissolved Fe plotted against median total dissolved Mn. There is no apparent correlation between the concentrations of the two elements... 6
Figure 1. 4 Concept of Zeta potential in electrical double layer............................. 9
Figure 1. 5 TEM image showing poor aggregation resulting from slow air oxidation of Waikato bore water 10
Figure 1. 6 TEM image of flocs formed by rapid air oxidation of Waikato bore water 10
Figure 1. 7 Disinfection by-products 15
Figure 1. 8 Hypochlorous acid dissociation in dependence with pH.................... 16
Figure 1. 9 Direct and indirect oxidation processes in divided and undivided cells – Pollutant removal pathways of electrochemical oxidation 19
Figure 1. 10 Liquid Mercury Chlor-Alkali process 20
Figure 1. 11 Diaphragm Separated Cell.. 21
Figure 1. 12 Chlorine generation using the chloride content present in the bulk solution using four different anode.. 24
Figure 1. 13 Surface modifications of titanium anodes by; a) pure oxide film, b) atmospheric oxide film, c) doped oxide, d) oxide-metal mixture, e) modification by surface states of oxide, f) surface states from metal deposition. D is the distribution of electrons in dependence of the energy E 26
Figure 1. 14 Current distribution when a) large bubbles are formed and b) small bubble are formed.. 27
Figure 1. 15 Difference between conventional and thin layered cell.................... 29
Figure 1. 16 Porous anode membrane cell... 32
Figure 1. 17 Breadbox design for treating iron laden water 32
Figure 1. 18 Flume design with reduced interelectrode gap 34
Figure 1. 19 PEFT cell Electrode set-up.. 34
Figure 1. 20 Staggered electrode set-up.. 35
Figure 2. 1 Schematic of the Multiple PEFT cell system 38

Figure 2. 2 Experimental set-up of the multiple PEFT cell 39

Figure 3. 1 Point contact between Stainless Steel leads and the electrode surface 45

Figure 3. 2 Drilled HIP sheet pressing the stainless steel leads onto the electrodes 46

Figure 3. 3 Titanium disc leads 46

Figure 3. 4 Flotation column design 48

Figure 4. 1 Iron removal from 20 mg/L iron solution at 1A (Flow Rate = 190 mL/min using 1, 2, 3, and 4 electrode pair of graphite anode and stainless steel cathode) 49

Figure 4. 2 The effect of NaCl concentration and current on iron removal efficiencies (Flow Rate = 190 mL/min) 51

Figure 4. 3 Aligned and Staggered electrode set-up 52

Figure 4. 4 Comparison of Aligned and staggered electrode set-up for iron removal (Flow Rate = 190 mL/min) 53

Figure 4. 5 Iron (II) oxidation efficiencies of Cell 1 and Cell 4 from 20 mg/L iron solution and 2 A DC (Flow Rate = 190mL/min) 55

Figure 4. 6 Comparison of iron oxidised by air, electro-oxidation of bore water (at 1 A and 2 A) and electro-oxidation of synthetic bore water (flow rate 190 mL/min) using a single PEFT cell 57

Figure 5. 1 Electro chlorination at varying chloride dosages and increasing current (flow rate = 190 mL/min, commercial DSA material) 61

Figure 5. 2 Total iron and manganese concentrations in the electrochemically treated bore water (measured directly after electrolysis and at t = 5 hours)….. 64

Figure 6.1 Gravity settling of oxidised bore water (Single cell at 190 mL/min, conductivity = 266 µS/cm at 15.8℃)……………………………………67

Figure 6.2 Gravity settling of oxidised bore water. (Double cell at 190 mL/min, conductivity = 266 µS/cm at 15.8 ℃)…………………………………………………..…….…...67

Figure 6.3 Oxidation and settling of synthetic iron water at different chloride dosages (Double cell at 190 mL/min)……………………………………..68

Figure 6.4 Preliminary DAF system……………………………………………..71

Figure 6.5 Pressurised DAF system…………………………………………….....72

Figure 6.6 Modified electro-flotation column..73

Figure A. 1 Calibration curve of ferrous ion concentration versus absorbance at 515 nm. 83

Figure A. 2 Calibration curve of chloride ion concentration versus absorbance at 460nm. 83

List of Tables

Table 1. 1 Chemicals used for iron and manganese treatment.............................. 13

Table 1. 2 Chlorine overpotential of different anode material.............................. 18

Table 1. 3 Comparison of Chlor-alkali cells.. 22

Table 1. 4 Mechanical properties of Graphite material.. 23

Table 1. 5 Mechanical properties of 99.2% Titanium material............................. 25

Table 2. 1 Electrode Material and spacer used in the development of the multiple PEFT cell 40

Table 3. 1 Individual cell performance using stainless steel leads (Conductivity = 150 µS/cm at 16℃, pH = 6.90 at 20℃, natural chloride = 26 mg/L, residual chlorine = 0.40 mg/L and flow rate = 190 mL/min).................................... 45

Table 3. 2 Individual cell performance using titanium dics (Conductivity = 150 µS/cm at 16 ℃, pH = 6.90 at 20 ℃, natural chloride = 26 mg/L, residual chlorine = 0.40mg/L and flow rate = 190 mL/min).................................... 46

Table 4. 1 Iron Removal efficiency of ME-PEFT cell from 20 mg/L iron water (Flow rate = 190 mL/min, NaCl = 100 mg/L, current = 1 A) 53

Table 4.2 Iron oxidation efficiency of ME-PEFT cell from 20 mg/L iron water (Flow rate = 190 mL/min, NaCl = 100 mg/L, current = 1 A)….......….….....54

Table 4. 3 Chlorine generation by graphite anode from 100 mg/L NaCl at increasing currents (Flow rate 190 mL/min) 56

Table 5. 1 Chlorine generation by laboratory prepared DSAs at different chloride and current values (Flow rate = 190 mL/min and pH = 5 at 20℃) 60

Table 5. 2 Electro-oxidation of iron in groundwater containing 7 mg/L natural chloride at flow rate of 190 ml/min (Conductivity = 266 µS/cm at 15.8 ℃)….. 62

Table 5.3 Electro-oxidation of iron in groundwater at flow rate of 190 mL/min……………………………..…………………………………….. 63

Table 6. 1 Oxidation and settling of a synthetic iron water (20 mg/L Fe(II) and 20 mg/L NaCl. (At 5A, 5.84 V, Flow rate = 190 mL/min, pH = 7.30 at 20 ℃, Conductivity = 463 µS/cm at 24 ℃) 69

Table C. 1 Chlorine generation by TiO2/RuO2/IrO2 at 190ml min-1 (pH ≈ 5 at 20℃)... 88

Table C. 2 Chlorine generation by TiO2/RuO2/IrO2 at 190ml min-1 (pH = 6.20 at 20℃) 88

Chapter 1: Introduction and Literature Review

1.1 General Introduction

Over 70% of the earth's surface is covered by water but 97.5% of this is salt water that cannot be used for most human needs. 70% of the remaining 2.5% is freshwater frozen in the icecaps of Antarctica whilst much of the rest is present in soil as moisture or lies in deep groundwater aquifers, inaccessible to humans. (Pal et al. 2010).

Less than 1% of the world's freshwater is accessible for direct human use and is found in lakes, rivers, reservoirs and underground water shallow enough to be withdrawn at affordable costs. Apart from fossil groundwaters, these sources of water are generally available on a sustainable basis as they are regularly recharged by rain and snowfall.

The shortage of clean usable water has been a major global concern for a long time and its primary impact has been upon developing countries. In such areas, water withdrawals have increased from 4% to 8% every year for the past decade (Falkenmark & Widstrand 1992). Furthermore, developed countries have experienced a critical need for wastewater management due to an ever increasing population, urbanization and improved living standards (Pal et al. 2010). Between the years 1900-1995 it has been estimated that the global freshwater water withdrawal increased over six times which was nearly twice the rate of population growth (Gleick & Miller 2002).

Groundwater is an integral part of human existence. Groundwater is trapped within the soil and underlying broken rocks, its major contributor being rain that infiltrates through the soil onto the aquifer where it is stored (Shibasaki et al. 2007). Groundwater is a very important freshwater source for humans and human activities. According to the Environmental Protection Agency (EPA), nearly 40% of the United States population use groundwater for drinking, cleaning, cooking etc. Moreover, 97% of the people living in rural area use groundwater and nearly 40% of the water is used for farming purposes (Dowd 1985). Fossil water is a form of groundwater that remains sealed in the aquifer for a very long period of time. Since it is a non-renewable resource, water mining leads to a drop in the water table and raises the water level in the hydrosphere contributing to the rise of sea level (Hays 2011).

In New Zealand, groundwater is known to contain elevated levels of iron and manganese which is derived naturally from the water rock interactions (Rosen 2001). Iron and manganese are more likely to be present in their reduced state when the dissolved oxygen levels are low and also because reduced states are more soluble and stable than their oxidised forms. Generally, aquifers with slow water flow, peat layers and oxygen depletion zones have elevated levels of iron and manganese (Ayotte J.D. 1999). At low concentrations, the water is unpalatable and, in extreme cases, unusable even for agricultural purposes.

In order to make use of this metal polluted ground water, new technologies need to be developed to reliably and efficiently remove contaminants present. One such technology is electrochemical oxidation. It is a process where the contaminants present in water are indirectly oxidised by oxidising species such as chlorine and oxygen formed by electrolysis with an applied DC current (White 1984).

In water and wastewater treatment industries, chlorine remains the most effective way of disinfecting water as it provides both the primary and secondary functions of a disinfectant (Worley et al. 1986). Traditionally, active chlorine is introduced into the water body as chlorine gas or hypochlorite. However, more recently, there has been a positive surge towards generating chlorine electrochemically onsite, thereby eliminating transportation costs, handling and storage of dangerous chlorine gas and hypochlorite (Zorpas 2011). One of the major drawbacks associated with the electrochemical oxidation of chloride to chlorine is the high cost at low chloride concentrations (Costaz et al. 1983).

The chloride concentration present in New Zealand groundwater ranges from 10 – 160 mg/L NaCl (Council 2005). Electrochemical chlorine generation from such low salt concentrations is costly because of high cell resistance, high voltage requirements, high power consumption and the need for expensive electrodes.

There are two ways of addressing concerns of cell resistance and associated power consumption. The inter electrode distance can be reduced or the active surface area of the electrodes can be increased. Recently a perforated electrode flow through (PEFT) cell has been described which uses low cost carbon (graphite) and stainless steel electrodes and has an inter electrode distance of less than 240 µm (Nath 2011; Nath et al. 2011). This cell configuration achieved high current densities at voltages below 25 V. The cell was able to decontaminate problem iron water with an added chloride concentration of 250 mg/L with four passes through the cell at an energy cost of 18 kWh/m^3 (Nath 2011). The present work had the general aim of optimising this technology to achieve single pass treatment of natural water, without added chloride and at lower energy cost.

1.2 Literature Review

1.2.1 Waikato bore water

Apart from the Waikato river, the predominant source of freshwater in Waikato region originates from groundwater. Groundwaters accounts for nearly 90% of the rural freshwater supply in the region and is extensively used for agricultural, domestic and industrial activities (Hadfield 2001). An estimated 400 wells are drilled every year to extract groundwater in the Waikato region (Figure 1.1)**.**

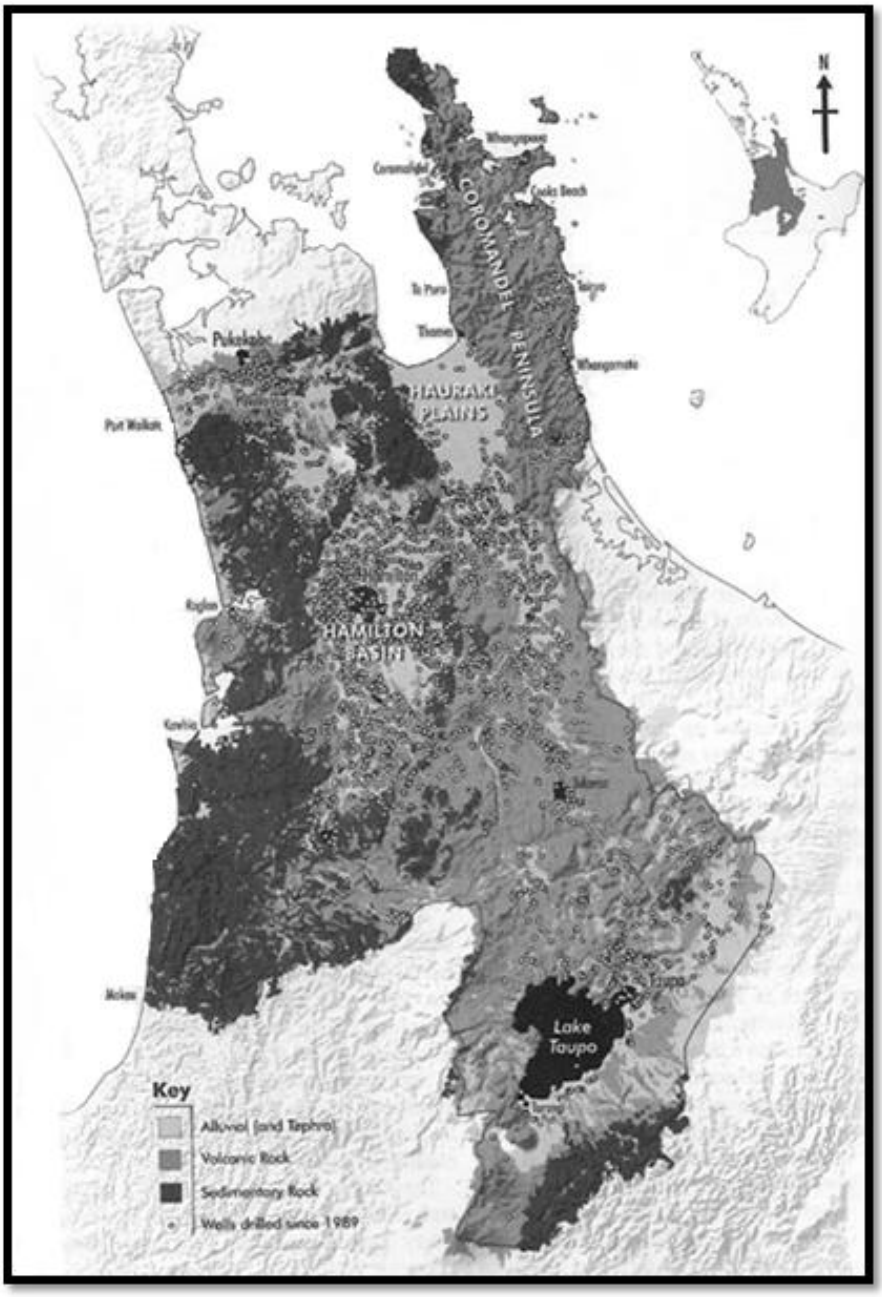

Figure 1.1 **Waikato Region geology and wells drilled since 1989 (Retrieved from (Hadfield 2001))**

Factors including shallow water tables and sediment accumulation affect the quality of groundwater extracted from bores (Rosen 2001). Additionally, proximity to road surfaces, sewage pipelines, septic tanks and farmland also increases the risk of contamination (Gleick & Miller 2002). Furthermore, streams are sustained by groundwater interaction during draught seasons which in turn has an influence on surface water quality (Piver 1993). Therefore, careful management of groundwater is essential to ensure the sustainability of the freshwater resource.

1.2.2 Issues relating to iron and manganese in groundwater

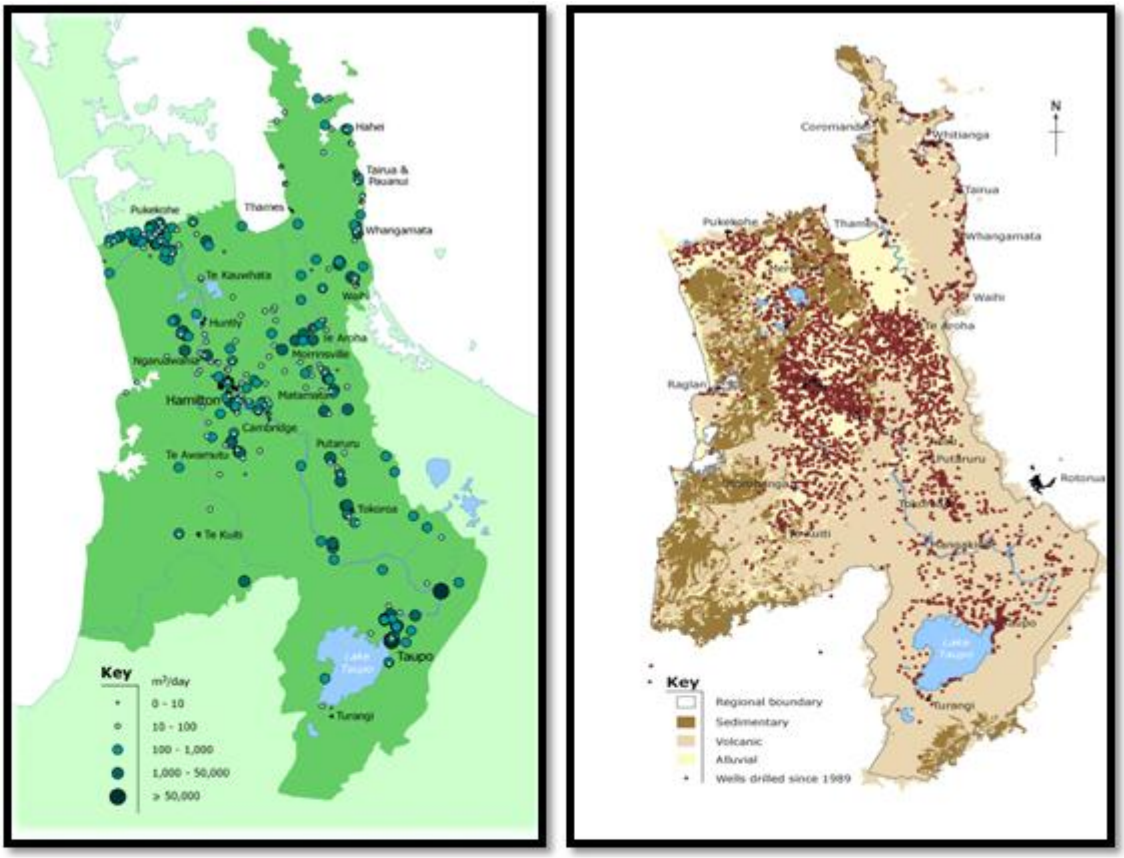

Figure 1.2 Left: Wells drilled with resource consent Right: Total number of wells drilled in Waikato Region (Retrieved from (WRC 2012))

The presence of iron and manganese is very common in groundwater. In unconfined shallow aquifers of New Zealand, slow movement of water facilitates oxygen consumption and reaction with organic matter leading to anoxic conditions and increased concentrations of iron and manganese (Hadfield 2001). Such is the case with most of Waikato's groundwater caused by the extraction of water from shallow aquifers instead of the best aquifer available in the area due to mere inconvenience (see figure 1.2).

In nature, Fe(II) is spontaneously oxidized to Fe(III) by oxygen. This process may also lead to the formation of partially oxidized ferrous-ferric intermediate species which are very difficult to predict (Rosen 2001). Depending on environmental conditions (such as pH, temperature and redox potential), the partially oxidized iron intermediates form stable iron oxides such as magnetite (Stumm & Sulzberger 1992). When iron contaminated water is used for irrigation, the iron concentration in the pasture is increased and has an adverse effect on the health of dairy animals (Linn 2006). It is recommended that the concentration of iron in bovine drinking water should be below 2 mg/L. More importantly, the New Zealand drinking water standards specify maximum acceptable values for iron and manganese of 0.2 mg/L and 0.04 mg/L respectively (Ministry of Health 2005).

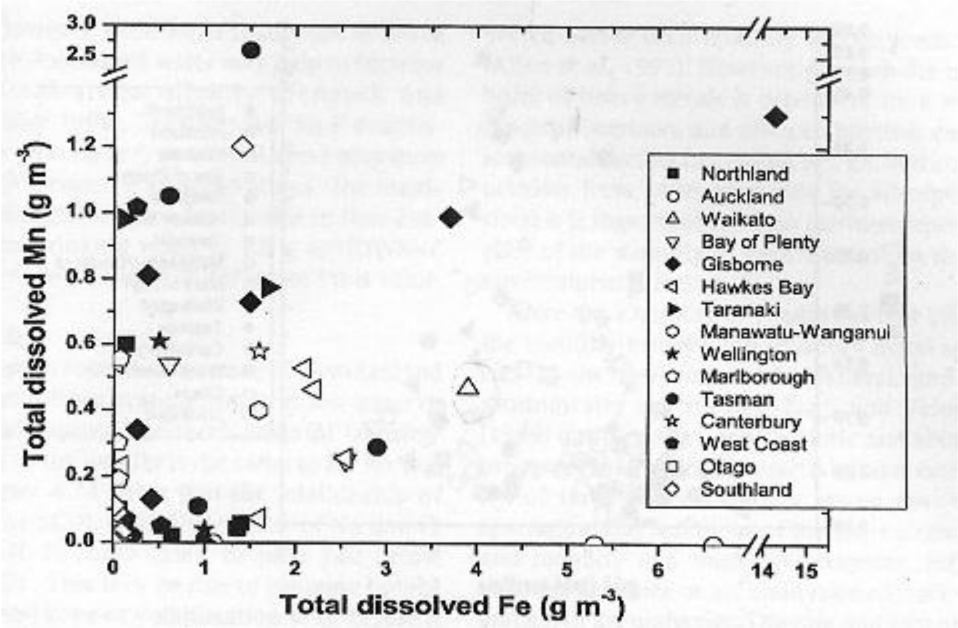

Figure 1.3 Median concentration of total dissolved Fe plotted against median total dissolved Mn. There is no apparent correlation between the concentrations of the two elements. (Retrieved from (Rosen 2001))

Figure 1.3 depicts elevated levels of iron present throughout the regions in New Zealand. According to drinking water standards for New Zealand (DWSNZ 1995), iron concentrations greater than 0.2 g/m^3 and manganese concentrations > 0.05 g/m^3 can stain laundry. Concentrations of manganese exceeding 0.5 g/m^3 impose a potential human health risk (DWSNZ 1995). Thirty six sampled wells had a median total dissolved manganese concentration > 0.05 g/m^3 and sixteen wells had concentrations exceeding 0.5 g/m^3 (Figure 1.3). While widespread throughout the country, Gisborne has by far the highest iron and manganese concentration in bore water. The aquifers in this region are very deep and characteristically contain organic matter (Rosen 2001).

Waikato region’s groundwater is known to contain elevated levels of iron and manganese (20.0 mg/L and 0.9 mg/L respectively) (Moore & Clarkson 2007). In oxygen rich surface soils, these metals exist in insoluble oxidised forms (Rosen 2001). In deeper peat soils, under anaerobic conditions, iron and manganese are found in their soluble reduced Fe(II) and Mn(II), oxidation states. (Ellis et al. 2000). The natural conditions present in the aquifer determine the concentration of dissolved iron and manganese. From Figure 1.3, it is clear that there is no correlation between the concentration of iron and manganese present in groundwaters of New Zealand. This can arise from two main causes. Firstly, since the redox potentials for the reduction of Fe(III) and Mn(IV) are different, the redox potential of the aquifer may lead to differential reduction and solubility of iron and manganese (Rosen 2001). Secondly, the abundance of iron relative to manganese in the minerals of soil and rocks can lead to high Fe(II) and low Mn(II) concentrations in the aquifer (Rosen 2001). These metals are known to form stable colloidal suspensions with organic carbon and silica. (Stumm & Morgan 1988). Bores with groundwater contaminated with iron and manganese as well as silica and/or organic carbon are often abandoned due to high costs of treatment to remove stable colloidal iron.

1.2.3 Colloidal chemistry

In nature, colloidal particles have associated surface charges that stabilize them in suspension (Priesing 1962). These stable surface properties can be altered by adding chemicals so that separation by gravity clarification or filtration is possible. This transformation of the suspension from a stable to an unstable state is achieved by coagulation and flocculation processes (Bratby 2006). Although these two processes are capable of co-existence, they are vastly disparate. In coagulation, colloids are destabilised (through charge neutralisation) using chemicals, whilst in flocculation, large agglomerates of colloid particles are formed facilitating settling under gravity. Coagulation also results in agglomerate formation but these are relatively small and more loosely bound as opposed to the larger flocs formed during flocculation (Priesing 1962).

Stability of Colloidal Suspension

In colloidal chemistry, the term *stability* entails the ability of a particle in the suspension to remain as separate entity (Shchukin et al. 1981). The surface charge present at the solid-liquid interface of the colloid and surface hydration layer of colloids are the two interfacial effects promoting colloidal stability (Bratby 2006).

Colloids are generally classified into two groups:

1. Hydrophobic colloids – repel water molecules, and
2. Hydrophilic colloids – strong affinity for water molecules

In water and wastewater, both types of colloids can be present (Priesing 1962; Birdi 2008).

The tendency to aggregate is caused by weak van der Waal forces of attraction. These attractive forces are opposed by the electrostatic repulsion of like surface charges on the particles (Priesing 1962). The strength of the electrostatic repulsion determines the stability of both hydrophobic and hydrophilic particles (Tripathy & De 2006). Additionally, stability of the colloidal suspension can be affected by adsorbed water molecules that act as a barrier to the close approach of the particles necessary for van der Waals forces to be operative (Birdi 2008).

Electrical Double Layer

In electrolytic solutions, charged surfaces acquire an ionic atmosphere of mobile ions such that the excess of the counter ions (same charge as surface) over the co ions (same charge as surface) balances the surface charge. The fixed layer of surface charge and the diffuse layer of charge in the ionic atmosphere together constitute the electrical double layer (Priesing 1962; Sprycha 1989; Tripathy & De 2006).

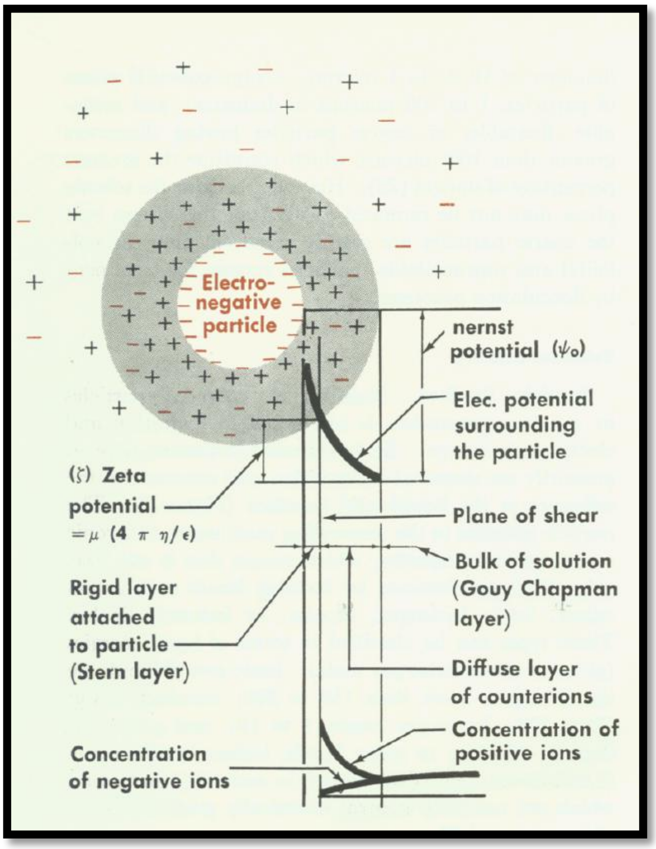

Figure 1.4 Concept of Zeta potential in electrical double layer (Retrieved from (Priesing 1962))

Figure 1.4 illustrates further refinement of the double layer theory where a layer of specifically adsorbed ions is envisaged at the particle surface. The inner layer of fixed charge is known as the Stern Layer (Priesing 1962). The outer diffuse layer is known as the Gouy-Chapman Layer. The stability of the colloidal suspension is significantly influenced by the potential of the Stern Layer (Tripathy & De 2006). The potential of Stern Layer cannot be calculated directly but is estimated by the electrical potential between the shear plane and the bulk solution, i.e., the Zeta potential (Sprycha 1989).

1.2.4 Colloid chemistry of Waikato’s problem bore waters

Natural air oxidation of iron and manganese contaminated bore water results in slow formation of hydrous oxide colloids which react with negative charged silica and/or organic species to form stabilised colloidal suspensions (Winchester 1983). When the metal hydrous oxide colloidal particles are coated with negatively charged particles, they acquire a net negative charge and become stabilised against aggregation.

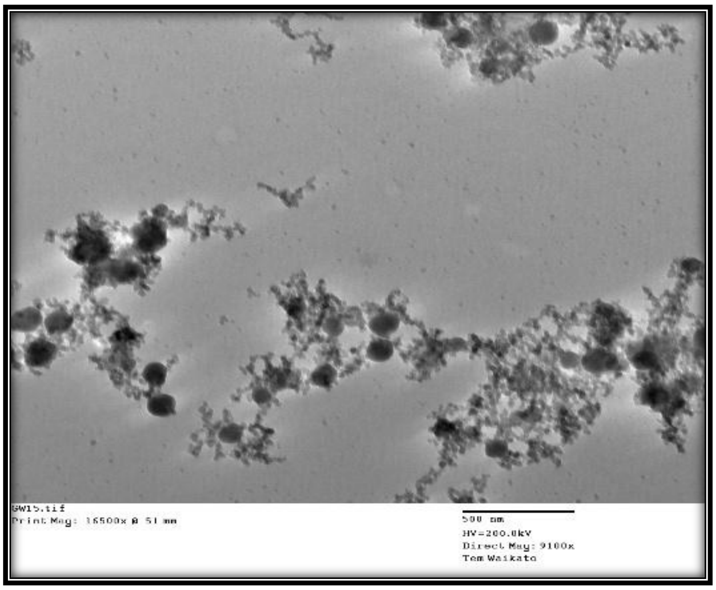

Figure 1.5 TEM image showing poor aggregation resulting from slow air oxidation of Waikato bore water (Nath 2011)

The process is illustrated by data taken from Nath (2011). Figure 1.5 shows how during slow oxidation, the iron particles (dark particles) become surrounded by a sheath of silica particles (lighter particles). In contrast, during rapid oxidation large aggregates of iron (dark particles) with silica particles interspersed are formed (Figure 1.6). The hydrous oxides aggregate before being coated with the negatively charge silica particles (Stumm & Sulzberger 1992). The size of the aggregates formed is large enough to allow rapid settling. (Stumm & Sulzberger 1992)

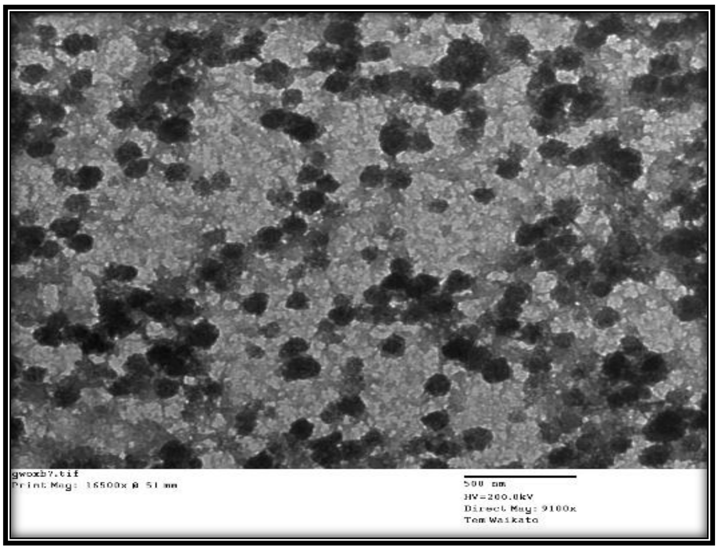

Figure 1.6 TEM image of flocs formed by rapid air oxidation of Waikato bore water (Nath 2011)

1.2.5 Existing technologies for treating iron and manganese water

Depending on the pH and oxygen status of the water, iron and manganese can be present as dissolved, particulate or colloidal forms. The speciation and concentration of these metals determines the best treatment process for removal. Normally the groundwater is chemically treated to oxidise the Fe(II) to Fe(III). At neutral and higher pHs, ferric (Fe(III)) is converted to ferric hydroxide ($Fe(OH)_3$) which eventually transforms to a rust (Fe_2O_3) like product that can be separated by sedimentation or gravity filtration (Casiday et al. 2008).

Some of the existing technologies used for treating iron and manganese laden waters are summarised below.

Air oxidation

Air oxidation is an effective, low cost and chemical free method for treating iron and manganese contaminated water. (Sugio & Kojima 1992). This treatment process uses aeration as the oxidizing agent and is typically conducted prior to filtration in conventional treatment plants. Under excess air, the soluble ferrous ion, Fe(II), is oxidized to ferric ion, Fe(III) which readily forms an insoluble iron hydroxide. Similarly, manganous ion, Mn(II), is oxidized to manganic ion, Mn(IV), forming insoluble manganese dioxide (Aydin et al. 2001). These insoluble metals are either allowed to settle (in a settling tank) or removed using filtration.

Consideration of standard reduction potentials (see below) for these processes indicates that whereas Fe(II) can be expected to be relatively easily oxidised by air, Mn(II) will be require a stronger oxidising agent for complete oxidation.

$$2Fe^{2+} - 2e^- \rightarrow 2Fe^{3+} \qquad E^0 = -0.77$$

$$1/2O_2 + 2H^+ + 2e^- \rightarrow H_2O \qquad E^0 = 1.23$$

The overall reaction is:

$$2Fe^2 + 1/2O_2 + 2H^+ \rightarrow 2Fe^{3+} + H_2O \qquad E^0 = 0.46$$

The Fe(III) will undergo hydrolysis according to:

$$2Fe^{3+} + 6H_2O \rightarrow 2Fe(OH)_3 + 6H^+,$$

so that the overall reaction will be:

$$2Fe^{2+} + 1/2O_2 + 5H_2O \rightarrow 2Fe(OH)_3 + 4H^+$$

Equation 1.1

Similarly for Mn we have:

$$Mn^{2+} + 2H_2O - 2e^- \rightarrow MnO_2 + 4H+ \qquad E^0 = -1.23$$

$$1/2O_2 + 2H^+ + 2e^- \rightarrow H_2O \qquad E^0 = 1.23$$

$$Mn^{2+} + 2H_2O + 1/2O_2 + 2H^+ \rightarrow MnO_2 + H_2O \qquad E^0 = 0.0$$

Equation 1.2

While the conditions in the air oxidations will not be standard conditions, standard data are indicative of the differences in the Fe and Mn systems and indicate why Mn(II) is more difficult to oxidise than Fe(II).

Air oxidation can be achieved using several methods. Water is either treated by dispersing into the air (e.g. passing it through porous trays under gravity which provides ample contact between air and water) or by passing air into water (as bubbles) (John 1997). Alkaline conditions are required for optimum manganese removal. Moreover, this treatment process is also capable of removing sulphides and volatile organic matter under optimum pH values (Serikov et al. 2009).

However, treatment using air oxidation requires careful monitoring of the water flow rate. When the flow rate is too high, sufficient air does not contact with the water and hence, oxidation of Fe(II) and Mn(II) does not occur. Likewise when the flow rate is too low, the water becomes saturated with dissolved oxygen and can subsequently lead to corrosion and elevated concentrations of other trace metals such as copper and lead present in the water (Kaya et al. 2005; Serikov et al. 2009).

Over the course of treatment, slime growth is one of the most common by-products that form on the aeration equipment. When untreated, slime can cause odour and palatability issues in treated water. However, slime can be controlled by the addition of a disinfectant such as chlorine and regular inspection and early treatment (Kaya et al. 2005).

Although air oxidation is a chemical free treatment process, there are some major disadvantages related to air treatment of iron and manganese laden water (Sarikaya 1990). Treating water contaminated with high concentrations of manganese requires a large reaction tank as the rate of oxidation is very slow (Li et al. 2005). Additionally, air oxidation depends upon the pH of the solution. Subtle changes in the water quality can alter the pH of the solution which in turn affects the rate of oxidation. In extreme cases, low pH can significantly reduce the rate of oxidation, exceeding the treatment plant’s capacity and promoting poor water quality (Aydin et al. 2001; Serikov et al. 2009).

Chemical oxidation

Chemicals are added in order to increase the redox potential of water and oxidise iron and manganese. Some of the most common chemicals used for chemical oxidation of iron and manganese are chlorine and potassium permanganate (White 1992).

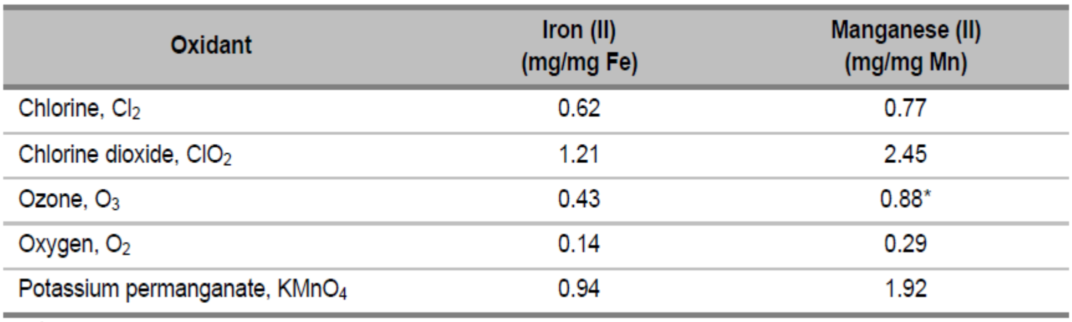

Oxidant	Iron (II) (mg/mg Fe)	Manganese (II) (mg/mg Mn)
Chlorine, Cl_2	0.62	0.77
Chlorine dioxide, ClO_2	1.21	2.45
Ozone, O_3	0.43	0.88*
Oxygen, O_2	0.14	0.29
Potassium permanganate, $KMnO_4$	0.94	1.92

Table 1.1 Chemicals used for iron and manganese treatment (Retrieved from (White 1992))

For example oxidation of iron by potassium permanganate is represented by the equation:

$$3Fe^{2+}_{(aq)} + MnO_{4\,(aq)}^{-} + 4H^{+} \rightarrow 3Fe^{3+}_{(aq)} + MnO_{2(s)} + 2H_2O_{(l)}$$

Equation 1. 3

Potassium permanganate is superior to air or chlorine as a manganese oxidizer. However, high dosages are required and over-dosage can result in colouring of the treated water (Ingram & Bean 1953).

Generally permanganate oxidation is carried out as part of a filtration process. Oxidation occurs while the solution is in a filter of manganese greensand, a granular filtration media that regenerates permanganate after backwash (Sayell & Davis 1975). Optimum oxidation is achieved when a considerable amount of time is allowed for the permanganate to regenerate after backwashing Overdosing with chlorine and subsequent addition of reducing agent can result in improper subsequent disinfection as excess reducing agent can also reduce the chlorine that is later added as a disinfectant. Careful monitoring is thus required.

Several drawbacks limit widespread usage of chlorination for iron removal. The major concern is the health issues caused by the so called disinfection by-products (DBP) (Ellis et al. 2000). Figure 1.7 shows a list of chlorine DBPs. Other concerns include the dangers of transporting, handling and storing of these dangerous chemicals (Tang et al. 2010).

DISINFECTANT RESIDUALS

- Free Chlorine
  - Hypochlorous Acid
  - Hypochlorite Ion
- Chloramines
  - Monochloramine
- Chlorine Dioxide

INORGANIC BYPRODUCTS

- Chlorate Ion
- Chlorite Ion
- Bromate Ion
- Iodate Ion
- Hydrogen Peroxide
- Ammonia

ORGANIC OXIDATION BYPRODUCTS

- Aldehydes
  - Formaldehyde
  - Acetaldehyde
  - Glyoxal
  - Hexanal
  - Heptanal
- Carboxylic Acids
  - Hexanoic Acid
  - Heptanoic Acid
  - Oxalic Acid
- Assimilable Organic Carbon

HALOGENATED ORGANIC BYPRODUCTS

- Trihalomethanes
  - Chloroform
  - Bromodichloromethane
  - Dibromochloromethane
  - Bromoform
- Haloacetic Acids
  - Monochloroacetic Acid
  - Dichloroacetic Acid
  - Trichloroacetic Acid
  - Monobromoacetic Acid
  - Dibromoacetic Acid
- Haloacetonitriles
  - Dichloroacetronitrile
  - Bromochloroacetonitrile
  - Dibromoacetonitrile
  - Trichloroacetonitrile
- Haloketones
  - 1,1-Dichloropropanone
  - 1,1,1-Trichloropropanone
- Chlorophenols
  - 2-Chlorophenol
  - 2,4-Dichlorophenol
  - 2,4,6-Trichlorophenol
- Chloropicrin
- Chloral Hydrate
- Cyanogen Chloride
- N-Organochloramines
- MX*

* 3-Chloro-4-(dichloromethyl)-5-hydroxy-2(5H)-furanone

Figure 1.7 Disinfection by-products (Retrieved from (White 1992))

1.2.6 The aqueous chemistry of chlorine

In water treatment applications, chlorine is typically supplied in the form of calcium/sodium hypochloride or chlorine gas. Chlorine can also be generated from the electrolysis of chloride ions present in brine solutions (Abdul-Wahab & Al-Weshahi 2009).

Depending upon the pH chlorine reacts with water to form HOCl, OCl^- or Cl^- (Equation 1.4 and Equation 1. 5) (Kott et al. 1975).

$$Cl_{2(aq)} + H_2O \rightleftharpoons HOCl + Cl^- + H^+ \qquad K_1 = 5 \text{ X } 10^{-4} \text{ mol/L}$$

Equation 1.4

$$HOCl \rightleftharpoons H^+ + OCl^- \qquad K_2 = 2.6 \text{ X } 10^{-8} \text{ mol/L}$$

Equation 1.5

Oxidizing and disinfecting capacities of chlorine stems from its ability to produce hypochlorous acid. The pH determines the relative concentrations of HOCl and OCl- (Kott et al. 1975). Since OCl^- predominates at high pH and Cl_2 predominates at low pHs, approximately neutral pHs, where HOCl predominates, provide the optimum conditions for disinfection (Sobral et al. 2000) (Figure 1.8). However free chlorine exists in water as a combination of OCl^-, HOCl and Cl_2 present in different concentrations.

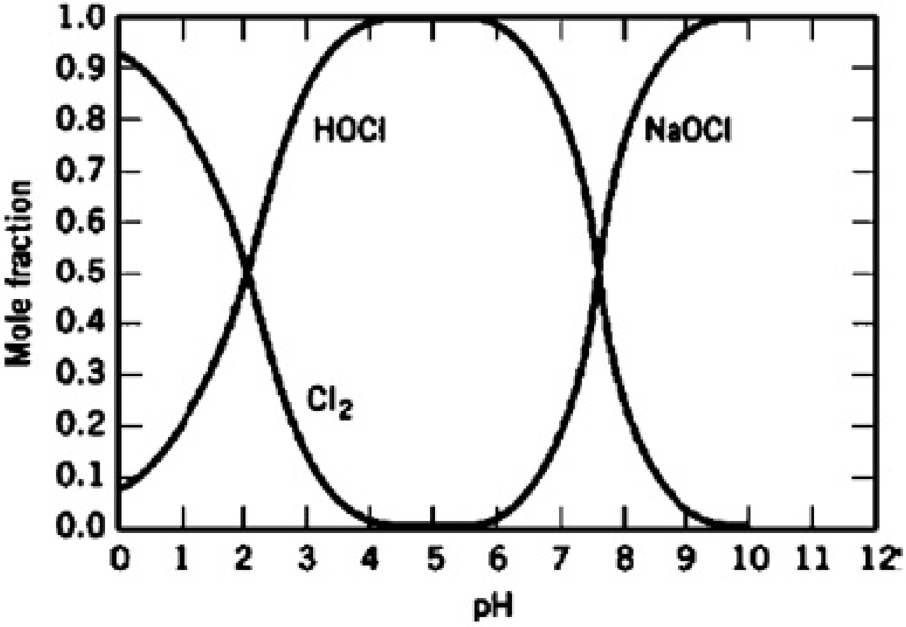

Figure 1.8 Hypochlorous acid dissociation in dependence with pH (Retrieved from (Sobral et al. 2000))

1.2.7 Electrochemical chlorine generators

The electrochemical generation of chlorine for chlorination possess many advantages over chlorination by addition of chemical chlorine. Chlorine can be generated on-site, eliminating the risks involved in storage and handling (Czarnetzki & Janssen 1989). Electrochemical production of gases such as Cl_2 and O_2 is achieved using vertical electrolysers with small inter-electrode gaps. In addition to disinfection, the Cl_2 and O_2 can also assist in mass transfer (Bennett 1980).

Chlorine generators, also known as chlorinators, electrochemically convert the chloride ions present in natural water or brine into a hypochlorite solution. Under an applied direct current (DC), the anode oxidises the chloride ions to form chlorine and hypochlorous acid and some electrolysis of water may also occur producing oxygen and acid (Key D.L. 2010). At the cathode, reduction takes place producing hydrogen and base (Miller 1985) (Liske 1965).

Divided and undivided cells for electrochemical chlorine generation

The two types of cell configurations used for electro chlorination are; undivided (hypochlorite is formed along with hydrogen and oxygen gases) and divided (where the hydrogen and oxygen gases are formed in separate streams) (White 1984).

Depending on whether the cell is divided or undivided, chlorine can be generated as a gas or in the hydrolysed hypochlorite form. Of the two cell configurations, undivided cells are more widely used as electro chlorinators (White 1992). The redox reactions occurring in an undivided cell are as follows;

- At the anode, chloride is oxidised to generate chlorine

$$2Cl^- \rightleftharpoons Cl_{2\,(g/aq)} + 2e^-$$

Equation 1.6

- During electrolysis, concomitant with chlorine production, water is reduced at the cathode to hydrogen according to equation 1.7.

$$2H_2O_{(l)} + 2e^- \rightarrow H_{2(g)} + 2OH^-$$

Equation 1.7

Overall (Equation 1. 6 and Equation 1.7):excluding water oxidation is:

$$2Cl^- + 2H_2O \rightarrow 2OH^- + Cl_2 + H_2$$

Equation 1.7

Key parameters affecting chlorine production include:

1. Conductivity of the electrolyte,
2. Electric potential between the anode and cathode, and
3. Flow rate of the electrolyte.

Hydrogen gas bubbles affect the electrochemical processes in several ways particularly by hindering the fluid dynamics in the cell and increasing cell resistance (Lantelme & Groult 2004). Gas bubbles on the electrodes cause a fraction of their surfaces to be inactive and result in high overpotential values (Thonstad et al. 2004). In addition to hydrogen gas bubbles, other gases also evolve from the electrodes (Ambler & Logan 2011). In particular, oxygen will be formed at the anode in competition to chlorine according to Equation 1.8.

$$2H_2O_{(l)} - 4e^- \rightarrow O_{2(g)} + 4H^+$$

Equation 1.8

The relative amounts of chlorine and oxygen produced will depend on the respective overpotentials of the material used for the anode (Table 1.2).

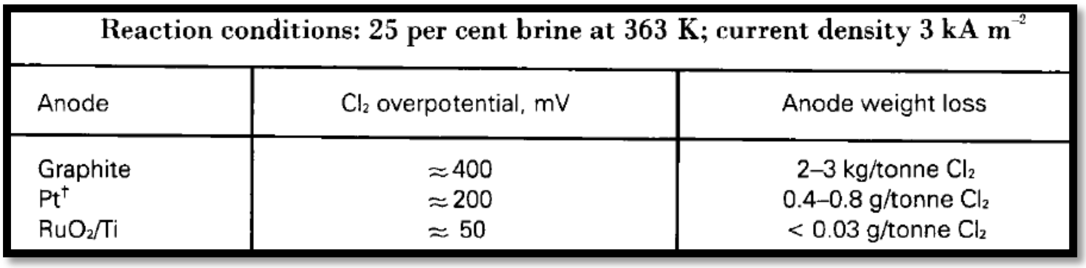

Reaction conditions: 25 per cent brine at 363 K; current density 3 kA m^{-2}

Anode	Cl_2 overpotential, mV	Anode weight loss
Graphite	≈400	2–3 kg/tonne Cl_2
Pt†	≈200	0.4–0.8 g/tonne Cl_2
RuO_2/Ti	≈ 50	< 0.03 g/tonne Cl_2

Table 1. 2 Chlorine overpotential of different anode material (Retrieved from (Chandler et al. 1997))

Often the surfaces of electrodes are coated with electrocatalytic materials in order to favour the generation of a desired product (Chandler et al. 1997). These materials increase the rate of chemical reaction of the target ions without being consumed in the process (Liu et al. 2004).

Direct and indirect oxidation by electrolysers

Electrolysers can bring about oxidation either directly or indirectly (Chiang et al. 1995). Direct oxidation is a two-step procedure, involving the diffusion of species from the bulk effluent onto the anode followed by its oxidation at the anode surface. Indirect oxidation is a process where a strong oxidising agent is generated at the anode which is then responsible for oxidising the target species present in the bulk solution (Figure 1.9). For disinfection and oxidation of water impurities, the general consensus favours the principal oxidation mechanism to be indirect oxidation by electrochemically generated chlorine. The main advantage of the undivided cell for water treatment is that it allows the indirect oxidation and disinfection and can be installed as an inline treatment device (Mathieson 2006).

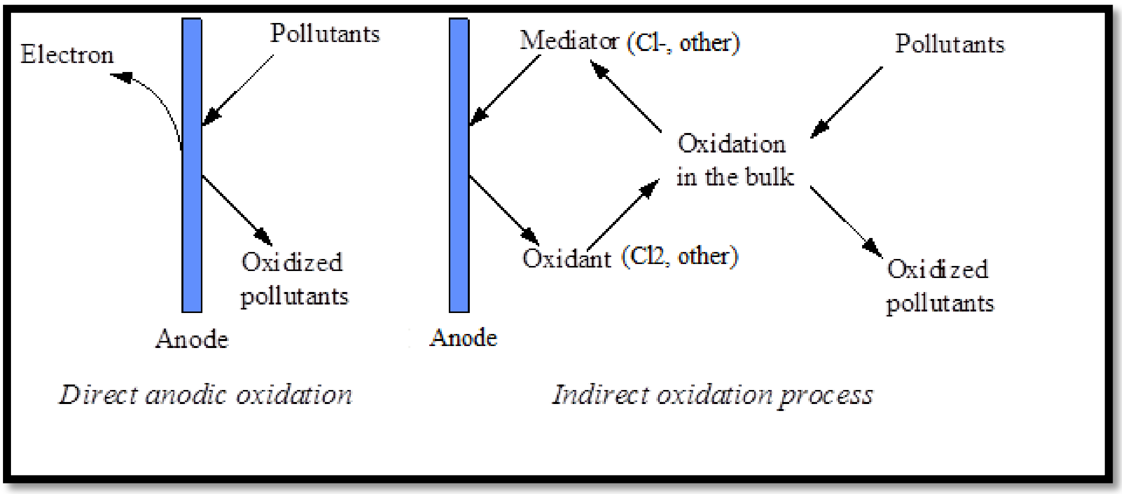

Figure 1.9 Direct and indirect oxidation processes in divided and undivided cells – Pollutant removal pathways of electrochemical oxidation (Retrieved from (Chiang et al. 1995))

Electrolytic chlorination of drinking water

Electro-chlorination offers the possibility of both metal removal and disinfection in a controlled way without the addition of chemicals (Miller 1985). Some of the potential advantages of electrochemical chlorination:

- fine control of amount produced,
- no storage or handling of dangerous chemicals,
- no expensive metering devices, and
- good for small scale applications

The aim of electrolytic chlorination is to generate active chlorine from the natural salt present in water through electrolysis (Guillet & Trancart 1988). The difficulty in achieving this is that most potable waters contain such low levels of electrolyte that their conductivities are so low that conventional cell resistances are too high for the process to be economic

Electrolytic chlorination of wastewater

Electro-chlorination also has potential applications in wastewater treatment (Li et al. 2002; Li et al. 2004).

Historically, chlorination has been used as an important final step in the wastewater treatment. However, due to the generation of organo-chlorinated species this disinfection process is now less favoured (Cano et al. 2011). The possibility of more controlled chlorine dosing and recent advances in anodic materials such as conductive-diamond (Rodrigo et al. 2010), producing BOD consuming reactive oxygen species (ROS), have resulted in renewed interest in electrochemical treatment of wastewater.

1.2.8 The chlor alkali industry

Liquid Mercury Chlor-Alkali process (Divided cell)

Chlor-alkali has been a well-established process for the electrolysis of brine to generate chlorine since the 1980s. Initially, the electrode materials used were graphite anode and mercury liquid cathode.

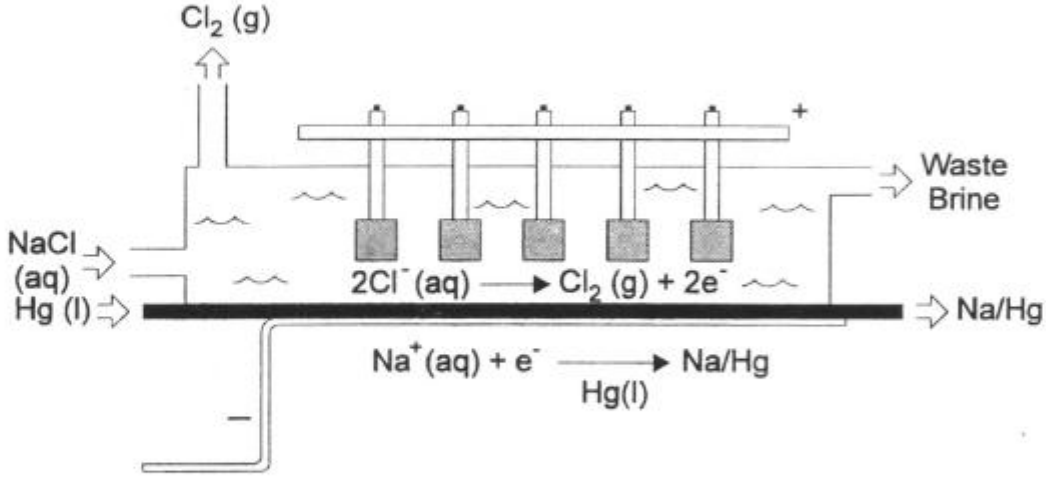

Figure 1.10 Liquid Mercury Chlor-Alkali process (Retrieved from (Harris 2007))

Liquid mercury flows along the bottom of the electrolyser acting as the cathode whereas graphite anodes are suspended parallel from the top. The chlorine gas evolved from the brine solution during electrolysis is released at the anode (Figure 1.10). This process produces chlorine and hydrogen gases in separate steps (Harris 2007).

One of the major disadvantages of this process is the cost associated with the mercury liquid cathode. Moreover, the loss of unrecovered mercury into the environment can lead to a rise in mercury levels in the fish population present in streams where the treated water is discharged (Díez et al. 2008).

Diaphragm and Membrane cell processes

High costs associated with mercury and its negative impact on the environment eventually led to the development of diaphragm and membrane separated cells, a technology that allows generation of chlorine and hydrogen gases in the same cell. (Florkiewicz 2007).

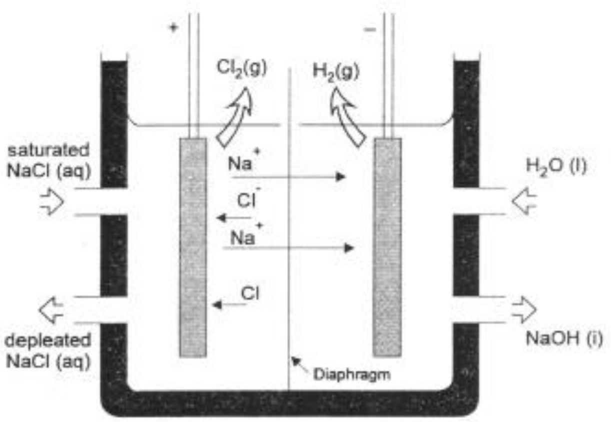

Figure 1.11 Diaphragm Separated Cell (Retrieved from (Harris 2007))

Nearly saturated brine solution enters the anode section. During this process the chloride ions are oxidised to chlorine gas at the anode whereas hydrogen gas and hydroxide are produced at the cathode. Sodium ions migrate to the cathode section through the diaphragm forming sodium hydroxide (Figure 1.11).

This technology is a technical advancement on the traditional mercury liquid flow cell due to its capacity to produce chlorine in a mercury free environment (Collings 2007). However, the cell produces low quality sodium hydroxide due to sodium chloride contamination as the diaphragm is not selectively permeable (McCluney & van Zee 1989; Collings 2007). This issue was overcome by replacing the diaphragm with a perfluorinated polymer cation exchange membrane. The membrane is cation selective, allowing passage of only water and sodium ions towards the cathode end and allowing production of high quality sodium hydroxide (Collings 2007)

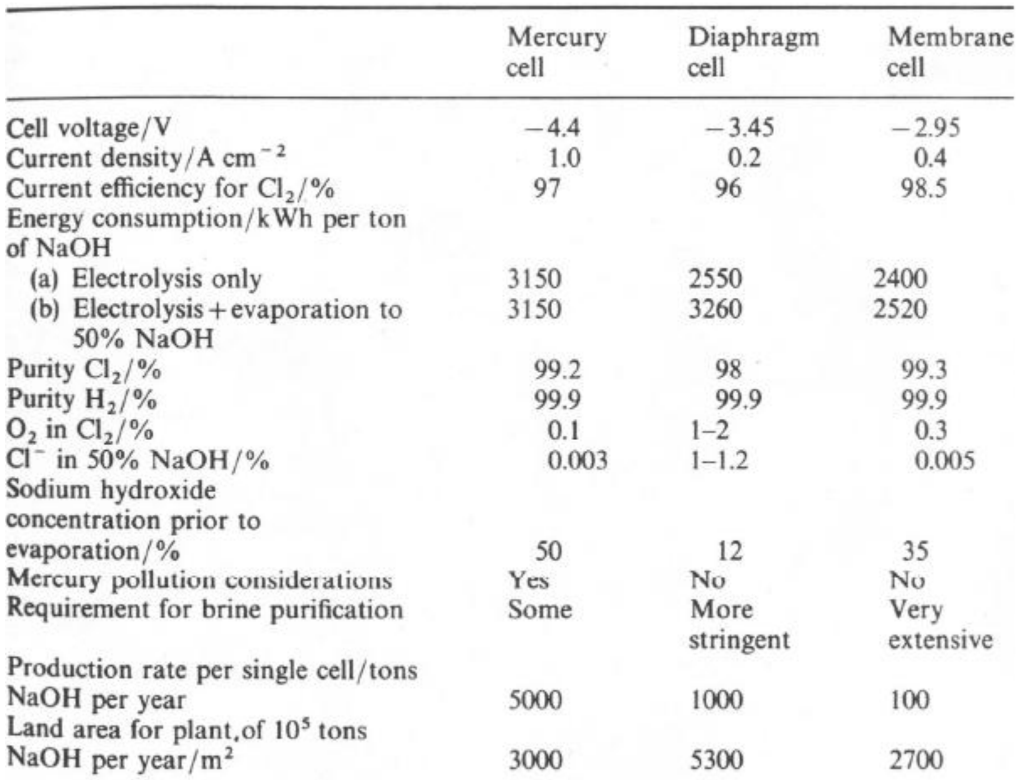

	Mercury cell	Diaphragm cell	Membrane cell
Cell voltage/V	−4.4	−3.45	−2.95
Current density/A cm^{-2}	1.0	0.2	0.4
Current efficiency for Cl_2/%	97	96	98.5
Energy consumption/kWh per ton of NaOH			
(a) Electrolysis only	3150	2550	2400
(b) Electrolysis + evaporation to 50% NaOH	3150	3260	2520
Purity Cl_2/%	99.2	98	99.3
Purity H_2/%	99.9	99.9	99.9
O_2 in Cl_2/%	0.1	1–2	0.3
Cl^- in 50% NaOH/%	0.003	1–1.2	0.005
Sodium hydroxide concentration prior to evaporation/%	50	12	35
Mercury pollution considerations	Yes	No	No
Requirement for brine purification	Some	More stringent	Very extensive
Production rate per single cell/tons NaOH per year	5000	1000	100
Land area for plant, of 10^5 tons NaOH per year/m^2	3000	5300	2700

Table 1.3 Comparison of Chlor-alkali cells (Retrieved from (Collings 2007))

Undivided cell hypochlorite generators

In water treatment, sodium hypochlorite (bleach) is widely used as a disinfectant instead of chlorine gas. (White 1992). This eliminates risks associated with chlorine gas leakage from storage cylinders. Alternatively sodium hypochlorite can produced on site by electrolysis of brine in an undivided cell (Asokan & Subramanian 2009). The, chlorine gas and sodium hydroxide generated in the undikvided cell react to form sodium hypochlorite solution (Martinez-Huitle & Ferro 2006) (Equation 1.9).

$$Cl_2 + 2NaOH \rightarrow NaOCl + NaCl + H_2O$$

Equation 1. 9

1.2.9 Electrode Materials

The type of electrode material used for electrochemical processes determines the current efficiency for the production of the desired species. In the case of chlorine production, three main anode materials have been used; graphite, dimensionally stabilised titanium and boron doped diamond.

Graphite

Physical parameter	**Value**
Bulk Density	>1.72 g/cm^3
Maximum particle size	0.8 mm
Specific Resistance	<8.0 μΩm
Thermal Conductivity	150.2 W/m-°C
Compressive Strength	>30MPa
Flexural Strength	13.5 MPa

Table 1.4 Mechanical properties of Graphite material (Retrieved from (Nath 2011))

Graphite has been widely used for the electrochemical production of chlorine since the nineteenth century. During chlorine generation, graphite anodes are inert and therefore efficient chlorination can be achieved at low polarizations. Graphite anodes undergo two general groups of reactions during electrolysis, the first of which is the electrochemical oxidation of water molecules (Equation 1.10 - Equation 1.12) and the second is, formation of oxidation species from the ingredients present in the solution (Entwisle 1974).

$$C + H_2O \rightarrow CO_2 + 4H^+ + 4e^- \qquad (E^0 = +0.144V)$$

Equation 1.10

$$C + H_2O \rightarrow CO + 2H^+ + 2e^- \qquad (E^\circ = +0.420V)$$

Equation 1.11

$$2H_2O \rightarrow O_2 + 4H^+ + 4e^- \qquad (E^\circ = +1.23V)$$

Equation 1.12

However, a predominance of oxygen generation promotes oxidization of the graphite anode to carbon dioxide. Graphite degradation also occurs at low pH, increased sulphate ion concentrations and high current densities (Entwisle 1974).

Of great importance when utilizing graphite as the anode material is the pressure build-up with applied voltage. Voltage fluctuates throughout electrolysis whereas current flow rate remains constant. Graphite electrodes degrade after repeated cycles of charging and discharging. This is mainly due to the deformation of the porous structure caused by chemical coating and pressure build up during electrolysis (Dresselhaus & Dresselhaus 1981). More importantly, graphite anodes generate poor quality chlorine whilst consuming large amounts of current during brine electrolysis, further limiting their practicality for inline electro-chlorine generation (Woo 1986). However, graphite offers the advantage of low cost and compatibility with New Zealand drinking water standards and a lesser likelihood of producing more toxic and highly oxidised forms of chlorine (DWSNZ 1995; MOE 2005).

Dimensionally Stabilized Anodes (DSA)

A major drawback associated of graphite anodes is their low current efficiency at low chloride concentrations. Dimensionally stabilized anodes (DSA) (Katsaounis 2010) are extremely energy efficient and have the ability to generate hypochlorite from very dilute brine solutions (Key D.L. 2010) (Figure 1.12).

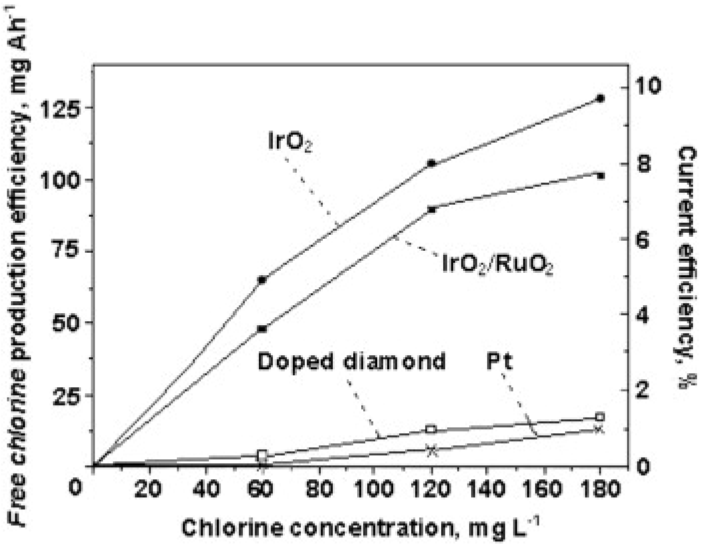

Figure 1.12 Chlorine generation using the chloride content present in the bulk solution using four different anode materials (Retrieved from (Ghernaout et al. 2011))

DSAs have excellent stability against surface and pitting corrosion and can thus be used as an inline chlorine generator (Lu et al. 2012). The development of DSA has resulted in innovative equipment design, better operation conditions and lower energy consumptions associated with electrochemical applications (Miller 1985).

Titanium metal is naturally coated with an insulating titanium oxide layer which makes it corrosion resistant (Liu et al. 2004). However, due to the insulating oxide layer, titanium metal cannot be directly used as an anodic material. It requires modification by a coating of other metals or oxides to make the surface electrically conducting and also impart electrocatalytic properties. (Katsaounis 2010).

Physical parameter	**Value**
Bulk Density	4.54 g/cm^3
Maximum particle size	-
Specific Resistance	42 μΩcm
Thermal Conductivity	19.2 W/m-K
Compressive Strength	>400MPa
Flexural Strength	275 MPa

Table 1.5 Mechanical properties of 99.2% Titanium material (Retrieved from (Liu et al. 2004))

Titanium electrodes can be modified by various techniques as illustrated in Figure 1.16 depending upon the electrocatalytic behaviour exhibited by the deposited conducting compound (Katsaounis 2010). Dimensionally stable titanium anodes can be derived by modifications using metallic oxides (by thermal decomposition) such as Ti/TiO_2/Pt. Furthermore, titanium can be also modified using conducting oxides (by anodic process) such as Ti/TiO_2/PbO_2 constituting low-cost DSAs (Li et al. 2006).

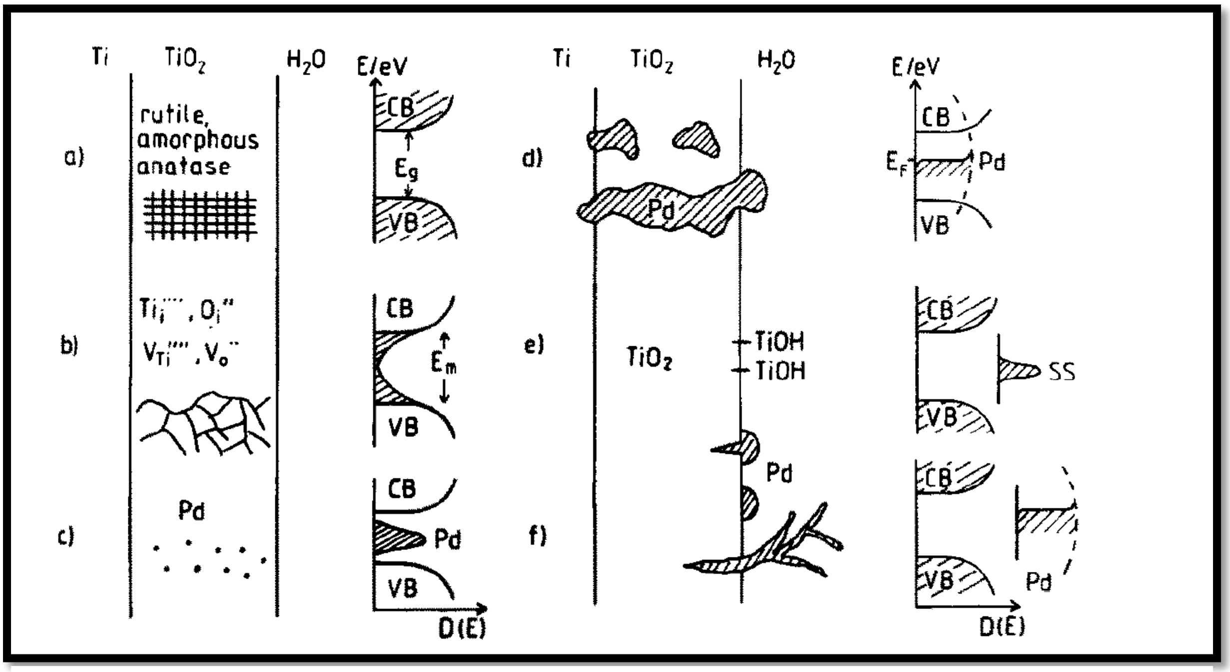

Figure 1.1 Surface modifications of titanium anodes by; a) pure oxide film, b) atmospheric oxide film, c) doped oxide, d) oxide-metal mixture, e) modification by surface states of oxide, f) surface states from metal deposition. D is the distribution of electrons in dependence of the energy E (Retrieved from (Schultze 1989))

Although DSAs have excellent electrocatalytic properties, the associated costs are much higher than graphite. Moreover, rigorous preparation techniques are required and can be quite long, involving multiple procedures. However, despite its cost ineffectiveness, DSAs have completely replaced graphite anodes for chlorine production primarily due to their longer service life as well as considerable reduction in anodic overpotential (Devilliers & Mahé 2010).

Boron Doped Diamond (BDD)

Boron doped diamond, with its excellent structural stability and oxidation ability, can produce species with high oxidation potential (such as ozone and hydrogen peroxide) during electrolysis (Michaud et al. 2003). BDD anodes are widely used for the electrochemical oxidation of organic matter to carbon dioxide. Additionally, BDD anodes are also useful in disinfection (Schmalz et al. 2009).

According to current literature, BDD anodes produce inorganic disinfection by-products. Initial studies have concluded that during electrolysis of chloride free water, oxidised form of sulphur from sulphate were effective (Bergmann et al. 2009). However utilization of BDD anodes for electrolysing synthetic drinking water containing chloride resulted in the generation of chlorate and perchlorates at high concentrations (Bergmann et al. 2009). Additionally, usage of BDD anodes were also found to produce precarbonates in sulphate containing water as well as bromate and perbromate when electrolysing bromide containing water (Rychen et al. 2010; Bergmann et al. 2011)**.** All these species are incompatible with drinking water. BDD anodes were thus not considered for this research.

1.2.10 Factors affecting electrochemical efficiency

In order to minimise energy consumption for a given rate of treatment, it is important to minimise the voltage required to achieve the necessary current flow. Formation of bubbles, the overpotential, the inter-electrode gap and the conductivity of the electrolyte all affect the applied voltage required (Sharma 1998).

Gas bubbles in the inter electrode gap

When gas bubble sizes are small with respect to the interelectrode gap, the lengthening of the current distribution paths is not considered. The free space around the bubble has no effect on the ohmic voltage drop. However, for larger bubbles, there is a strong non-uniform current distribution in the bubble free space (Figure 1.14). The vertical flow direction of the current is hindered resulting in an ohmic voltage drop in the bubble free space. (Thonstad et al. 2004).

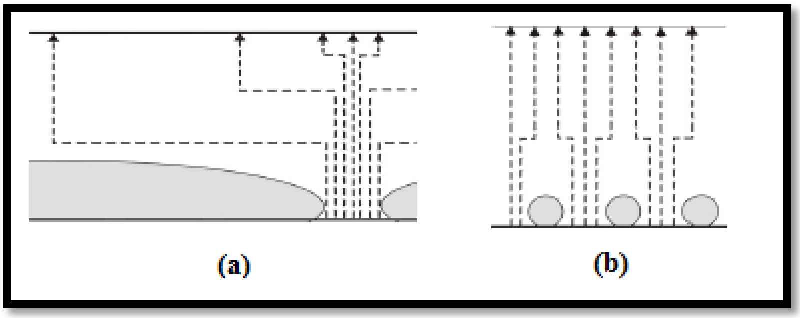

Figure 1.14 Current distribution when a) large bubbles are formed and b) small bubble are formed (Retrieved from (Thonstad et al. 2004)

Effect of Current Density on Cell efficiency

Operational current density is a vital factor in electro-oxidation process as it is the only parameter that can be controlled externally. An increase in current increases the anode potential, the rate of oxidation and the gas bubble formation.

In theory, three components determine the potential of the cell;

$$\eta_{AP} = \eta_k + \eta_{Mt} + \eta_{IR}$$

Equation 1. 13

where,

η_{AP} = applied overpotential (V)
η_k = kinetic overpotential (V)
η_{Mt} = mass transfer overpotential (V)
η_{IR} = overpotential caused by resistance or IR drop (V)

The drop in resistance (IR) is directly related to the interelelctrode distance, surface area of the electrodes, the conductivity of the solution and the applied current (Queeney 2003). However, decreasing the interelectrode gap, increasing the cross sectional area of the electrodes and increasing the conductivity of the electrolyte can minimize the drop in IR (Queeney 2003).

Current density not only influences the systems run time but it also determines the rate of oxidation. Often, the highest achievable current density may not be the most effective way of treatment but rather, depends on a combination of optimum current density and cell configuration (Augustin 1998). Current density is greatly influence by pH, conductivity and temperature as well as flow rate of the electrolyte (Czarnetzki & Janssen 1989)

Effect of inter-electrode gap on current density

When the inter-electrode gap is within the micron range, electrolyte resistance, R_{el} (present between the electrodes) is largely eliminated resulting in a large decrease in the ohmic resistance R_d of the cell as shown in Figure 1.15 (Küpper et al. 2003). Moreover, minimisation of the thickness of the diffusion-layer (present on the electrode surface) decreases the residual potential drop $\Delta\varphi$. This is achieved by reducing the electrode gap ($< 500\mu m$) until the minimum ohmic drop is reached (Küpper et al. 2003). In other words, $R_d \ll R_a + R_c$.

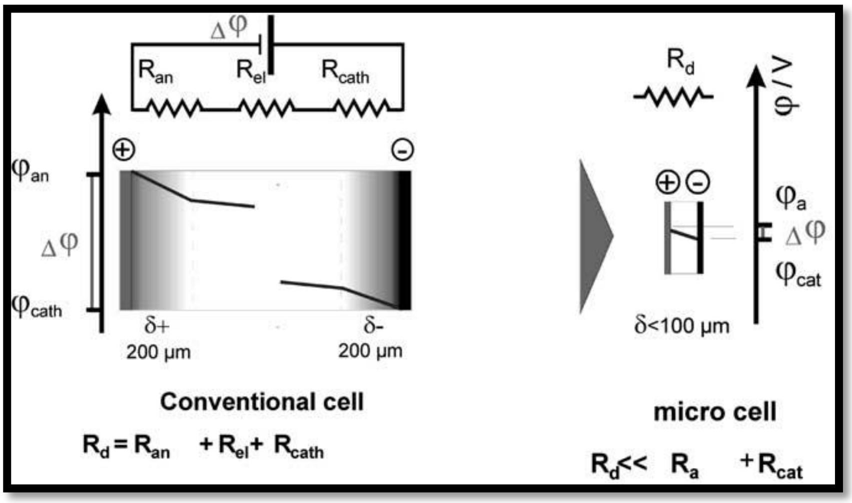

Figure 1.15 Difference between conventional and thin layered cell (Retrieved from (Küpper et al. 2003))

Reducing R_d assists in lowering the amount of salt required to produce adequate conductivity (Küpper et al. 2003).

Effect of pH and Conductivity

pH is another critical aspect of electro-oxidation treatment. According to the Nernst equation, the standard oxygen potential drops at higher pH.

$$E_{O_2} = 1.229 - 0.05916 \text{ pH}$$

Equation 1.14

The standard potential for the production of chlorine from chloride (1.358 V) does not vary much with pH as compared to oxygen. At pH = 0, E_{O_2}= 1.229 V; at pH = 7, E_{O_2}= 0.815 V; at pH = 14, E_{O_2}= 0.401 V. When voltages are higher than chlorine potential, the chlorine current fraction can be increased by decreasing the anodic pH (by increasing the current density) at the expense of oxygen production that can be balanced by chloride depletion. However, raising the pH of the bulk solution does not directly lower the minimum voltage for electrolysis since the change in hydrogen potential instates a change in oxygen potential (At pH = 1, E_{O_2}= 0 V; at pH = 7, E_{O_2}= - 0.414 V; at pH = 14, E_{O_2}= - 0.828 V).

$$E_{H_2} = -0.05916 \text{ pH}$$

Equation 1.15

Therefore, for all uniform pH values at 25°C, the standard potential for the electrolysis of water is 1.229 V. The surface of the cathode will be strongly alkaline whereas the anode surface would be strongly acidic. This implies that the cell voltage of the overall electrolysis of water can easily exceed 2.05 V (1.229 - (- 0.828)). Altering the flow rate is one of the few ways of altering this affect. Lowering the flow rate will aggravate the lowering of anodic pH whereby favouring chlorine production ahead of oxygen. Likewise, increasing the flow rate will offset the acidity of the anode and therefore favour oxygen production (Macka et al. 1998)

In chemical treatment, the pH of the solution decreases with the addition of coagulant and thus needs to be adjusted. However, for electro-oxidation, the pH of the solution increases due to the production of H_2 gas at the cathode, particularly true at a pH range between 4 and 9. A pH > 9 results in a pH decrease after treatment (Brillas et al. 2004). However, in order to avoid the development of chlorine bubbles (which may lead to the loss of chlorine gas during electrolysis) and to minimise the production of O_2 gas, electrolysis should be carried out at a pH range between 9 and 12 (Czarnetzki & Janssen 1989).

Conductivity is defined as the ability of a material to withstand electric current (Priesing 1962). In an electrochemical system, the current efficiency decreases when the electrolytic conductivity is low. In order to increase the current efficiency, the conductivity of the electrolyte is increased by adding salt. (Sharma 1998).

1.2.11Clarifier Design

The electrolysis of dilute chloride solutions will always produce hydrogen at the cathode and in addition to hypochlorite, at least some oxygen at the anode due to water electrolysis. The gas is produce as very fine bubbles which adhere to any particles present promoting their buoyancy (Haarhoff & Edzwald 2012). Therefore, substances with densities similar to water rise to the water surface assisted by gas bubbles by a process known as electro-flotation (Trahar & Warren 1976).

Dissolved air flotation (DAF)

DAF is used for floating particles which have specific gravity higher than 1.0. (Trahar & Warren 1976). Contact between the gas bubbles and the solid can occur by adhesion, trapping and adsorption. (Trahar & Warren 1976). Providing their combined density is less than unity, the particle-bubble pair will rise to the surface of the liquid where the solid material can be skimmed off. For adequate flotation, the bubble size should be between $10 - 100\,\mu$m. Gas bubbles generated from a pressurized liquid produces a milky white appearance of this size range once the liquid is depressurized (Haarhoff & Edzwald 2012).

1.3 Previous work at the University of Waikato

Prior research at the University of Waikato has dealt with the development of electrochemical methods for chlorine generation, disinfection, iron removal and effluent treatment

1.3.1 Divided cell using porous anode

Wang (2005) developed a divided cell using porous anodes to generate chlorine from dilute brine solutions for small scale water treatment plants and treatment of swimming pools.

The cell comprised of an anode compartment which consisted a porous titanium anode plate, an anode back plate and a product chamber and a parallel cathode compartment consisting a porous titanium cathodic plate, a cathode back plate and a product chamber. The electrodes are supported with ion exchange membranes which selectively allow the ions, present in the aqueous solution, to enter into either compartment (Figure 1.16).

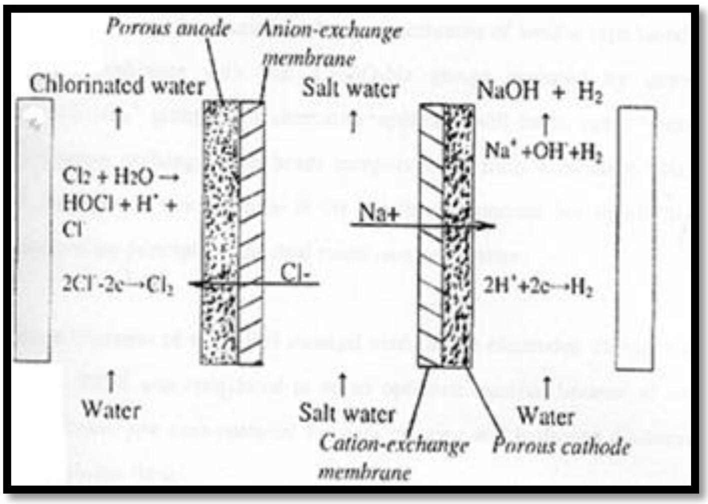

Figure 1.16 Porous anode membrane cell (Retrieved from (Wang 2005))

In order to improve the cell’s ability to generate chlorine at low power consumptions, the ion exchange membrane was chemically modified with platinum which acts as a catalyst and improves the surface properties of the membrane. The Pt-catalysed membrane resulted in a 50% drop in cell voltage, increasing the cell’s current efficiency by 87% at a cell voltage of 6.4 V at 5 A. However, it was also found that decreasing the concentration of the brine resulted in an increase in membrane resistance, resulting in poor energy efficiencies.

1.3.2 Online Chlorine generation using natural chloride in novel undivided cells

Mathieson (2006) developed two cells for wastewater treatment.

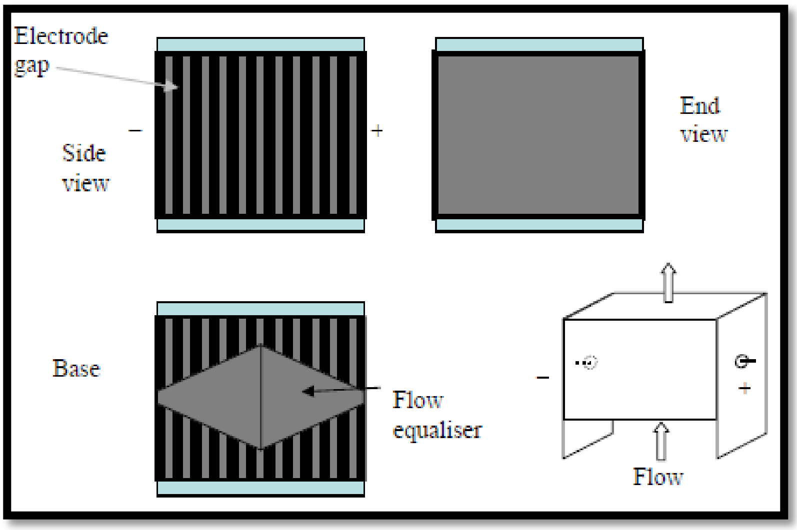

Figure 1.17 Breadbox design for treating iron laden water (Retrieved from (Mathieson 2006))

Breadbox cell

The breadbox cell (see Figure 1.17) so called because of its parallel alignment of the electrodes, is a bipolar stack of twelve 316-stainless steel electrodes (having an active area of 0.04 m^2). The electrodes were hollow rectangular prisms each with a small hole in the top face to allow the generated gases to escape. The thickness of the hollow electrodes was 15 mm and the inter-electrode gap between the parallel electrodes was set to 1 mm. This undivided cell design was capable of achieving rapid oxidation of Fe(II) to insoluble Fe(III). The Fe(III) formed aggregated flocs which rose in the settling tank due to the gas bubbles produced during electrolysis. The floc was then allowed to settle and removed using gravity filtration.

While the system is capable of producing high quality water using the chloride present in bore water, it involved a lengthy filtration step. Additionally, since the breadbox design is an undivided cell system and doesn't have a separating membrane between the anodes and the cathodes, the reduction of Fe(III) back to Fe(II) at the cathode is an added possibility. Furthermore, high current densities were required for optimum electrolysis, promoting high power consumption and rapid degradation of the anodes. Reducing the current density led to poor chlorine generation and poor oxidation of Fe(II) to Fe(III).

Flume cell

Mathieson's second cell design represented a major advance. He was able to reduce the inter-electrode gap to 0.1 mm (thickness of a nylon insulating membrane) and avoided hydraulic resistance by passing the effluent to be treated through an anode bed of aluminium shavings separated from a stainless steel cathode flume by the nylon mesh. Essentially this was a cell with a porous anode separated from a sheet cathode. (Figure 1.18).

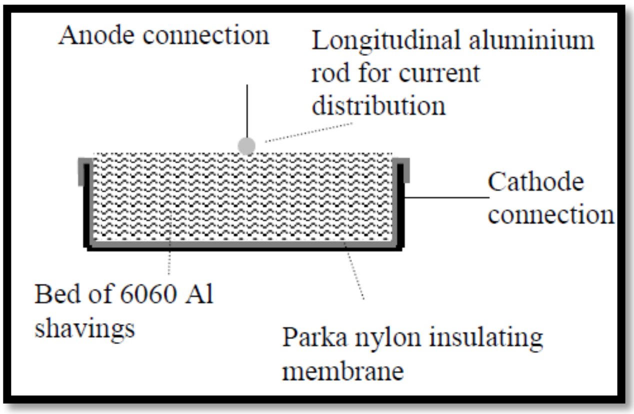

Figure 1.18 Flume design with reduced interelectrode gap (Retrieved from (Mathieson 2006))

1.3.3 Micro-gap perforated electrode flow through (PEFT) cell

Nath (2011) further developed the concept of passing the liquid to be treated through the electrodes rather than between them by developing a cell based upon two perforated electrodes. The cell was used for the *in situ* generation of chlorine for various water and wastewater treatment applications. The cell had some similarities to the Zappi cell (Zappi & Weinberg 2001) which, like the Mathieson cell, used an insulating electrode spacer. However, unlike the Zappi cell, this cell has a closed housing to facilitate in situ high pressure operation as an inline chlorine generator/oxidiser.

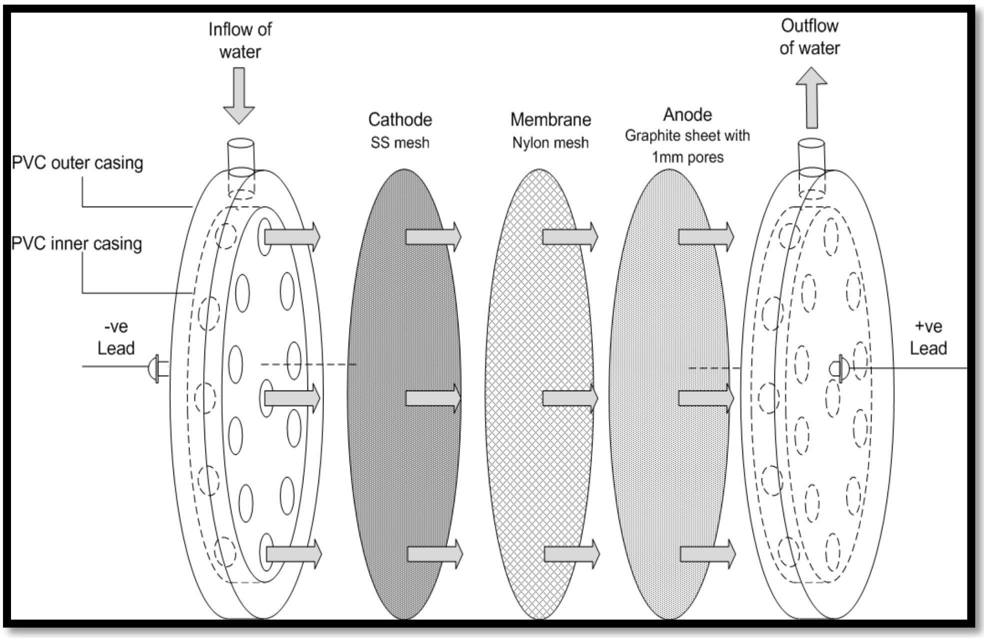

.

Figure 1.19 PEFT cell Electrode set-up (Nath 2011)

Perforations in the electrodes were precision drilled and the electrodes assembled in such a way that optimised symmetrical flow paths of identical and minimum path length for flow between each perforation of the anode and each perforation of the cathode (see Fig 1.21). Even though the flow gap between the electrodes was very narrow (50 µm or less) the flow path was very short. In this way good volumetric flow rates through the cell were obtained at modest applied pressures The PEFT cell is capable of *in situ* generation of chlorine using natural chloride.

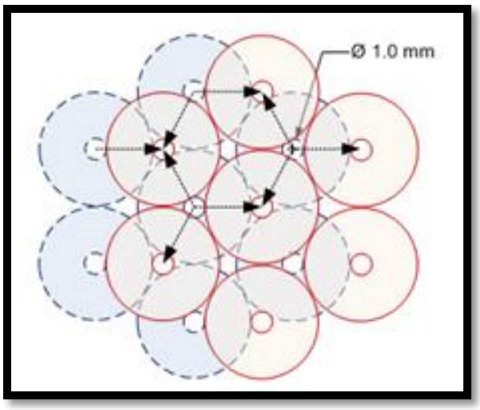

Figure 1.20 Staggered electrode set-up (Retrieved from (Nath 2011))

Nath found that by using the PEFT cell, 100% Fe(II) oxidation of iron in bore water was achieved after four cycles through a single cell at chloride concentration of 250 mg/L and with a power consumption of 18.4 kWh/m^3.

The present work is based upon Nath's PEFT cell design and investigates methods for improving the PEFT cell's performance for treating iron and manganese laden bore water. The central idea was that by using a stack of multiple electrode pairs connected in parallel, single pass oxidation at lower power consumption should be achievable.

1.4 Objectives of the Present Study

The first objective was to assemble and test a multi-electrode PEFT cell design with graphite anodes. The use of multiple electrodes should require lower concentrations of chloride as the chloride oxidised in the first cell and then reduced while oxidising Fe(II) will be available for re-oxidation by the second cell in a stacked multiple cell system. Furthermore, if the cells are electrically connected in parallel, for a constant current flow through the system, the resistance and, consequently the power consumed should be reduced by a factor equal to the number of cells connected in parallel.

In initial work, graphite anodes will be used to see if this low cost material can be used to achieve satisfactorily oxidise the iron and manganese of a problem Waikato bore water. Depending upon the outcomes of this work, DSAs may be trialled.

A final objective of the study, if the initial work was successful, was to design and develop an electro-flotation clarifier system for the online floc removal after the inline oxidation.

1.5 Thesis Outline

Chapter 1 defines the area of study with a general introduction, and examines the literature on the importance of chlorine in water and wastewater treatment industries leading to the evolution of electrochemical technology and applications of various electrochemical techniques for iron and manganese removal followed by the specific objectives of this research.

Chapter 2 describes the materials and methods used in this research.

Chapter 3 describes the development of the ME-PEFT cell system and the evolution of the electro-flotation column.

Chapter 4 investigates graphite as the anode material and the effect of multiple electrode pairs, electrically connected in parallel, on iron oxidation, iron removal and electro-chlorination.

Chapter 5 investigates the effect of a better anode material (DSA) on electro-chlorination, iron oxidation and iron removal from low chloride concentrations.

Chapter 6 investigates the performance of the electro-flotation column with respect to gravity settling.

Chapter 7 is the general discussion and main conclusions along with recommendations for future research.

Chapter 2: Material and Methods

2.1 Perforated electrode flow through cell (PEFT)

Traditionally, static plate electrodes are immersed into a water bath and separated by distance of a few millimetres to centimetres. While satisfactory for use with concentrated electrolytes, such configurations, because of their high resistance, are unsatisfactory because of cost and high voltage requirement for dilute electrolyte systems such as natural water. The development of PEFT cell design has enhanced the efficiency of the electrolytic system. Unlike conventional systems, PEFT cell is completely sealed and it can be subjected to varying pressure and flow rates allowing it to be directly in cooperated into an existing water treatment plant. More importantly, the cell design based upon electrodes perforated with a regular hole pattern and staggered to give symmetrical short flow paths between the electrodes, allows the electrodes to be brought very close together while maintaining good cell flow characteristics. Inter electrode gaps of $\leq$ 50 µm can be used dramatically reducing cell resistances and hence power consumption (Nath 2011).

The details of the PEFT cell design, its electrodes and construction have been summarised in Section 1.2. The adaptation of this design to provide multiple electrode contacts during a single pass and so avoid the need for recycling is discussed in Section 2.2 below.

2.2 Development of the multi-electrode PEFT (ME-PEFT) cell

The outer casing of the PEFT cell was made of high density plastic (Poly(methyl methacrylate)) and the electrodes were held together by eight stainless steel nuts and bolts. Each electrode compartment comprised of an anode and a cathode separated by a spacer. The distance between each electrode compartment was set at 10 cm in order to achieve optimum oxidation efficiencies from each cell as it gives enough time for the electrochemically generated chlorine to oxidise Fe(II) to Fe(III) and also for the reduction of chlorine to chloride. The longer column (57 cm) following the four cells was incorporated in order to allow flocculation to occur with the help of the bubbles generated during electrolysis. Bubbles attached to the floc allow them to float and aggregate at the top of the column. Ideally, the concentrated aggregated floc is collected inside the tray (at the top) and removed through the sludge outlet whereas the clear effluent is retrieved from the treated effluent outlet as shown in Figure 2.1.

Initially, stainless steel wires were used as the electrical connecting leads however, due to high resistance and improper current distribution onto the electrodes they were replaced with titanium foil discs. The electrode separator used was 50 µm strip of inert cellulose (3M Scotch^{TM} tape 375, USA) giving a cell constant of $\approx 1 \times 10^{-6}$ cm^{-1} (calculated from cell geometry). The influent enters into the cathodic end of the PEFT cell and moves vertically through the electrodes and discharged as treated electrolyte (Figure 2. 1).

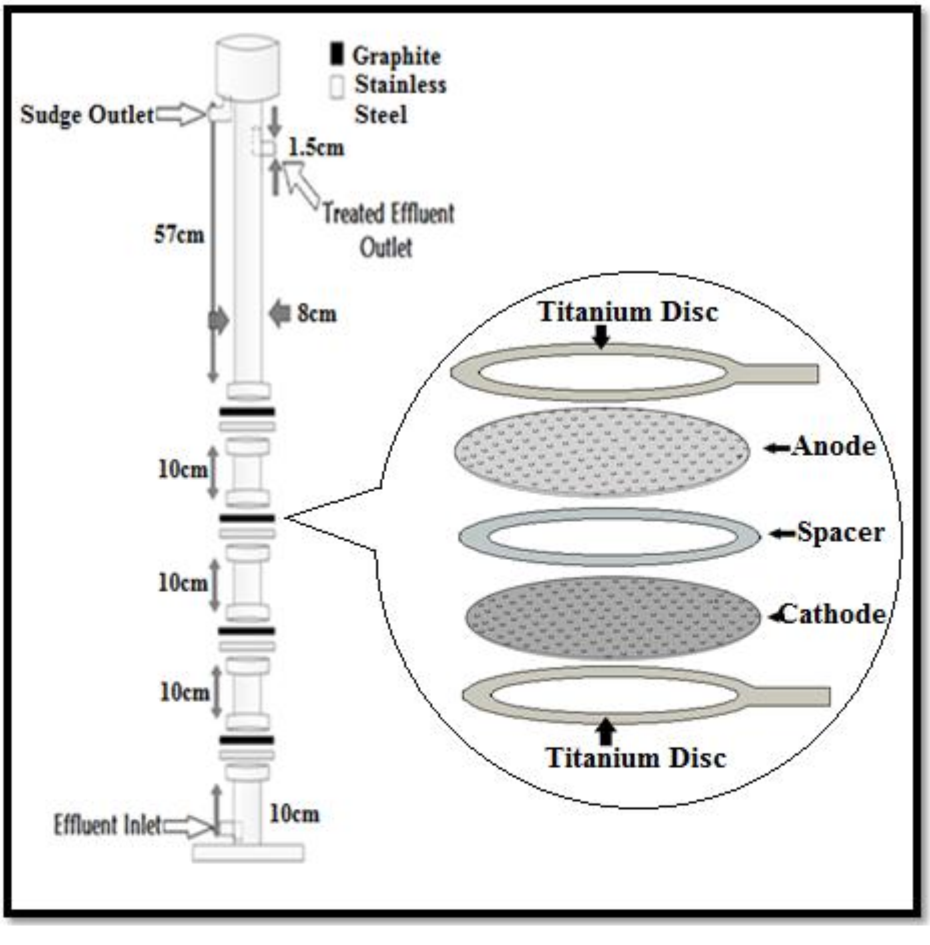

Figure 2.1 Schematic of the Multiple PEFT cell system

Figure 2.2 illustrates the experimental setup of the PEFT cell system. The cell was connected to a direct current source with a maximum of 20 A and 35 V (TRIO Regulated DC Power Supply PD 35-20). The applied current and voltage were measured using FLUKE 37 multimeters. A peristaltic pump (Watson Marlow 504S, with regulated DC power supply) with a flow controlling knob was feeding the influent into the cell and the effluent was collected into a measuring cylinder.

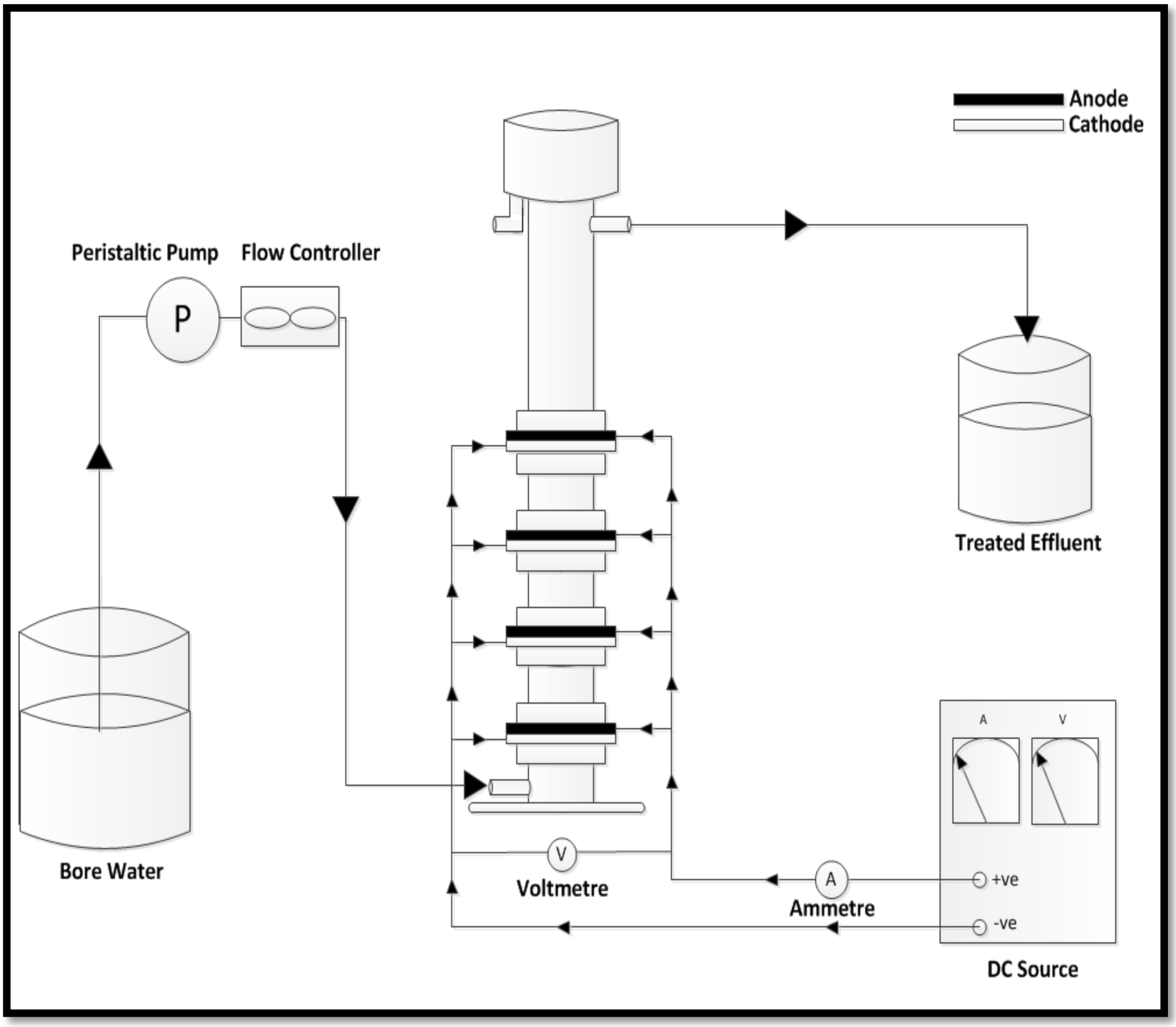

Figure 2.1 Experimental set-up of the multiple PEFT cell

2.3 Electrode Materials

The electrode materials used in this research were chosen on the basis of their compatibility with water treatment, New Zealand drinking water standards, cost effectiveness and the ability to withstand corrosion. The anode and cathode materials used during this research are summarised in Table 2.1.

Anode	**Cathode**	**Spacer – electrode gap**	**Flow gap**
Graphite	Stainless steel	Polyurethane – 50 µm ± 2µm	50 µm
TiO_2/RuO_2	Stainless steel	Polyurethane – 50 µm ± 2µm	50 µm
$TiO_2/RuO_2/IrO_2$	Stainless steel plate	Polyurethane – 50 µm ± 2µm	50 µm

Table 2.1 Electrode Material and spacer used in the development of the multiple PEFT cell

2.3.1 Anode Materials

Graphite (thickness = 2.5 mm) was chosen as the anode in the study conducted previously using the PEFT cell for iron and manganese removal from bore water (Nath 2011). In order to compare the differences in iron and manganese removal efficiencies using the multi-electrode PEFT cell system graphite was used as the anode for initial studies.

For the later part of this research graphite anodes were replaced by dimensionally stabilised titanium anodes (thickness = 2 mm). They were chosen due to their superior mechanical properties, compatibility with the drinking water supplies and primarily because of their excellent ability to generate chlorine from very low chloride levels as found in Waikato groundwater.

2.3.2 Cathode Material

The material used as the cathode was 316-stainless steel (thickness = 2 mm) for this research. This particular stainless steel composition was selected because of its high corrosion resistant properties.

Both the electrodes were precisely drilled using a CNC-1350-A Galaxy computer numerical controlled machine with the same hole density of 8 holes/cm^2 (diameter = 1 mm) giving an effective electrode surface area of 48.3 cm^2.

2.4 General procedure for electrolysis experiments

Iron and manganese (up to 25 and 0.9 mg/L) contaminated water used for this research was collected from a groundwater bore located in 956, Tuhikaramea road, Hamilton, New Zealand. Synthetic iron water were prepared using double distilled water which had a fixed pH range between 4.2-4.5 and conductivity < 2 µS/cm at 20°C.

The electrochemical treatment was carried out by passing groundwater through the ME-PEFT cell which electro oxidizes the metal ions which subsequently aggregate and settle in the column. The percentage oxidation of ferrous into ferric ions was determined by the 1, 10 Phenanthroline spectrophotometric method and detected using JENEWA 7300 SPECTROPHOTOMETER (Vogel 1997). The effluent from the cell was filtered with a 0.45 μm filter and analyzed using ICP-MS PerkinElmer SCIEX ELAN DRC II for metal ion content. BDH Analar grade reagent sodium chloride was added to the groundwater for effective chlorine production under electrolysis. The pH was measured using a BA350 series 3 EDT Instrument pH meter and the conductivity was measured using a CyberScan100 Con Eutech Instrument. Turbidity of the treated groundwater samples was measured using HACH 2100P Turbidimeter, in Nephelometric Turbidity Units (NTU) and the dissolved oxygen level was measured using a CyberScan 100 DO instrument. The active chlorine level in treated water was determined by an iodometric titration and the initial chloride level in groundwater was determined using mercury (II) thiocyanate spectrophotometric method (Vogel, 1997).

2.5 Analytical Methods

2.5.1 Ferrous ion Analysis

The ferrous ion concentration in the effluent was measured using the 1,10 Phenanthrolein spectrophotometric method (Vogel 1997). A dilution series of known ferrous ion ($FeSO_4.7H_2O$, MW 278.02, BDH Analar reagent) solutions (0 - 4.0 mg/L) were used to prepare a calibration curve (absorbance versus ferrous ion concentration (Appendix A). A volume of 10 mL oxidized effluent was transferred into a 50 mL falcon tube to which 5.0 mL of 0.2 mol/L sodium acetate (UNILAB Ajax, Analar reagent) and 4.0 mL of 0.25% 1, 10 Phenanthrolein (SERVA, Feinbiochemica, Heidelberg, Analar reagent) were added and made up to the 50 mL mark with distilled water. The solution was mixed well and allowed to stand for 10 minutes for the colour to develop and the absorbance was measured at 515 nm using JENEWA 7300 UV-VIS spectrophotometer.

Preparation of 20 mg/L iron solution

M.W. of $FeSO_4.7H_2O$ = 278.02 g/mol

M.W. of Fe = 55.847 g/mol

55.847 g/mol → 278.02 g/mol

55.847 g (Fe) → 278.02 g ($FeSO_4.7H_2O$)

∴ 1 g (Fe) → 278.02/55.847 = 4.978 g ($FeSO_4.7H_2O$)

Thus, **20 mg** (Fe) = 4.978 x 20 = **99.56 mg** ($FeSO_4.7H_2O$)

2.5.2 Chlorine Analysis

The chlorine concentrations of synthetic water having the same electrolytic concentrations (containing no iron or manganese) as groundwater were calculated using the Iodometric titration method. NaCl (BDH Analar reagent) was used to prepare the sodium chloride solutions in single distilled water (conductivity < 2 mS/cm). Sodium iodide (10% solution, BDH Analar reagent), sodium thiosulfate (BDH Analar reagent, made up to concentrations of 0.1, 0.05, 0.025 and 0.0125 mol/L), glacial acetic acid (Merck Laboratory Reagent), and starch glycollate indicator (BDH Analar reagent) were used as required. In order to resist chlorine to escape, a known amount (100 mL) of the electrolysed solution was transferred into a beaker containing 10% sodium iodide (20 mL). The solution was acidified using glacial acetic acid (10 mL) along with the starch indicator (~ 1 mL). The samples were titrated against standardized sodium thiosulpfate solution.

2.5.3 Chloride Analysis

The chloride ion concentration present in groundwater samples was measured using a spectrophotometric method. A dilution series of known chloride ion (BDH Analar grade reagent) concentrations (0 – 40 mg/L Cl^-) were used to prepare the calibration curve (absorbance versus chloride ion concentration (Appendix A). A volume of 6 mL colour reagent was transferred into a 15 mL falcon tube to which 3 mL of the sample was added. The solution was well mixed and made up to the

15 mL mark with distilled water. After the colour had developed (15 minutes) absorbance was measured at 460 nm using JENEWA 7300 UV-VIS spectrophotometer.

Preparation of the Colour Reagent for chloride analysis

Mercury Thiocyanate (0.013 mol/L $Hg(SCN)_2$; Mr = 316.77)
4.17gram of $Hg(SCN)_2$ was added to 1 L methanol. The solution was filtered using ash less filter paper.
Ferric Nitrate (0.5 mol/L $Fe(NO_3)_3.9H_2O$; Mr = 404.00)
202 gram of $Fe(NO_3)_3.9H_2O$ was added to 250 mL distilled water along with 21 mL conc. HNO_3. The solution was made up to 1 L using distilled water and filtered using ash less filter paper. It was then stored in an amber bottle.

Colour Reagent
90 mL of 0.5 mol/L ferric nitrate was added to 90 mL 0.013 mol/L mercuric thiocyanate. The solution was then made up to 600 mL using distilled water.

Chapter 3: Evolution of the multi-electrode PEFT cell and DAF clarifier system

3.1 Multi-electrode PEFT cell

The poly(methyl methacrylate) outer casing of the prototype of the Multi-electrode PEFT (ME-PEFT) cell had been prepared prior to the commencement of this research. This was a major advantage as getting the prototype built can be a time taking process depending upon the availability of the material and the workload on the University workshop. All the components in the cell, however, were prepared during the course of this research. Initially, the cell was assembled and tested for leakage using tap water. It was ensured that the water sealant prepared were of diminutive thicknesses so that it does not interfere with the desired inter-electrode gap of 50 μm (thickness of cello tape used as the spacer). The sealants were positioned between the electrode and the outer covering of the cell in order to avoid leakage and short circuiting. However, preparing the sealants was a tedious procedure as the preparation stage required >24 hours for the silicon seal to form and often the retrieval of the thin sealant resulted in tearing. Eventually the seals were prepared and the cells were working without any leakage.

Initially, the cells were powered from the DC supply using stainless steel leads. The leads were coiled in order to cover a large surface area of the electrodes. The preparation stage of the coils was not easy as the stainless steel wires were 1.5 mm thick which made it very hard to bend. Moreover, the coiling process was done by hand leading to irregularities in the shape of the coils. It was also found that the coils, when placed inside the cell, did not sit evenly on the surface of the electrode due to the unevenness of the coil surface (Figure 3.1). This resulted in point contacts between the power leads and the electrode surface and thus current distribution across the electrode was not even.

Figure 3.1 Point contact between Stainless Steel leads and the electrode surface.

During the tests it was found that electrolysis was not occurring evenly over the surface of the electrodes as a result of uneven current distribution.

Table 3.1 Individual cell performance using stainless steel leads (Conductivity = 150 µS/cm at 16℃, pH = 6.90 at 20℃, natural chloride = 26 mg/L, residual chlorine = 0.40 mg/L and flow rate = 190 mL/min)

Cell	Current (A)	Voltage (V)
1	1	12.4
2	0.32	31.2
3	1	3.6
4	1	13.8

From the currents and voltages of Table 3.1 it is clear that individual cells resistances differed widely. Cells 1 and 4 require similar voltages to produce 1 A current indicating that the contact resistances between the current leads and the electrodes are similar. However, Cell 2 has lower current for a higher voltage indicating much higher contact resistances. The very low resistance of cell 3 was a result of obvious short circuiting.

In order to have an even power distribution throughout the cell a new pressing mechanism was developed. This pressing technique would ensure that the leads are in proper contact with the electrodes (Figure 3.2). The results were very similar to what was observed for cell 1 and 4 in Table 3.1 however, using this technique it was observed that stainless steel leads started to corrode over a period of time forming a resistive layer between the surface of the lead and the electrode causing an increase in cell resistance.

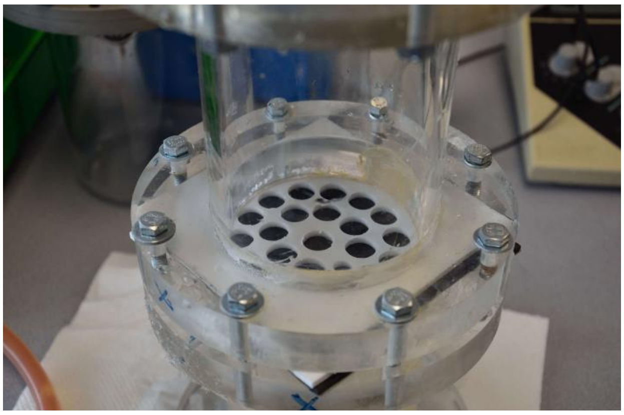

Figure 3.2 Drilled HIP sheet pressing the stainless steel leads onto the electrodes

Therefore the stainless steel leads were replaced with more corrosion resistant leads. It was also decided that the leads should be in the form of a disc rather than a coil in order to improve electrode contact and current distribution between the electrodes (Figure 3.3).

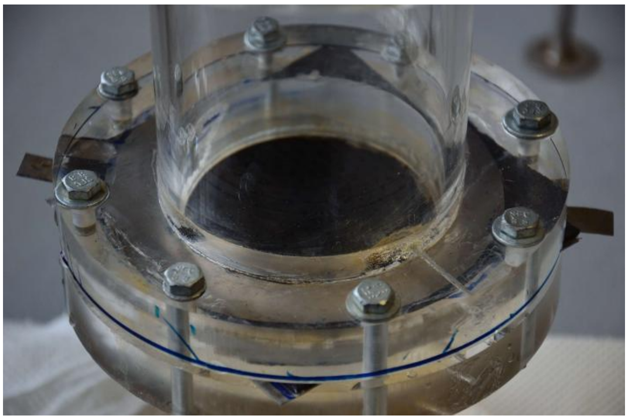

Figure 3.3 Titanium disc leads

This new contact system worked successfully. The discs were clamped between the electrodes and the outer diameter of the cell's casing (Figure 3.3) so that the discs are not in contact with the solution during electrolysis. This is required as titanium forms a resistive oxide layer if in contact with the solution during electrolysis. During the tests, it was observed that electrolysis occurred evenly over the electrode surface..

Table 3.2 Individual cell performance using titanium dics (Conductivity = 150µS/cm at 16℃, pH = 6.90 at 20℃, natural chloride = 26 mg/L, residual chlorine = 0.40mg/L and flow rate = 190 mL/min)

Cell	Current (A)	Voltage (V)
1	1	7.85
2	1	6.99
3	1	7.23
4	1	7.19

From Table 3.2 it can be seen that the current distribution is similar in all the individual cells. Even more, the cell resistance has decreased from what was observed using stainless steel leads (Table 3.1) implying that the power distribution has improved from the coiled set up.

3.2 DAF clarifier

The DAF clarifier was initially designed as shown in Figure 3.4 (a). The effluent from the cell enters the clarifier from the bottom of the column. The floc aggregating at the top of the riser column (due to electro-flotation) is removed via the sludge outlet (situated on the top of the column) whereas eluent is removed at the base of the riser column. This design did not perform well due to the positioning of the inlet and the eluent outlet which were located very close together allowing contamination of the product water by the floc suspension. Therefore the inlet position was raised to the middle of the clarifier column as shown in Figure 3.4 (b). This new design performed well as the floc rose with the top of the riser column without interfering with the retrieval of clean product water. However, at higher current densities it was found that the large gas bubbles formed during electrolysis interfered with the floc formation process. Due to these large bubbles floc removal was inefficient as the floc mixed with product waters. A third clarifier design is shown in Figure 3.4 (c). The treated water is fed into a narrow riser column which allows the floc to rise and aggregate at the top of the column. The circumference of the sludge removal outlet was reduced in order to allow removal both large gas bubbles and concentrated floc simultaneously even at high current densities.

Data for the first two clarifier designs were not recorded due to the poor/no floc removal achieved. The third clarifier design showed some promise but the large bubbles still caused problems. Further development of this design is described in Chapter 6.

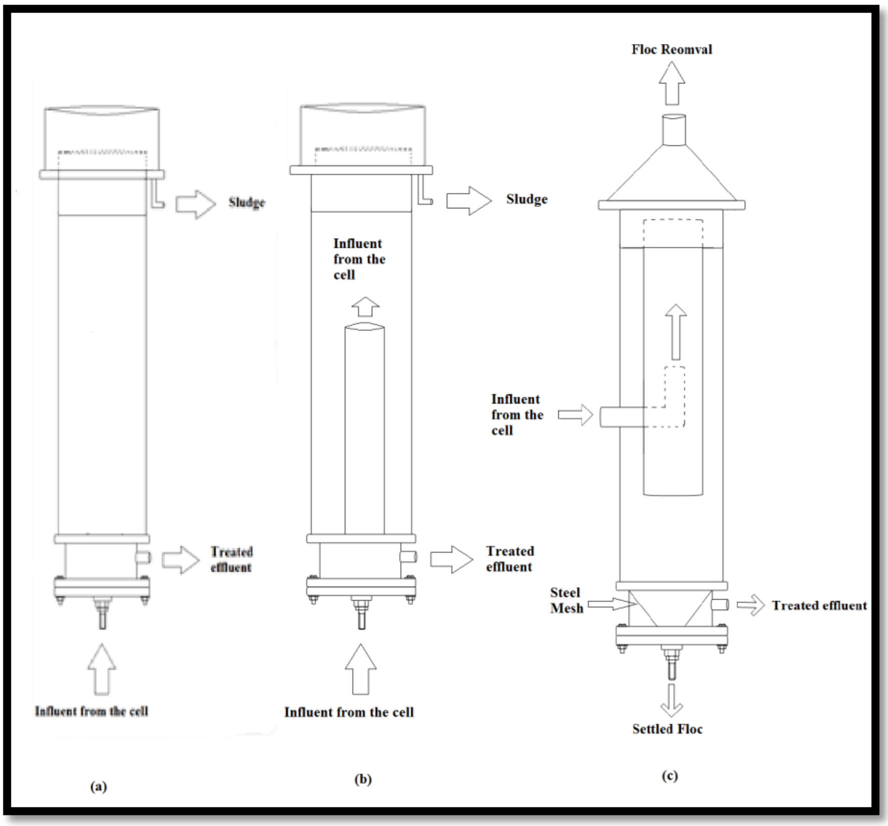

Figure 3.4 Flotation column design

Chapter 4: Multi-electrode PEFT (ME-PEFT) Cell Using Graphite Anodes

4.1 Trials of the ME-PEFT cell using synthetic bore water

4.1.1 Effect of increased number of electrode pairs.

Initial trials of the ME-PEFT cell were performed using synthetic bore water prepared by 20 mg/L Fe (see Section 2.5.1) made up with ferrous sulphate and tap water to provide the other mineral constituents likely to be present.

The synthetic bore water was passed through the ME-PEFT cell at 190 mL/min (Current density = 20 mA/cm^2, conductivity = 189.7 µS/cm at 18°C). Samples of the electrolysed water were filtered through 0.45 µm filter and analysed for Fe using ICP-MS. Data for system fitted with 1, 2, 3, and 4 electrode pairs are presented in Figure 4.1.

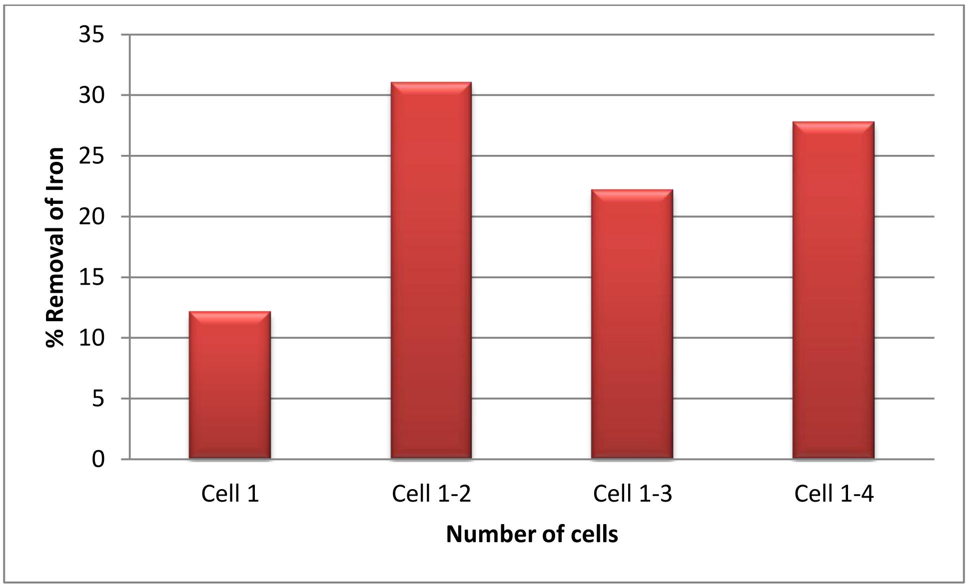

Figure 4.1 Iron removal from 20 mg/L iron solution at 1A (Flow Rate = 190 mL/min using 1, 2, 3, and 4 electrode pair of graphite anode and stainless steel cathode)

It is clear that at 1 A current, the maximum iron removal was 30% with the use of two electrode pairs. It is apparent that even without the addition of chloride, significant oxidation of the Fe was achieved. This could have been brought about either by the oxygen species formed as a result of water electrolysis and/or the chlorine produced from the chloride added to the synthetic bore water with the tap water used to prepare the solution. Tap water was found to contain 25 mg/L chloride.

While the increase in Fe removal by the two electrode pair system relative to the one pair system is easily understood, the reduced removal with three and four electrode pair is not easily explained.

4.1.2 Effect of chloride concentration and current density

A series of experiments was conducted on the 20 mg/L synthetic bore water to show the effect of NaCl concentration and current on iron oxidation and removal. Data are presented in Figure 4.2.

From Figure 4.2 it can be observed that while the cell’s efficiency did improve with increasing chloride concentration up to a chloride concentration of 225 mg/L, the effect of increasing the number of electrode pairs had if anything, a negative effect on Fe removal. With the electrode pairs connected electrically in parallel, current would be distributed between them. Thus the total passage of charge per unit volume would remain the same and so the amount of oxidation would be not affected. In order to test this possibility experiments at 2, 2.5 and 3 A and 100 mg/L chloride were conducted. However even the passage of more current per unit volume of the solution had little effect on iron removal.

One possible explanation for the contradictory result obtained from these preliminary results for the ME-PEFT cell was the sub-optimal alignment of the electrode perforations. This aspect will be considered in the next section.

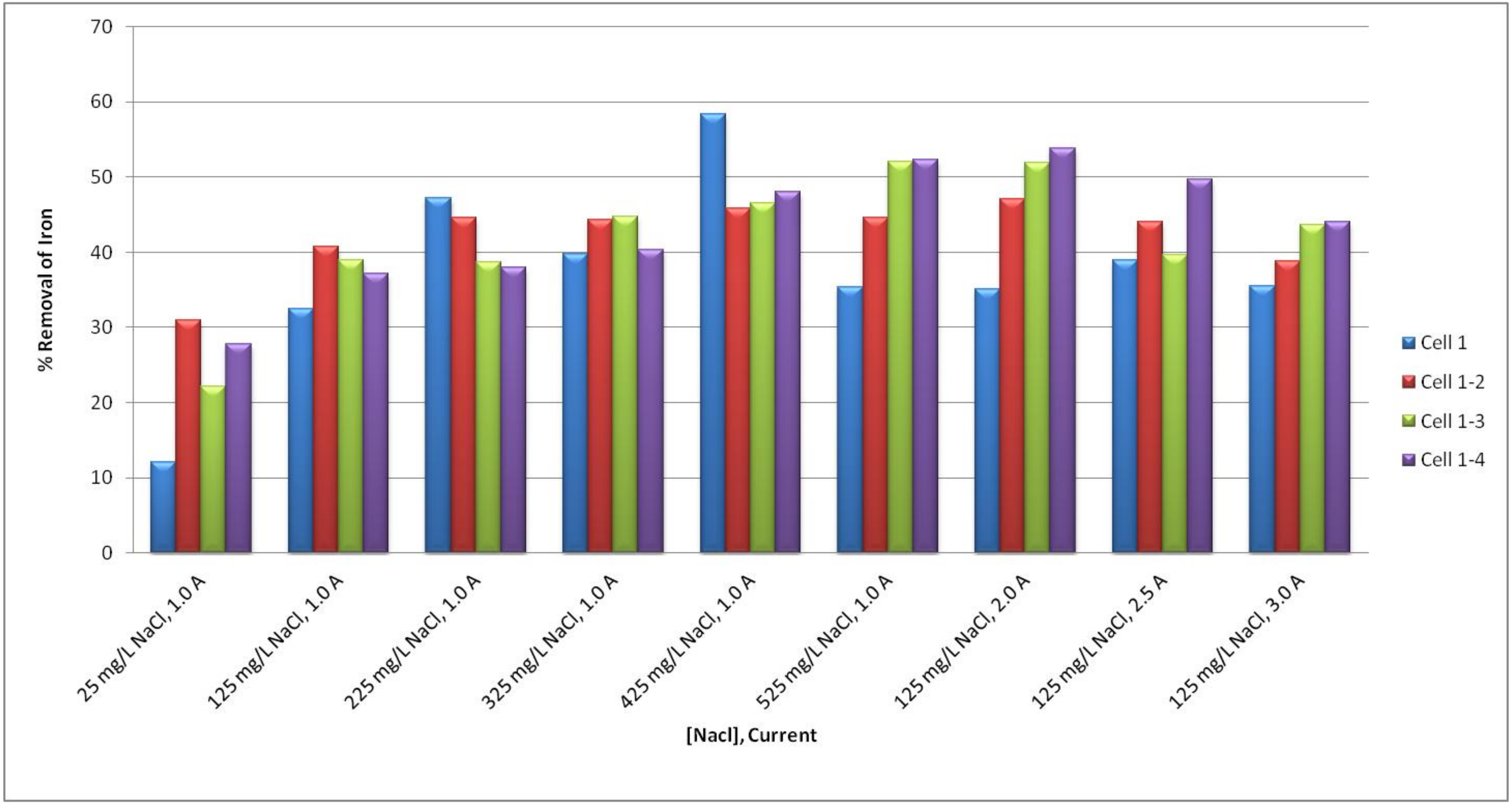

Figure 4.2 The effect of NaCl concentration and current on iron removal efficiencies (Flow Rate = 190 mL/min)

4.1.3 Effect of Perforation Configuration

Initially the electrodes were aligned with the perforations in the electrodes directly aligned. In this configuration the solution between the electrodes will tend to be stagnant and not renewed by the flow through the cell.

In order for the surfaces of the electrodes to be continuously exposed to fresh solution, it is necessary that the perforations be configured in a staggered array to ensure symmetric paths of minimum path length from the perforations of one electrode to the perforations of the other electrode. This is illustrated in figure 4.3.

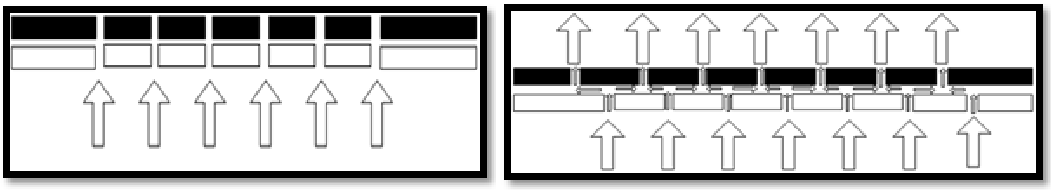

Figure 4.3 Aligned and Staggered electrode set-up

The results achieved for iron removal for one cell with a staggered perforation pattern were 69%, 56% and 63% respectively at 1 A, 2 A and 3 A. The 3 A iron removal results with staggered perforations were approximately 50% greater than for the aligned perforations (Figure 4.4). Therefore, staggered electrode configuration was used for further studies in this research.

However, Figure 4.4 also indicates that increasing the applied DC current through the staggered configuration did not improve the iron removal efficiency of the graphite anode. Quite to the contrary, the highest iron removal efficiency (≈ 70%) was achieved at the lowest current of 1 A DC. This result cannot be easily explained. Possibly at the higher voltages electrolysis of water to form oxygen is favoured with this oxygen reacting with the carbon anode rather than with the iron.

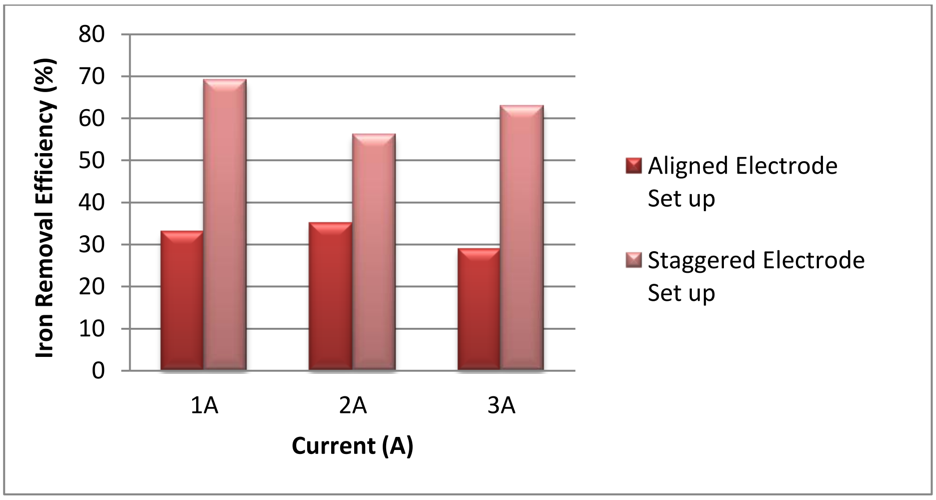

Figure 4.4 Comparison of Aligned and staggered electrode set-up for iron removal (Flow Rate = 190 mL/min)

Data for the staggered configuration for multi-electrode PEFT cells using the same synthetic bore water and 1 A current are summarised in Table 4.1. Increasing the number of electrode pairs had no effect on the iron removal. This is consistent with the iron removal requiring a given amount of charge transfer irrespective of the number of electrode pairs used.

Table 4.1 Iron Removal efficiency of ME-PEFT cell from 20 mg/L iron water (Flow rate = 190 mL/min, NaCl = 100 mg/L, current = 1 A)

Electrode Pair	Voltage (V)	Fe+2 Concentration (mg/L)		Iron Removal Efficiency (%)
		Initial	Final	
1	5.47	10.88	3.32	**69**
1-2.	4.46	9.59	3.54	**64**
1-3.	4.2	9.05	3.17	**64**
1-4.	3.75	8.52	2.47	**63**

4.2 Oxidation versus iron removal with staggered perforations.

In experiments up until this time, the % iron removal has been used as the criterion for cell efficiency. Iron removal requires two steps: oxidation and filtration through 0.45 µm filters. It is possible that less than 100 % removal was a consequence of inefficient filtration of sub 0.45 µm oxide particles rather than incomplete oxidation and colloidal hydrous oxide particle formation. Even though the electrolytically treated solutions were clear and nonturbid after 0.45 µm filtration, it was considered prudent to check that there was good correlation between iron oxidation and iron removal. In other words it was felt necessary to show that poor iron removal was a result of poor iron oxidation not poor filtration.

The oxidation efficiency of the ME-PEFT cell system for synthetic 20 mg/L iron solution containing 100 mg/L NaCl electrolysed at 1 A was determined by collecting samples of the electrolysed water immediately after passage through the cell and analysing the Fe(II) content according to the procedure described in Section 2.5.1. Data are summarised in Table 4.2.

Table 4.2 Iron oxidation efficiency of ME-PEFT cell from 20 mg/L iron water (Flow rate = 190 mL/min, NaCl = 100 mg/L, current = 1 A)

Electrode Pair	**Voltage (V)**	**Current Density (mA/cm^2)**	**Fe^{+2} Concentration (mg/L)**		**Absorbance (NTU)**	**% Fe^{+2} oxidised**
			Initial	**Final**		
1	5.47	19.90	20	6.19	0.218	**69**
1-2.	4.46	9.95	20	6.96	0.245	**65**
1-3.	4.2	6.63	20	6.96	0.245	**65**
1-4.	3.75	4.98	20	6.79	0.239	**66**

From Table 4.2 it is clear that complete oxidation of Fe(II) was not achieved and that distributing the current over an increasing number of cells had no effect. However comparison of the data (Table 4.2) with that of Table 4.1 reveals that the % of iron oxidised was essentially the same as the % removed in the previous experiment. Here again it can be noted that using multiple cells connected in parallel did not improve the efficiency of oxidation. Current densities were all very low (19.9 mA/cm, 9.95 mA/cm, 6.63 mA/cm and 4.98 mA/cm respectively) making it unlikely that lowered current density would contribute to improved current efficiency.

4.3 Effect of chloride concentration with staggered perforations

It is clear from the results of Section 4.2 that, even with the improved performance achieved with the staggered perforation, insufficient oxidation had been achieved to oxidise and precipitate all of the iron. A chloride concentration of 100 mg/L electrolysed in the ME-PEFT cell system produced insufficient chlorine to oxidise all the Fe(II) of a 20 mg/L solution to Fe(III). Even though chloride concentrations above 100 mg/L had little effect on iron removal with the aligned perforation configuration, it was considered worthwhile to see if chloride concentration was more effective with the staggered perforation configuration. Also it was considered worthwhile to see if the performances of electrode pair combinations were similar. Experiments were conducted with two single electrode pair cells with staggered perforation configuration at three chloride concentrations. Data are presented in Figure 4.5.

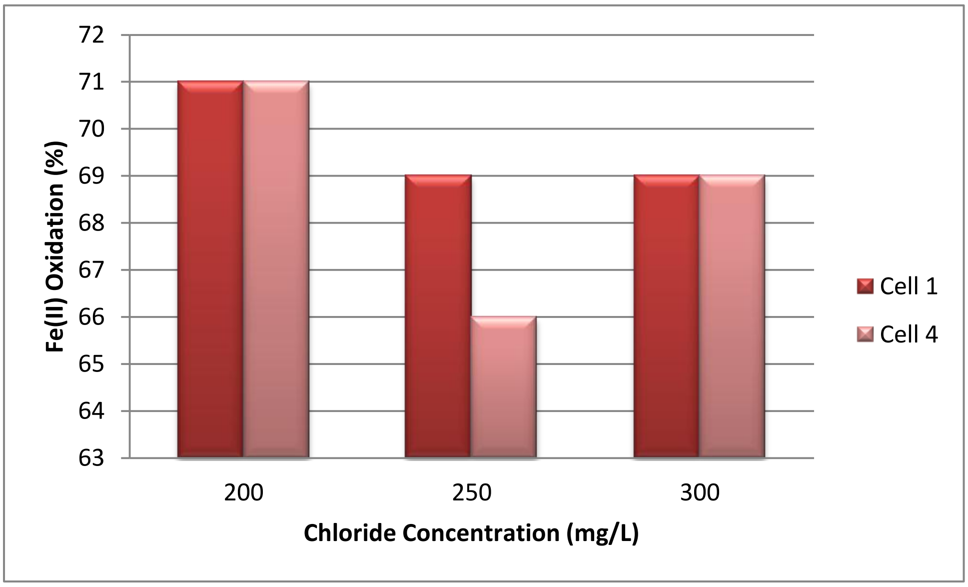

Figure 4.5 Iron (II) oxidation efficiencies of Cell 1 and Cell 4 from 20 mg/L iron solution and 2 A DC (Flow Rate = 190mL/min)

It is apparent that the two cells used performed similarly and that chloride concentration had little effect on oxidation efficiency.

4.4 Electrochemical chlorine generation using graphite anodes

It is commonly believed that electrochemical oxidation of species occurring in water proceeds through initial oxidation of chloride naturally present (or added) to chlorine. It was thus of interest whether the incomplete oxidation and removal of iron that has been observed was due to inadequate generation of chlorine or whether adequate chlorine was being produced but was ineffective in oxidising the iron under the conditions of the experiment.

Considerations of the currents used indicate that more than adequate charge was passed through the cell to bring about complete oxidation. For example when a current of 1 A is passed through a single electrode pair PEFT cell where the average residence time of the sample in the cell at a flow rate of 190 mL/min is 0.078 seconds, the amount of charge transferred will be 316 coulombs per litre or 3.27 x 10^{-3} Faradays. This should be able to oxidise 3.27 x 10^{-3} moles of Fe(II). The actual amount of iron that would have passed through the cell was calculated to be 3.21 x 10^{-5} mol. Thus a 100 fold excess of charge over that required to oxidise the iron would have been passed through the cell.

If the mechanism for iron oxidation involves initial production of chlorine, then the amount of chlorine produced will indicate the amount of iron oxidation to be expected. It was thus of interest to determine the amount of chlorine produced in the absence of any reducing agent.

A single cell consisting of graphite anode (see Figure 3. 3) was used to electrolyse a NaCl solution (Conductivity = 212 µS/cm at Temperature = 24.6℃, 100 mg/L NaCl) at a flow rate of 190 mL/min and at currents ranging from 1 to 5 A. The amount of chlorine generated was measured following the procedure described in Section 2.5.2. Results are summarised in Table 4.3.

Table 4.3 Chlorine generation by graphite anode from 100 mg/L NaCl at increasing currents (Flow rate 190 mL/min)

Current (A)	Voltage (V)	Current Density (mA/cm^2)	Cl_2 Production (mg/L)
1	8.93	19.90	**0.55**
3	15.64	59.67	**0.66**
5	20.08	99.45	**1.14**

It is clear that even at the highest current density (99.45 mA/cm) and voltage used (5 A, 20.08 V) the chlorine production (1.14 mg/L or 3.21 x 10^{-5} mol/L) is much less than what is required to oxidise the levels of iron used in the synthetic bore water trial reported above (20 mg/L or 3.61 x 10^{-4} mol/L). So even if the chloride was repeatedly re-oxidised in a series of 4 PEFT cells, insufficient chlorine would be produced to effect complete oxidation of the iron.

In order for the stoichiometric oxidation of 20 mg/L Fe by Cl_2, the graphite anode must be able to generate at least 13 mg/L chlorine as shown below.

Mr(Fe) = 55.4

$0.020\ g/L \rightarrow 0.020 / 55.4 = 3.61 \times 10^{-4}\ mol/L$

Mr(Cl) = 35.5

$3.61 \times 10^{-4} \times 35.5 \rightarrow 0.0128\ g/L = 13\ mg/L$

4.5 Trials with bore water

Up until this stage of the work, all tests were conducted using synthetic solution containing 20 mg/L ferrous ion with known concentrations of NaCl. Even though iron removal from this water was less than desirable it was considered to be useful to get some data for the performance of the staggered perforation ME-PEFT system on a real iron containing bore water. Bore water is known to contain ferrous ion, concentrations ranging from 20 – 25 mg/L, along with various other inorganic and organic constituents that can affect oxidation and coagulation processes. In order to be able to make comparison with the synthetic iron water results of figure 4.5, 250 mg/L NaCl was added (Conductivity = 255 µS/cm at 17.5 ℃). Data are given in Figure 4.6 in which PEFT cell oxidation at two applied currents is compared with natural air oxidation for a sample passed through the cell without any current.

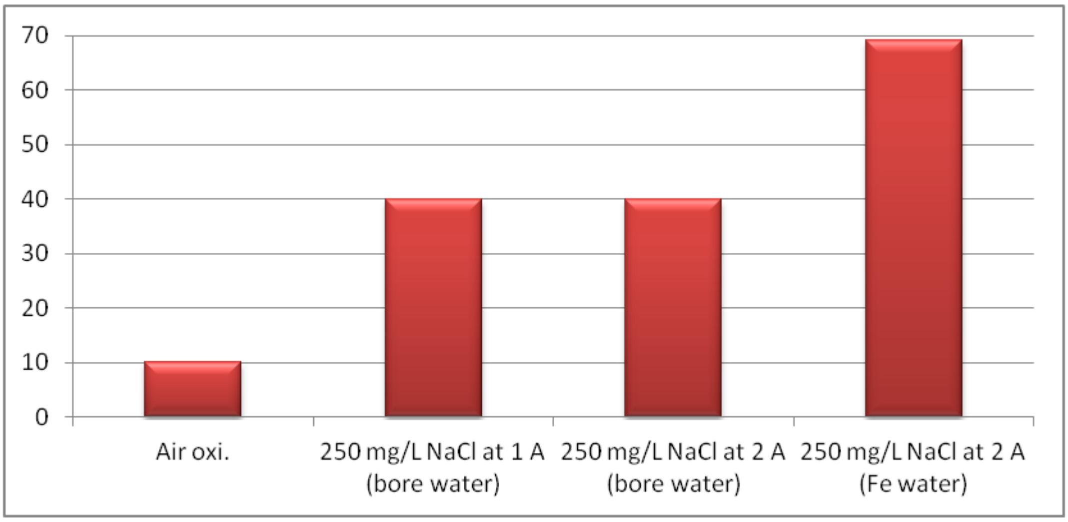

Figure 4.6 Comparison of iron oxidised by air, electro-oxidation of bore water (at 1 A and 2 A) and electro-oxidation of synthetic bore water (flow rate 190 mL/min) using a single PEFT cell

Figure 4.6 shows that bore water was only 40% oxidised, irrespective of current, whereas synthetic water of similar iron content was 69% oxidised under the same conditions.

4.6 Conclusion

From the evidence provided by the present findings, stacking four cells connected in parallel did not achieve complete oxidation of Fe(II) in bore water even with the addition of 250 mg/L NaCl when graphite was used as the anode material. The graphite anodes did not produce nearly enough chlorine to oxidise the iron.

Thus while Nath was able to achieve 100% oxidation with graphite electrodes in a single pass through the PEFT cell, he used much higher chloride dosages (≈ 1-3 g/L) and higher current densities (78.6 mA/cm) (Nath 2011). These conditions are not compatible with the treatment of domestic farm water supplies. Moreover, increasing the chloride concentration will result in the formation of residual chlorine in the treated bore water (which is not used up during electrolysis) leading to the formation of chlorinated organics (Bull et al. 1995; Hsu et al. 2001) which could be carcinogenic.

It was clear from the results of this chapter that a more electrically efficient anode material would be necessary to achieve the objective of single pass removal of iron from bore water from the chloride concentrations available.

Chapter 5: Multi-electrode system using dimensionally stabilised titanium anodes (DSAs)

In Chapter 4, it was shown that even with the use of multi-electrode PEFT cells the maximum amount of oxidation in a synthetic iron water system was approximately 66% and with bore water the oxidation and removal for the same initial concentration was significantly less. Increasing the number of cells, the chloride concentration or the current density had little effect on this amount of oxidation. It is believed that the generation of chlorine is an essential step in the oxidation process and that at least 1 mole of HOCl is required to oxidise 1 mole of Fe(II). Apparently, in order to improve the oxidation of Fe(II) it is necessary to produce more chlorine. In this chapter the production of chlorine has been studied with the aim of ensuring sufficient chlorine would be available to oxidise all the Fe(II).

It is well known in the water treatment industry that titanium electrodes generate much more chlorine than graphite electrodes particularly at low chloride levels. However, during electrolysis titanium generates an oxide layer (titanium oxide layer) and hence it cannot be directly used as an anodic material. Titanium when coated with ruthenium oxide layer forms the dimensionally stabilized anodes (DSAs) and they are widely used in water treatment industry as electro chlorinators.

5.1 Laboratory preparation of Ruthenium stabilised DSAs

The dimensionally stabilised titanium anodes were prepared by first electrodepositing of a ruthenium layer onto a sheet of commercial 99.2% titanium (Grade 2) metal following the procedure of Zheng et al., 2008 using an acidic solution of ruthenium chloride. Prior to electro-deposition, the titanium electrodes were mechanically polished using silicon carbide grit 600 powder and diamond compound paste. The electrodes were then placed in an acetone ultrasonic bath (for 30 minutes) to remove any contaminants remaining followed by a degreasing step (using soap and water). Oxide layers were removed by etching using oxalic acid (HO_2COO_2H) at 90℃ for 1.5 hours. The electrodes were then cleaned (using double distilled water) and placed in the plating solution. Electrodeposition was carried out at room temperature in a plating solution comprising of 5 mM $RuCl_3.3H_2O$, 0.01 mol/L HCl, and 0.1 mol/L KCl at a constant pH value of 2.

$RuO_2 \cdot nH_2O$ film was coated on the pre-treated titanium electrodes using a cathodic deposition technique. Electro-deposition was carried out at 25 mA cm^{-2} (for 8 minutes) using pre-treated titanium electrode as the cathode and platinum gauze as the anode. After deposition the ruthenium film was converted to the oxide by heating to 150 ℃ for 2 hours (Zheng et al. 2008).

5.2 Electrochemical chlorine generation using laboratory prepared DSAs

Data for electrochemical chlorine production from sodium chloride solutions ranging from 10 to 50 mg/L chloride and currents ranging from 1 to 3 A are given in Table 5.2.

Table 5.1 Chlorine generation by laboratory prepared DSAs at different chloride and current values (Flow rate = 190 mL/min and pH = 5 at 20℃)

[NaCl] = 10 mg/L and conductivity = 36µS/cm at 20℃

Current (A)	Voltage (V)	Cl_2 Production (mg/L)
1	7.20	**1.5**
2	13.60	**4.2**
3	21.15	**7.2**

[NaCl] = 20 mg/L and conductivity = 51µS/cm at 20℃

Current (A)	Voltage (V)	Cl_2 Production (mg/L)
1	6.60	**2.3**
2	11.60	**5.5**
3	16.40	**9.8**

[NaCl] = 50 mg/L and conductivity = 118µS/cm at 20℃

Current (A)	Voltage (V)	Cl_2 Production (mg/L)
1	4.10	**4.1**
2	6.20	**10.2**
3	8.50	**18.4**

At an influent concentration of just 10 mg/L chloride (working at 3 A DC) the free chlorine generated was 7.20 mg/L. This is a dramatic improvement in chlorine production compared with the 0.66 mg/L produced using a graphite anode at the same current but using the higher chloride concentration of 100 mg/L. Thus DSAs were used as the anodes in the remainder of this thesis.

A major issue encountered with laboratory prepared DSAs was the degradation of ruthenium oxide layer after prolonged use. Loss of the ruthenium oxide layer exposed the titanium metal which was rapidly oxidised to form an insulating coating. The instability of the ruthenium coating was probably due to insufficient annealing of the electrodes before use. Fortunately a source of commercial titanium sheet coated with ruthenium oxide and iridium oxide was located and this material was used for all subsequent studies. Iridium oxide protects the ruthenium oxide layer from degrading during electrolysis and extends the service life for several years (Duby 1993).

5.3 Electrochemical chlorine generation using commercial DSAs

Data for chlorine generated using the commercial anode material at different chloride dosages and current densities are depicted in Figure 5.1. From the figure it can be observed that chlorine generation is twenty six times greater than what was observed for graphite anodes (see Table 4.3) at the same flow rate (190 mL/min), influent NaCl concentration (100 mg/L, conductivity = 212 µS/cm at 24.6°C) and operating current (3 A).

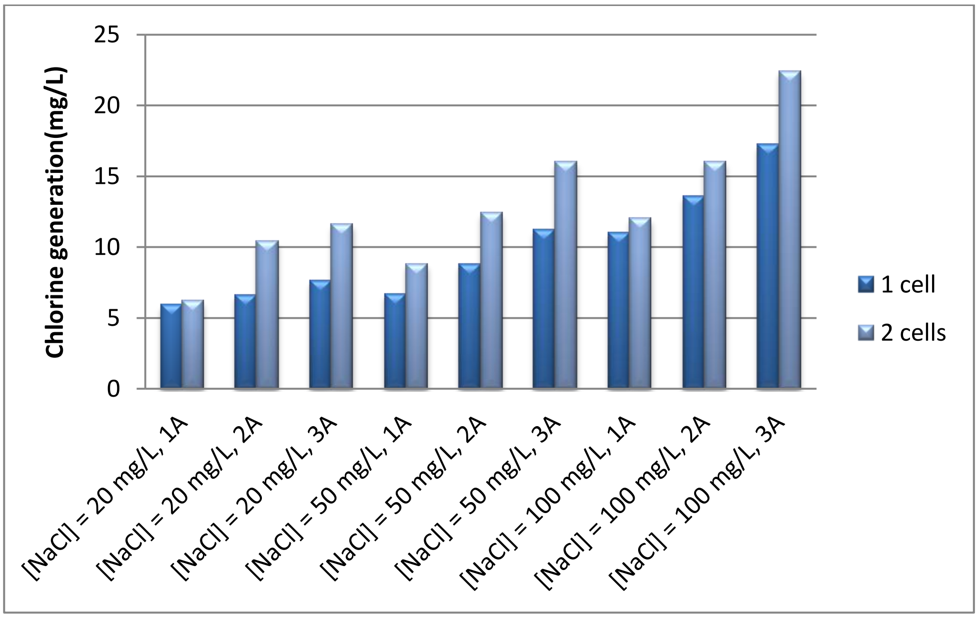

Figure 5.1 Electro chlorination at varying chloride dosages and increasing current (flow rate = 190 mL/min, commercial DSA material)

Furthermore there are much more pronounced effects of chloride concentration and the increased number of electrode pairs from one to two.

It has been previously reasoned that in order to oxidise the ferrous ions (concentrations ranging from 20 - 25 mg/L) present in bore water, 13-16 mg/L of chlorine will be required unless there are other oxidising species formed. However, with a ME-PEFT system, it might be possible to achieve complete oxidation at lower chloride levels because the chloride oxidised to chlorine which is then reduced back to chloride as it oxidises the iron in the first compartment, can be re-oxidised to chlorine in the subsequent compartment(s).

5.4 Rapid oxidation of Fe(II) in bore water using DSAs

5.3.1 Single Cell Electrolysis

In order to determine how much Fe(II) could be oxidized in a single pass through the cell, an experiment was performed in which bore water was passed through the cell at a flow rate of 190 mL/min and treated with varying currents. The natural groundwater had a conductivity of 266 µS/cm at 15.8℃ (containing 7 mg/L natural chloride – estimated by the procedure described in Section 2.5.3).

Data are presented in Table 5.2 and show that almost complete instantaneous oxidation (99%) was achieved at 9 A and 16.09 V.

Table 5. 2 Electro-oxidation of iron in groundwater containing 7 mg/L natural chloride at flow rate of 190 ml/min (Conductivity = 266 µS/cm at 15.8℃)

Electrode Pair	Current (A)	Current Density (mA/cm^2)	Voltage (V)	Fe^{+2} Concentration (mg/L)		% Fe^{+2} Oxidised	Power Consumption (kWh/m^3)
				Initial	Final		
1	0	0	-	21.52	21.52	**0**	**0**
1	1	19.9	4.49	21.52	11.67	**46**	**0.39**
1	2	39.8	5.75	21.52	7.98	**63**	**1.01**
1	3	59.7	7.34	21.52	4.57	**79**	**1.93**
1	4	79.6	9.21	21.52	3.21	**85**	**3.23**
1	5	99.5	10.58	21.52	3.07	**86**	**4.64**
1	6	119.4	11.56	21.52	2.5	**88**	**6.08**
1	7	139.3	13.51	21.52	1.39	**94**	**8.29**
1	8	159.2	14.95	21.52	0.85	**96**	**10.49**
1	9	179.1	16.09	21.52	0.28	**99**	**12.70**

From Table 5.2 it can be observed that with increasing current, an increase in the oxidation efficiency was achieved without the addition of NaCl. At currents as low as 2 A, the DSAs successfully oxidized 63% of Fe(II) from bore water without the addition of salt whereas using graphite anode and with the addition of 250 mg/L NaCl, just 40% of the iron was oxidized (Figure 4.6). Assuming stoichiometric oxidation of the Fe by the $Cl_{2,}$ oxididation of 100% of the 25 mg/L Fe(II) in a single pass would require a minimum of 16 mg/L of $Cl_{2.}$ Even if all the chloride was oxidized, a minimum chloride concentration of 20 mg/L would be required. It is clear that oxidizing agents other than chlorine are contributing to the oxidation. These could be the oxygen produced by the electrolysis of water or the transient reactive oxygen species (ROSs) which may be formed during electrolysis of water (Fiessinger et al. 1981; Kerwick et al. 2005) or, less likely, be the result of direct oxidation of the metals at the electrode surface (Chiang et al. 1995).

5.3.2 Multiple Cell Electrolysis

In order to determine whether power consumption and thus costs could be reduced by including more cells, an experiment was performed with a two electrode pair ME-PEFT cell connected in such a way that water flow was in series but were electrically connected in parallel.

Data are summarized in Table 5.3. Electro-oxidation of natural groundwater with a conductivity of 266 µS/cm at 15.8℃ and containing 7 mg/L natural chloride achieved 100% immediate iron oxidation at 5 A and 8.57 V using a two electrode pair ME-PEFT cell.

Table 5.3 Electro-oxidation of iron in groundwater at flow rate of 190 mL/min

Electrode pairs	**Current (A)**	**Current Density (mA/cm^2)**	**Voltage (V)**	**Fe^{+2} Concentration (mg/L)**		**% Fe^{+2} Oxidised**	**Power Consumption (kWh/m^3)**
				Initial	**Final**		
2	0	0	0	22.20	22.20	**0**	**0**
2	1	39.8	4.19	22.20	12.07	**46**	**0.37**
2	2	79.6	5.55	22.20	5.91	**73**	**0.97**
2	3	119.4	6.53	22.20	2.50	**89**	**1.72**
2	4	159.2	7.28	22.20	0.99	**96**	**2.55**
2	5	199.0	8.57	22.20	0.14	**99**	**3.76**

It is clear that reduced voltage and less current and thus less power were required when two cells electrically connected in parallel were used. The reduced resistance of the parallel connection contributes to lowered voltage requirement and increased current efficiency which is consistent with improved current efficiency that can be obtained from reducing current density (from 99.6 mA/cm to 49.8 mA/cm) (Nath 2011).

An indicative estimate of the effect of flow rate on current efficiency was determined by doubling the flow rate while maintaining the current at 5 A. The % oxidation decreased to 87%, similar to the value obtained for a flow rate of 190 mL/min for which a current of 3 amps was required. In other words a roughly equivalent amount of oxidation at the lower flow rate was achieved by passing 0.94 coulombs per mL but 1.07 coulombs per mL were required at the higher flow rate.

5.5 Metal ion removal

Samples of the electrolysed bore water (from Sections 5.3.1 and 5.3.2) were filtered through 0.45 µm filter and analysed for Fe and Mn using ICP-MS. Data for the metal ions remaining after filtration for a single and two electrode pair ME-PEFT cell at different currents are shown in Figure 5.2.

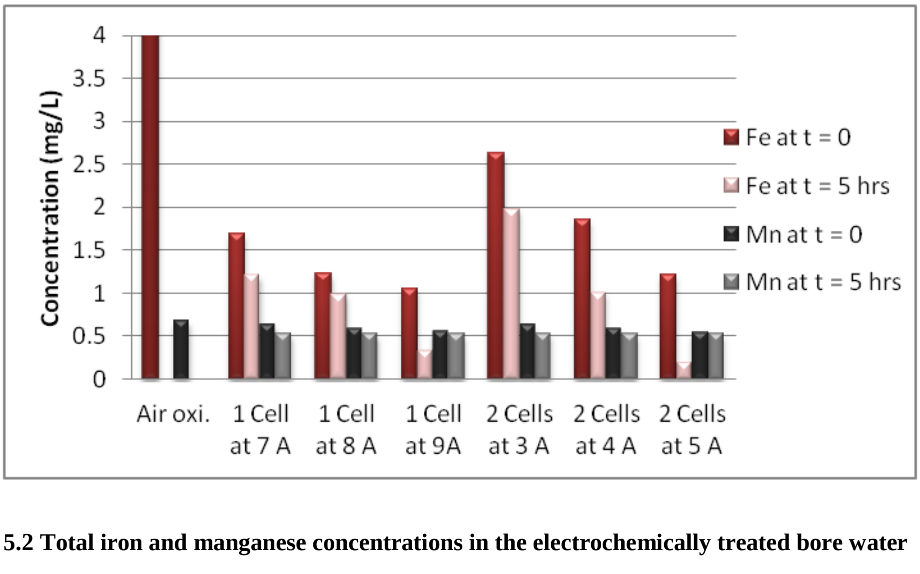

Figure 5.2 Total iron and manganese concentrations in the electrochemically treated bore water (measured directly after electrolysis and at t = 5 hours)

From the figure it can be seen that iron concentration was brought down to 0.198 mg/L by the two electrode pair ME-PEFT cell when operating at 5 A and 8.57 V after 5 hours settling time. This value falls within the New Zealand drinking water standards which require the iron concentration to be below 0.2 mg/L (Ministry of Health 2005).

The ME-PEFT cell was found to be effective in achieving rapid oxidation and removal of iron. However it was less effective in manganese removal. The manganese concentrations remained almost the same and increasing current and settling time had very little effect.

5.6 Summary

In this chapter it has been shown that DSAs perform much better in both chlorine production and Fe(II) oxidation than graphite anodes. A single electrode pair PEFT cell was able to achieve 99% oxidation at a power consumption of 12.70 kWh/m^3 whereas 100% oxidation was achieved at nearly 1/4th of the power consumption (3.76 kWh/m^3) when two electrode pair PEFT cells were used. The oxidized iron settled rapidly such that after five hours all the oxidized iron had settled. The amount of Fe(II) oxidized was much greater than what could have been achieved if all the chloride present had been oxidized to chlorine. It was thus concluded that oxygen species produced during the electrolysis must also have contributed to the oxidation.

Chapter 6: Clarification of oxidised bore water

Trials using DSAs in the ME-PEFT cell have shown that complete oxidation of the Fe(II) of bore water can be achieved with a two electrode pair ME-PEFT cell at 5 A and 8.57 V (Flow rate = 190 mL/min, conductivity = 266 µS/cm at 15.8℃ and natural chloride = 7 mg/L)

The oxidised iron formed a reddish brown suspension that settled completely in 5 hours. This chapter reports on work towards the ultimate aim of treated the water to achieve instantaneous iron removal.

6.1 Settling characteristics of oxidized bore water

Tests were conducted on the coagulation and settling of the treated bore water samples in which the settling of the Fe was followed by measuring turbidity as a function of time.

Bore water (≈ 20 mg/L Fe) was electrically oxidised following the procedure described in Sections 5.3.1 and 5.3.2.

6.1.1 Oxidation of bore water with a single electrode pair PEFT cell

In an initial experiment, using a single electrode pair PEFT cell and varying current densities, oxidised bore waters were produced in which 46 to 99 % of the Fe(II) was oxidised (Figure 6.1). A sample of the water was transferred to a 1 L measuring cylinder and turbidity measurements were taken at 30 minute and then 60 minute intervals for samples withdrawn from the top of the cylinder.

Data are presented in figure 6.1. It can be seen that the lowest value (2 NTU) at 9 A was achieved after 5 hours settling time. The final turbidity is consistent with incomplete oxidation of Fe(II) to Fe(III) using a single electrode pair cell. However the effectiveness of the electro-oxidation relative to air oxidation is clear from the difference in the settling curves for air oxidation relative to those for which varying current densities were used. The increasing turbidity of the air oxidized Fe showing no tendency to settle, illustrates the nature of the problem caused by the formation of stable colloidal suspensions in these systems.

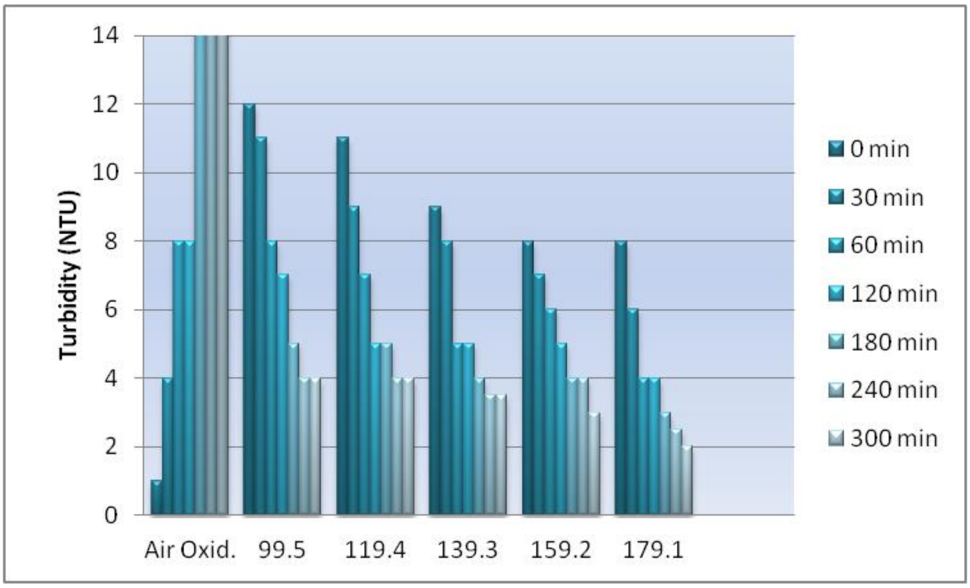

Figure 6.1 Gravity settling of oxidised bore water (Single cell at 190 mL/min, conductivity = 266 µS/cm at 15.8℃)

6.1.2 Oxidation with a two electrode pair PEFT cell

Because the electro-oxidized Fe took 5 hours to settle completely, the experiment was repeated with a two electrode pair device. Data are given in Figure 6.2. Even though complete oxidation of Fe(II) was achieved using two electrode pairs, full clarification was slow with the lowest turbidity measurement of 1.5 NTU being obtained after 5 hours. This is higher than the drinking water turbidity threshold (<1 NTU) (Figure 6. 2) (DWSNZ 2008).

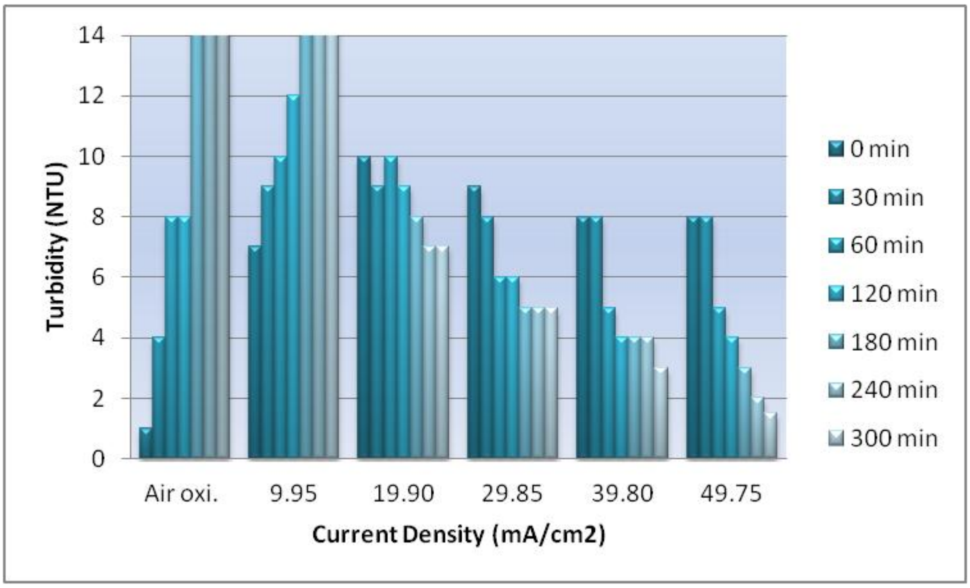

Figure 6.2 Gravity settling of oxidised bore water. (Double cell at 190 mL/min, conductivity = 266 µS/cm at 15.8℃)

6.1.3 The effect of chloride concentration on settling after oxidation of bore with a two electrode pair PEFT cell

When using the two electrode pair ME-PEFT cell system, while the Fe(II) was completely oxidised to Fe(III), settling was incomplete after 5 hours. It was considered possible that the settling rate might be increased by increasing the level of chlorine present to make the oxidation of the iron more rapid and also oxidise organic species present in the water that could stabilise the iron colloids formed. Sodium chloride was added to bore water to provide NaCl concentrations ranging from 7 to 757 mg/L. the bore water was then electrolysed as described in Section 6.1.1.

Data presented in Figure 6.3 show that the chloride ion concentration had little effect on settling. Added to this, 28 – 60 mg/L residual chlorine was generated at higher chloride concentrations. However, there did appear to be a continuing trend toward lower turbidities after extended settling time for the higher chloride concentrations resulting in turbidity below 0.5 NTU upon standing for 48 hours for the highest chloride concentration.

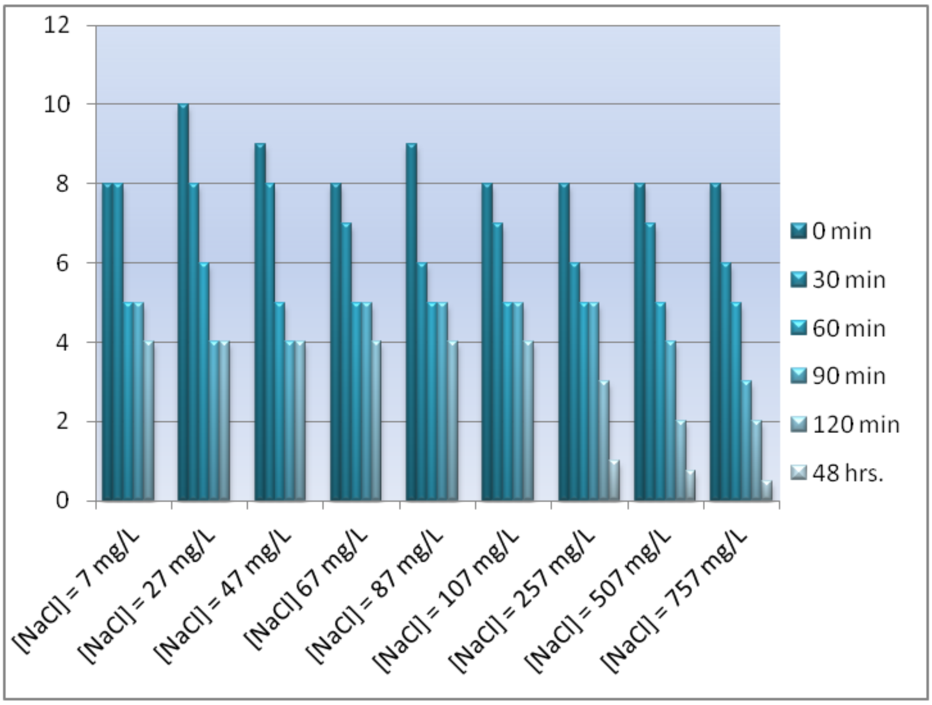

Figure 6.3 Oxidation and settling of synthetic iron water at different chloride concentrations (Two electrode pair ME-PEFT cell at 190 mL/min)

6.1.4 Oxidation and settling of a synthetic iron water

In order to determine whether there are species present in bore water that inhibit the rapid settling of the oxidised and precipitated Fe, an experiment was performed using synthetic bore water prepared from a solution of iron sulphate with and without the addition of sodium bicarbonate for pH control.

By treating a synthetic solution consisting 20 mg/L Fe(II) and 20 mg/L NaCl at 5 A (flow rate = 190 mL/min) it was found that the pH dropped from 5.5 to 3.0 after electrolysis. This was expected as the hydrolysis of Fe(III) formed during electrolysis can release up to 3 protons per Fe(III) into the solution causing the pH to fall. Low pHs are known to stabilise iron oxide colloids through acquisition of positive charge by the particles. Therefore, while complete oxidation was achieved, settling was incomplete. In order to have instantaneous precipitation the pH should be maintained between 6 and 8. This was achieved by adding sodium bicarbonate. Groundwater is known to contain elevated levels of bicarbonates which act to buffer the water against pH changes.

It was found that in the presence of sodium bicarbonate the synthetic iron solution rapidly oxidised in air alone. Purging to strip out dissolved oxygen was necessary to ensure that the oxidation was achieved electrochemically. Under these conditions, the synthetic iron water, buffered with sodium bicarbonate and containing only 0.92 mg/L of dissolved oxygen, both rapidly oxidised and flocculated when treated electrochemically. However the flocs formed, while appeariung more aggregated, did not settle any more rapidly than the oxidised and precipitated Fe of bore water samples (see Table 6.1).

Table 6.1 Oxidation and settling of a synthetic iron water (20 mg/L Fe(II) and 20 mg/L NaCl. (At 5A, 5.84 V, Flow rate = 190 mL/min, pH = 7.30 at 20℃, Conductivity = 463 µS/cm at 24℃)

Electrode Pairs	Time (min)	Turbidity (NTU)	
		Without filtration	With Filtration
2	0	12	1
2	30	11	0
2	60	8	0
2	90	7	0
2	120	6	0

The low turbidity results summarised in Table 6.1 also show that 100% removal of Fe is achieved when the oxidised solution was filtered through a 0.45 µm filter, indicating that the particle size of the oxidised iron is greater than 0.45 µm. The fact that the particles are relatively large but do not settle, points to the possibility that they might be removed by flotation. The fact that fine bubbles of hydrogen and oxygen resulting from electrolysis of water were invariably present in electro-oxidation experiments, enhances the attractiveness of developing a dissolved air flotation (DAF) type process to remove the oxidised iron.

6.2 Development of a DAF apparatus for oxidised bore water clarification

During electrolysis it was observed that large gas bubbles were formed at high currents. These bubbles disturbed the floc blanket at the top of the column of the ME-PEFT cell and the three DAF clarifiers described in Section 3.2 making it impossible to retrieve iron free treated water.

6.2.1 Preliminary design

In order to effectively remove iron precipitates with electro-flotation it is important to prevent large gas bubbles from entering the electro-flotation column. DAF design (c) was modified to allow venting of the large gas bubbles from the oxidised solution as it exited the ME-PEFT cell (Figure 6.4).

While the system efficiently removed the large gas bubbles prior to the DAF riser column, floc formation was not as expected. This was due to the fact that along with the large gas bubbles most of the fine bubbles also escaped through the vent leaving insufficient bubbles to adequately raise the floc. Turbidity measurements taken from the bottom of the flotation column indicated that over a period of 10 minutes, the turbidity was reduced from 12 to between 6 and 8 NTU (20 mg/L Fe(II) and 20 mg/L NaCl, electrolysed at 5A, 5.74 V, Flow rate = 190 mL/min, pH = 7.22 at 20°C, Conductivity = 470 µS/cm at 26°C).

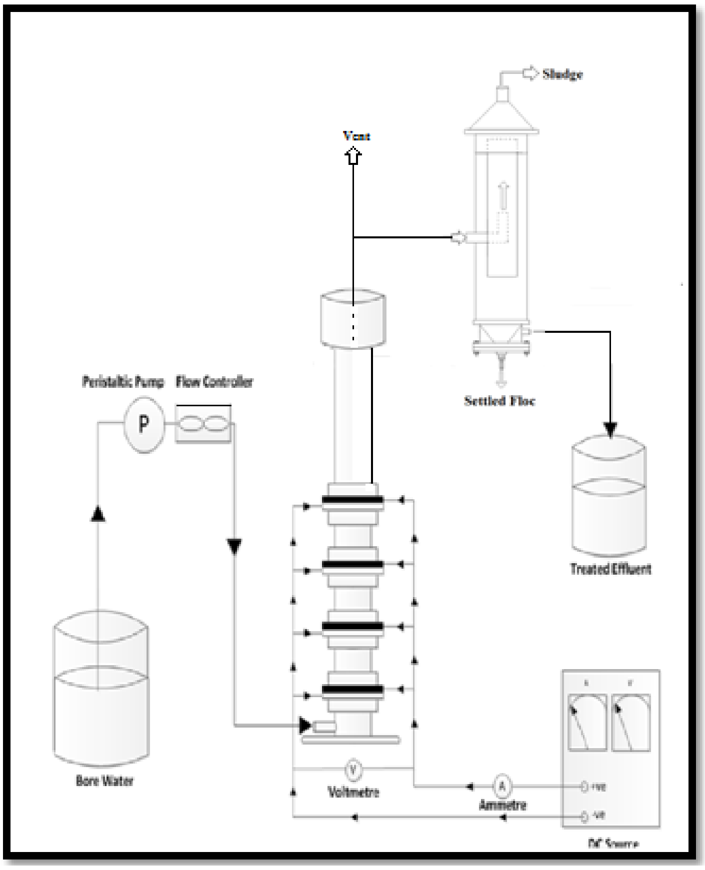

Figure 6.4 Preliminary DAF system

6.2.2 Pressurised DAF system

The results obtained from the system described above, while promising, were still less than satisfactory because fine bubble concentration was too low and some large bubbles escaped past the venting system. The system was redesigned to allow pressurisation of the water/gas system within the PEFT cell in order to supersaturate the water with the electrolytically produced gas. The system is shown in Figure 6.5.

Pressurising the oxidised effluent to 100 kPa resulted in the elimination of the large gas bubbles. The effluent entering the riser column was milky, indicative of the presence of very fine gas bubbles. It was also observed that a layer of clear and largely colourless solution was formed at the bottom of the riser column as the bubbles rose.

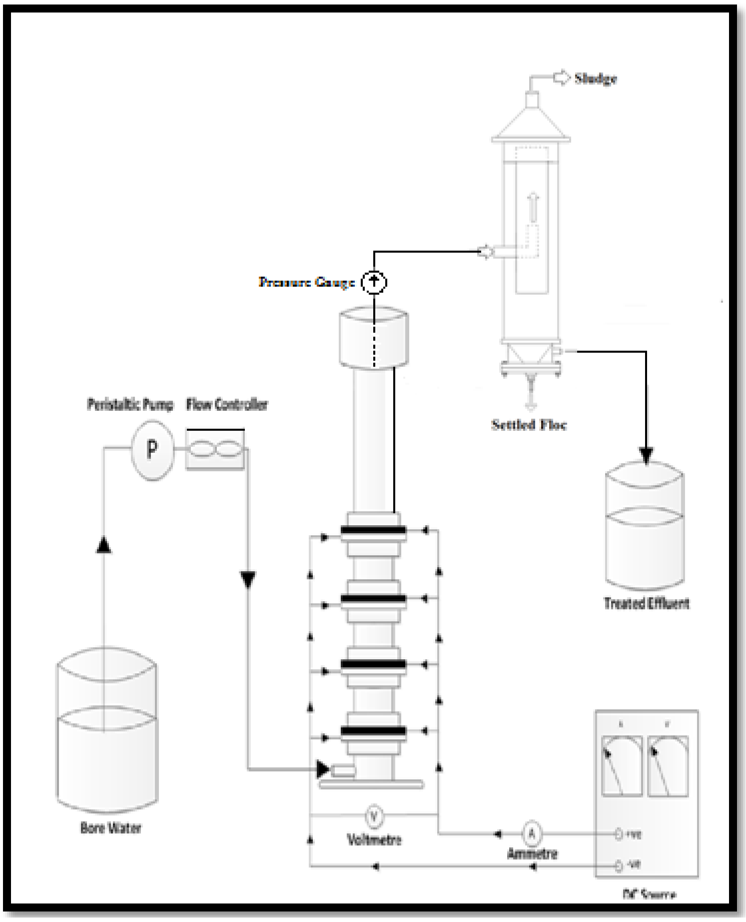

Figure 6.5 Pressurised DAF system

Unfortunately a region of turbulence formed at the top and bottom of the riser column as the oxidised effluent reached the top of the column. This caused mixing of the floc with the clarified solution. Thus while the turbidity reduction was greater than for the preliminary design, 12 NTU reduced to 5 NTU, it was still not able to achieve adequate floc removal.

6.2.3 Modified Pressurised DAF System

The initial observations of the pressurised DAF system indicated that oxidised iron can be effectively removed with further modification to the electro-flotation column. Turbulence can be minimised having the inner tube sealed at the bottom and extending it closer to the floc outlet. This set-up would force the floc to rise inside the riser column and, due to an increased width, the rising floc will not mix with the solution as it exits the flotation stage. Efficient removal through the outlet would be then possible (Figure 6.6). This system, although very promising, was not tested because construction of the modified design had not been completed.

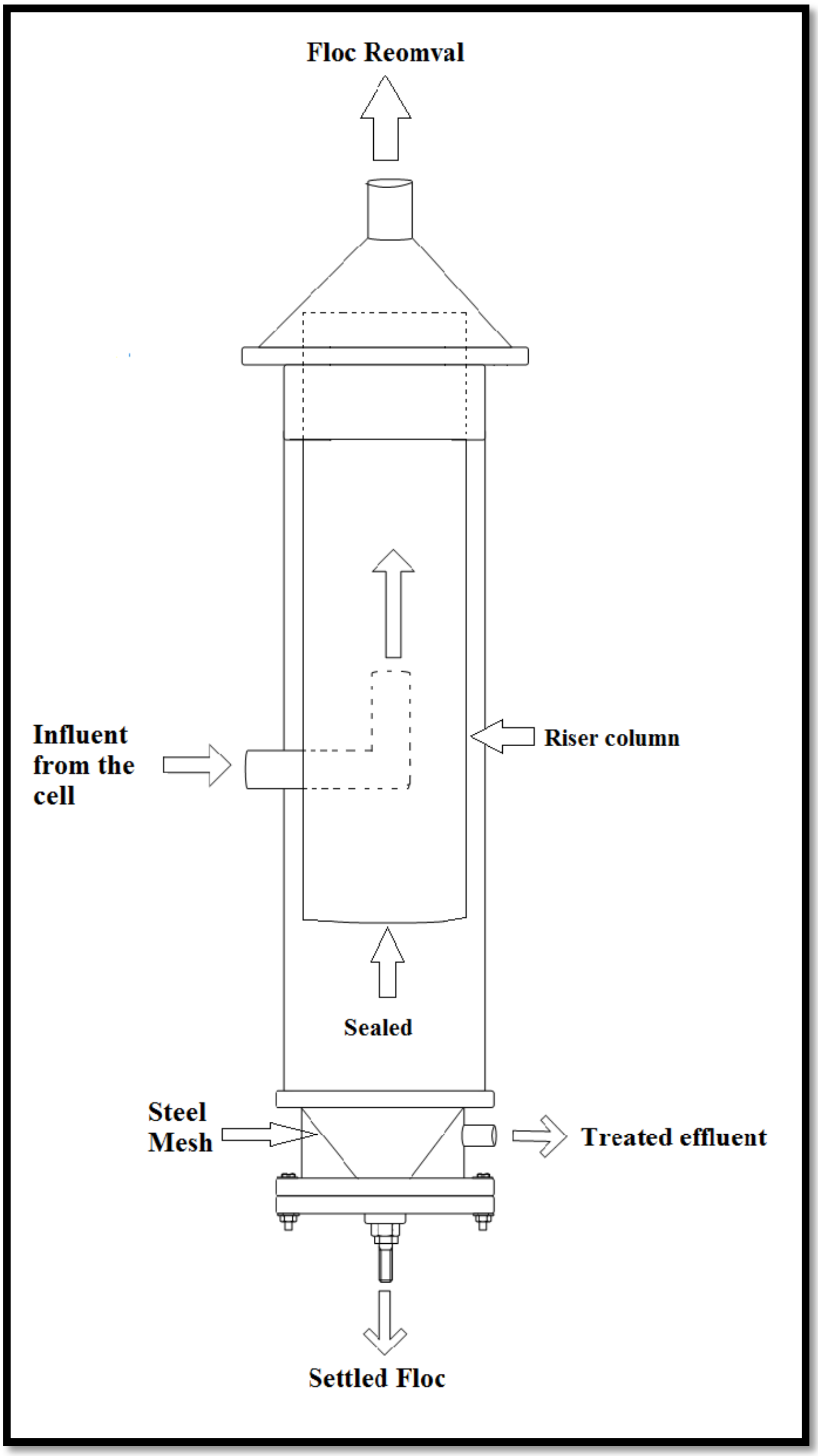

Figure 6.6 Modified electro-flotation column

Chapter 7: Summary and Conclusion

7.1 The importance of rapid oxidation of iron and manganese

Waikato groundwaters are known to contained elevated levels of iron and manganese and are often accompanied by silica and organic matter. Air oxidation and hydrolysis leads to the formation of hydrous oxide. Often the hydrous oxide particles form stable colloidal suspensions in the presence of silica and/or organic material. It is believed that the particles acquire a net negative charge stabilizing them from further aggregation (see Figure 1.5). However, under rapid oxidation the hydrous oxide particles instantaneously aggregate and flocs form before particle surfaces become protected (presumably by negatively charge) allowing the oxidised metal to settle over time.

The ME-PEFT cell was found to be effective in achieving rapid oxidation and removal of iron but less effective in manganese oxidation and removal. The poor manganese removal efficiency of the ME-PEFT cell is consistent with the greater magnitude of the manganese reduction potential ($E^0(Fe^{3+}/Fe^{2+}) = +0.77$ V, $E^0(MnO_2/Mn^{2+}) = +1.23$ V) (Rosen 2001) (Figure 5.2). The oxidation of Fe(II) could be expected to occur before the oxidation of Mn(II).

7.2 Importance of the electrode material

Low cost graphite anodes generated very low amounts of chlorine even at high chloride dosages and current inputs. The maximum iron removal achieved from a 20 mg/L iron solution (containing 100 mg/L NaCl operating at 1 A and 190 mL/min) was 69%. This was achieved by a single electrode pair PEFT cell and increasing the number of electrode pairs did not increase the amount of iron removed. Identical observations were made for the % iron oxidised.

Replacing graphite with dimensionally stabilised titanium anodes improved the current efficiency of the ME-PEFT cell several-fold. A single titanium electrode pair cell generated more chlorine from the available chloride and chlorine generation increased when the number of electrode pair connected electrically in parallel was increased. Because the current density was less, the current efficiency was increased. The current efficiency improved from 4% (for 99% iron oxidation with a single electrode pair PEFT cell at 12.70 kWh/m^3) to 7.5% for 100% iron oxidation with a dual electrode pair PEFT cell (at 3.76 kWh/m^3).

7.3 Oxidised iron removal

It was shown that the completely oxidised bore water completely settled over a period of 5 hours. Floc settled more rapidly at high chloride dosages (250 – 750 mg/L NaCl) however it resulted in the formation of residual chlorine ranging from 28 – 60 mg/L Cl_2.

Preliminary tests using the flotation system gave promising results. It was observed that gas bubbles attached to the precipitates form from completely oxidised synthetic bore water causing them to float. They might thus be removed via flotation. Preliminary work gave promising results but was hindered by complications caused by the presence of large bubbles. An improved pressurised DAF design was developed and will be tested once construction is complete.

7.4 Conclusions

From the results summarised in this thesis it can be concluded that;

- Dimensionally stabilised titanium anodes (DSA) performed much better than graphite anodes and performance improved with increasing number of electrode pairs.
- Graphite is a poor material for the anodes of cells designed for treatment of low electrolyte aqueous system. Current efficiencies for chlorine production are low and no improvement in chlorine generation or metal oxidation is achieved when used in a ME-PEFT cell.
- When DSAs are used, the ME-PEFT cell achieved markedly improved chlorine generation and Fe(II) oxidation at lower power consumption.
- A dual electrode pair ME-PEFT cell with DSAs achieved 100% iron oxidation and removal to a level of less than 0.2 mg/L from bore water in a single pass using naturally available chloride (7 mg/L). Power consumption was 3.76 kWh/m^3.
- The ME-PEFT system combined with a DAF clarifier offers the possibility of instantaneous online oxidation and removal of at least iron from problem bore waters.

7.5 Suggestions for future research

- Since Mn(IV) has a higher reduction potential than Fe(III), Fe(II) will tend to be oxidised before Mn(II). An extra cell installed inline after the complete oxidation of Fe should allow the chlorine produced to be available exclusively for Mn(II) oxidation.
- In order to use ME-PEFT cell-pressurised DAF system to be used as an online iron oxidation and removal technology, further work needs to be done to further optimise the riser column. Trialling of the design developed in Section 6.2.3 is envisaged.
- The PEFT cell offers opportunities for further studies of water and wastewater treatment, disinfection, electric field effects and electrochemistry of very dilute electrolyte solutions.

References

Abdul-Wahab SA, Al-Weshahi MA 2009. Brine Management: Substituting Chlorine with On-Site Produced Sodium Hypochlorite for Environmentally Improved Desalination Processes. Water Resources Management 23(12): 2437-2454.

Ambler JR, Logan BE 2011. Evaluation of stainless steel cathodes and a bicarbonate buffer for hydrogen production in microbial electrolysis cells using a new method for measuring gas production. International Journal of Hydrogen Energy 36(1): 160-166.

Asokan K, Subramanian K 2009. Design of a Tank Electrolyser for In-situ Generation of NaClO. Ao SI, Douglas C, Grundfest WS, Burgstone J ed. Hong Kong, Int Assoc Engineers-Iaeng. 139-142 p.

Augustin CO 1998. 'Transition current density' a new parameter in electrochemistry. Transactions of the Indian Institute of Metals 51(5): 427-430.

Aydin S, Tufekci N, Arayici S 2001. Oxidation of manganese (II) with air in water treatment. Fresenius Environmental Bulletin 10(4): 386-391.

Ayotte J.D. NMG, Robinson Jr., Gilpin R., Moore R.B. 1999. Relation of arsenic, iron, and manganese in ground water to aquifer type, bedrock lithogeochemistry, and land use in the New England Coastal Basins 99-4162. 61 p.

Bennett JE 1980. Electrodes for generation of hydrogen and oxygen from seawater. International Journal of Hydrogen Energy 5(4): 401-408.

Bergmann MEH, Rollin J, Iourtchouk T 2009. The occurrence of perchlorate during drinking water electrolysis using BDD anodes. Electrochimica Acta 54(7): 2102-2107.

Bergmann MEH, Iourtchouk T, Rollin J 2011. The occurrence of bromate and perbromate on BDD anodes during electrolysis of aqueous systems containing bromide: first systematic experimental studies. Journal of Applied Electrochemistry 41(9): 1109-1123.

Birdi KS 2008. Handbook of Surface and Colloidal Chemistry, Third Edition. In: Birdi KS ed. Industrial and Applied Chemistry. 3rd ed. Denmark, CRC Press. Pp. 756.

Bratby J 2006. Coagulation and Floculation in Water and Wastewater Treatment. In: TechBooks ed. 2nd ed, IWA Publishing.

Brillas E, Baños MA, Camps S, Arias C, Cabot PL, Garrido JA, Rodríguez RM 2004. Catalytic effect of Fe2+, Cu2+ and UVA light on the electrochemical degradation of nitrobenzene using an oxygen-diffusion cathode. New Journal of Chemistry 28(2): 314-322.

Bull RJ, Birnbaum LS, Cantor KP, Rose JB, Butterworth BE, Pegram R, Tuomisto J 1995. Water chlorination: Essential process or cancer hazard? Fundamental and Applied Toxicology 28(2): 155-166.

Cano A, Cañizares P, Barrera C, Sáez C, Rodrigo MA 2011. Use of low current densities in electrolyses with conductive-diamond electrochemical - Oxidation to disinfect treated wastewaters for reuse. Electrochemistry Communications 13(11): 1268-1270.

Casiday R, Noelken G, Frey R 2008. Treating the Public Water Supply : What is in your water, and how is it made safe to drink? Retrieved 7 March 2012 http://www.chemistry.wustl.edu/~edudev/LabTutorials/Water/PublicWaterSupply/PublicWaterSupply.html

Chandler GK, Genders JD, Pletcher D 1997. Electrodes based on Noble Metals. Platinum Metals Rev. 41(2): 54-63.

Chiang L-C, Chang J-E, Wen T-C 1995a. Indirect oxidation effect in electrochemical oxidation treatment of landfill leachate. Water Research 29(2): 671-678.

Chiang LC, Chang JE, Wen TC 1995. Indirect oxidation effect in electrochemical oxidation treatment of landfill leachate. Water Research 29(2): 671-678.

Collings S 2007. Chlor-Alkali Membrane Electrolyser. Modern Chlor-Alkali Technology, Blackwell Science Ltd. Pp. 225-236.

Costaz P, Miquel J, Reinbold M 1983. Simultaneous electroflotation and disinfection of sewage. Water Research 17(3): 255-262.

Council NR 2005. Groundwater Monitoring. Retrieved 20 March 2012 http://www.nrc.govt.nz/upload/1961/Groundwater%20pdf%20vs.pdf

Czarnetzki LR, Janssen LJJ 1989. Electrode current distribution in a hypochlorite cell. Journal of Applied Electrochemistry 19(5): 630-636.

Devilliers D, Mahé E 2010. Modified titanium electrodes: Application to Ti/TiO2/PbO 2 dimensionally stable anodes. Electrochimica Acta 55(27): 8207-8214.

Díez S, Barata C, Raldúa D 2008. Exposure to Mercury: A Critical Assessment of Adverse Ecological and Human Health Effects. Trace Elements as Contaminants and Nutrients, John Wiley & Sons, Inc. Pp. 343-371.

Dowd RM 1985. EPA's groundwater research. Environmental Science and Technology 19(11): 1031.

Dresselhaus MS, Dresselhaus G 1981. Intercalation compounds of graphite. Advances in Physics 30(2): 139-326.

Duby P 1993. History of progress in dimensionally stable anodes. JOM 45(3): 41-43.

DWSNZ 2008. A Guide to the Ministry of Health Drinking-water Standards for New Zealand. New Zealand. Pp. 1 - 38.

DWSNZ NZ 1995. Drinking-water standards for New Zealand.

Ellis D, Bouchard C, Lantagne G 2000. Removal of iron and manganese from groundwater by oxidation and microfiltration. Desalination 130(3): 255-264.

Entwisle JH 1974. Consumption of graphite anodes in chlorine manufacture by brine electrolysis. Journal of Applied Electrochemistry 4(4): 293-303.

Falkenmark M, Widstrand C 1992. Population and water resources: a delicate balance. Population Bulletin 47(3): 1-36.

Fiessinger F, Richard Y, Montiel A, Musquere P 1981. Advantages and disadvantages of chemical oxidation and disinfection by ozone and chlorine dioxide. Science of the Total Environment 18(APR): 245-261.

Florkiewicz TF 2007. Advanced Diaphragm Cell Technology (ADCT)™. Modern Chlor-Alkali Technology, Blackwell Science Ltd. Pp. 165-172.

Ghernaout D, Naceur MW, Aouabed A 2011. On the dependence of chlorine by-products generated species formation of the electrode material and applied charge during electrochemical water treatment. Desalination 270(1-3): 9-22.

Gleick PH, Miller RW 2002. The world's water, 2000-2001: The biennial report on freshwater resources. Electronic Green Journal(16).

Guillet P, Trancart M 1988. Electrochlorination of water and its various applications. L'electrochloration des eaux et ses diverses applications(119): 49-51.

Haarhoff J, Edzwald J 2012. Dissolved Air Flotation for water clarification. United States, McGraw-Hill Professional Publishing. 352 p.

Hadfield J 2001. Waikato. In: Rosen MR, White PA ed. Groundwaters of New Zealnd. Wellington, New Zealand Hydrological Society Inc. Pp. 315-326.

Harris M 2007. Phase-Out Issues for Mercury Cell Technology in the Chlor-Alkali Industry. Modern Chlor-Alkali Technology, Blackwell Science Ltd. Pp. 19-43.

Hays J 2011. Desert, Water, Water Shortages, Conservation and Resources. Retrieved 29 March 2012 http://factsanddetails.com/world.php?itemid=1185&catid=52&subcatid=331

Hsu CH, Jeng WL, Chang RM, Chien LC, Han BC 2001. Estimation of potential lifetime cancer risks for trihalomethanes from consuming chlorinated drinking water in Taiwan. Environmental Research 85(2): 77-82.

Ingram BL, Bean L 1953. Removal of Manganese Prior to Calcium and Magnesium Precipitations. Analytical Chemistry 25(8): 1217-1219.

John AV 1997. Diffused air - a superior alternative for aeration and mixing in waste water treatment facilities. Chemical Engineering World 32(12): 149-151.

Katsaounis A 2010. Recent developments and trends in the electrochemical promotion of catalysis (EPOC). Journal of Applied Electrochemistry 40(5): 885-902.

Kaya N, Karadurmus E, Alicilar A 2005. Catalytic air oxidation of manganese in synthetic waters. Central European Journal of Chemistry 3(3): 511-519.

Kerwick MI, Reddy SM, Chamberlain AHL, Holt DM 2005. Electrochemical disinfection, an environmentally acceptable method of drinking water disinfection? Electrochimica Acta 50(25–26): 5270-5277.

Key D.L. KJD, Okolongo G., Siguba M. 2010. Development of a small-scale electro-chlorination system for rural water supplies. Water Research Commission 1442/1/09.

Kott Y, Nupen EM, Ross WR 1975. Effect of ph on efficiency of chlorine disinfection and virus enumeration. Water Research 9(10): 869-872.

Küpper M, Hessel V, Löwe H, Stark W, Kinkel J, Michel M, Schmidt-Traub H 2003. Micro reactor for electroorganic synthesis in the simulated moving bed-reaction and separation environment. Electrochimica Acta 48(20-22): 2889-2896.

Lantelme F, Groult H 2004. Interfacial properties and gas bubble formation during the electrolytic preparation of fluorine. Journal of the Electrochemical Society 151(12): D121-D126.

Li D, Zhang I, Wang HT, Yang H, Wang B 2005. Operational performance of biological treatment plant for iron and manganese removal. Journal of Water Supply Research and Technology-Aqua 54(1): 15-24.

Li J, Zheng L, Li L, Shi G, Xian Y, Jin L 2006. Photoelectro-synergistic catalysis at Ti/TiO2/PbO2 electrode and its application on determination of chemical oxygen demand. Electroanalysis 18(22): 2251-2256.

Li XY, Ding F, Lo PSY, Sin SHP 2002. Electrochemical disinfection of saline wastewater effluent. Journal of Environmental Engineering 128(8): 697-704.

Li XY, Diao HF, Fan FXJ, Gu JD, Ding F, Tong ASF 2004. Electrochemical wastewater disinfection: Identification of its principal germicidal actions. Journal of Environmental Engineering 130(10): 1217-1221.

Linn J 2006. Impact of minerals in water on dairy cows. Beauchemin K, Doepel L ed. Edmonton, University Alberta Dept Agr, Food & Nutr Sci. 235-247 p.

Liske G 1965. Chlorine alkali electrolysis. Zellstoff Und Papier 14(12): 362-&.

Liu XY, Chu PK, Ding CX 2004. Surface modification of titanium, titanium alloys, and related materials for biomedical applications. Materials Science & Engineering R-Reports 47(3-4): 49-121.

Lu Q, An LC, Zhong Q, Hu Y 2012. Electro-chemical properties comparison and application in water-treatment of different DSA anodes. Pp. 279-285.

Macka M, Andersson P, Haddad PR 1998. Changes in Electrolyte pH Due to Electrolysis during Capillary Zone Electrophoresis. Analytical Chemistry 70(4): 743-749.

Martinez-Huitle CA, Ferro S 2006. Electrochemical oxidation of organic pollutants for the wastewater treatment: direct and indirect processes. Chemical Society Reviews 35(12): 1324-1340.

Mathieson GA 2006. Electrolytic purification of water. Unpublished thesis. xxvi, 230 p.

McCluney SA, van Zee JW 1989. Optimization analysis of a diaphragm cell/evaporator system for NaOH production. Journal of the Electrochemical Society 136(9): 2556-2564.

Michaud PA, Panizza M, Ouattara L, Diaco T, Foti G, Comninellis C 2003. Electrochemical oxidation of water on synthetic boron-doped diamond thin film anodes. Journal of Applied Electrochemistry 33(2): 151-154.

Miller MG 1985. ON SITE ELECTROLYTIC CHLORINE GENERATION. Water Services 89(1069): 104.

Ministry of Health NZ 2005. Drinking-water Standards for New Zealand. New Zealand.

MOE 2005. New Zealand Drinking-Water Standards. Retrieved 10 February 2012 http://www.mfe.govt.nz/publications/water/nz-drinking-water-standards-00.html

Moore TR, Clarkson BR 2007. Dissolved organic carbon in New Zealand peatlands. New Zealand Journal of Marine and Freshwater Research 41(1): 137-141.

Nath H 2011. The development and applications of a micro-gap perforated electrode flow through cell. Unpublished thesis, University of Waikato, Hamilton. 225 p.

Nath H, Wang XJ, Torrens R, Langdon A 2011. A novel perforated electrode flow through cell design for chlorine generation. Journal of Applied Electrochemistry 41(4): 389-395.

Pal A, Gin KYH, Lin AYC, Reinhard M 2010. Impacts of emerging organic contaminants on freshwater resources: Review of recent occurrences, sources, fate and effects. Science of the Total Environment 408(24): 6062-6069.

Piver WT 1993. Contamination and restoration of groundwater aquifers. Environmental Health Perspectives 100: 237-247.

Priesing CP 1962. A Theory of Coagulation Useful for Design. Industrial and Engineering Chemistry 54(8): 38-45.

Queeney KM 2003. Principles and hardware of electrolytic conductivity measurements. Pp. 49-58.

Rodrigo MA, Cañizares P, Sánchez-Carretero A, Sáez C 2010. Use of conductive-diamond electrochemical oxidation for wastewater treatment. Catalysis Today 151(1-2): 173-177.

Rosen MR 2001. Hydrochemistry of New Zealnd's aquifers. In: Rosen MR, White PA ed. Groundwaters of New ealand. Wellington, New Zealand Hydrological Society Inc. Pp. 77-110.

Rychen P, Provent C, Pupunat L, Hermant N 2010. Domestic and Industrial Water Disinfection Using Boron-Doped Diamond Electrodes

Electrochemistry for the Environment. In: Comninellis C, Chen G ed, Springer New York. Pp. 143-161.

Sarikaya HZ 1990. Contact aeration for iron removal - A theoretical assessment. Water Research 24(3): 329-331.

Sayell KM, Davis RR 1975. Removal of iron and manganese from raw water supplies using manganese greensand zeolite. Ind Water Eng 12(5): 20-23.

Schmalz V, Dittmar T, Haaken D, Worch E 2009. Electrochemical disinfection of biologically treated wastewater from small treatment systems by using boron-doped diamond (BDD) electrodes - Contribution for direct reuse of domestic wastewater. Water Research 43(20): 5260-5266.

Schultze JW 1989. A comparison of various modifications of titanium and other valve metal electrodes. Materials Chemistry and Physics 22(3-4): 417-430.

Serikov LV, Tropina EA, Shiyan LN, Frimmel FH, Metreveli G, Delay M 2009. Iron oxidation in different types of groundwater of Western Siberia. Journal of Soils and Sediments 9(2): 103-110.

Sharma BK 1998. Electro Chemistry. In: Sharma M, Sharma, I. ed. Fifth Edition ed. Meerut, Krishna Prakashan Media (P) LTD. Pp. 476.

Shchukin ED, Amelina EA, Yaminsky VV 1981. Adhesion of particles in liquid media and stability of disperse systems. Colloids and Surfaces 2(3): 221-242.

Shibasaki N, Le PF, Kamata A 2007. Evaluation of deep groundwater development for arsenic mitigation in western Bangladesh. Journal of Environmental Science and Health Part a-Toxic/Hazardous Substances & Environmental Engineering 42(12): 1919-1932.

Sobral LGS, Santos RLC, Barbosa LAD 2000. Electrolytic treatment of mercury-loaded activated carbon from a gas cleaning system. Science of the Total Environment 261(1-3): 195-201.

Sprycha R 1989. Electrical double layer at alumina/electrolyte interface. I. Surface charge and zeta potential. Journal of Colloid And Interface Science 127(1): 1-11.

Stumm W, Morgan JJ 1988. Citation classic - aquatic chemistry - an introduction emphasizing chemical-equilibria in natural-waters. Current Contents/Agriculture Biology & Environmental Sciences(41): 18-18.

Stumm W, Sulzberger B 1992. The cycling of iron in natural environments: Considerations based on laboratory studies of heterogeneous redox processes. Geochimica et Cosmochimica Acta 56(8): 3233-3257.

Sugio N, Kojima S 1992. Biological treatment of chlorhexidine digluconate-containing waste-water .3. Effect of long-time aeration on the treatment efficiency in batch activated-sludge treatment. Japanese Journal of Toxicology and Environmental Health 38(5): 458-464.

Tang Y, Wu L, Fu J, Bi X 2010. The research on removal of manganese and iron from portable water by chlorine dioxide/coagulant process. Shenyang Jianzhu Daxue Xuebao (Ziran Kexue Ban)/Journal of Shenyang Jianzhu University (Natural Science) 26(3): 542-546.

Thonstad J, Kleinschrodt HD, Vogt H 2004. Improved design equation for the interelectrode voltage drop in industrial aluminium cells. In: Tabereaux AT ed. Light Metals 2004. Warrendale, Minerals, Metals & Materials Soc. Pp. 427-432.

Trahar WJ, Warren LJ 1976. The flotability of very fine particles — A review. International Journal of Mineral Processing 3(2): 103-131.

Tripathy T, De BR 2006. Flocculation : A New Way to Treat the Waste Water. Journal of Physical Sciences 10: 93-127.

Vogel AI 1997. Textbook of Quantitative Chemical Analysis. 5 ed. London, Longman.

Wang X 2005. Development of electrochemical cell for the production of chlorine in dilute solutions. Unpublished thesis, New Zealand, Hamilton. 92 p.

White GC 1992. The Handbook of Chlorination and Alternative Disinfectants. Third ed. United States, John Wiley & Sons, Incorporated.

White RE 1984. Electrochemical Cell Design. Selected Contributions from a Symposium on Recent Advances in Electrochemical Cell Design. In: White RE ed. Electrochemical Cell Design. Selected Contributions from a Symposium on Recent Advances in Electrochemical Cell Design, 27-31 March 1983. Pp. viii+398.

Winchester JW 1983. Aquatic chemistry - an introduction emphasizing chemical-equilibria in natural-waters, 2nd edition - STUMM,W, MORGAN,JJ. Bulletin of the American Meteorological Society 64(5): 504-504.

Woo MYC 1986. Titanium as anode (and cathode) substrate material for industrial electrolytic applications. ASTM special technical publication 4(917): 3-6.

Worley SD, Williams DE, Burkett HD, Barnela SB, Swango LJ 1986. potential new water disinfectants. Pp. 1269-1283.

WRC 2012. Groundwater. Retrieved 17 May 2012, from http://www.waikatoregion.govt.nz/Environment/Natural-resources/Water/Groundwater/

Zappi GD, Weinberg NL; 2001 11/12/2001. Electrolytic apparatus, methods for purification of aqueous solutions and synthesis of chemicals. USA patent 6328875.

Zheng YZ, Ding HY, Zhang ML 2008. Hydrous-ruthenium-oxide thin film electrodes prepared by cathodic electrodeposition for supercapacitors. Thin Solid Films 516(21): 7381-7385.

Zorpas AA 2011. Alternative treatment of urban wastewater using electrochemical oxidation. Desalination and Water Treatment 27(1-3): 268-276.

Appendices

Appendix A: Calibration curves

A.1 Analysis of ferrous ion concentration in water using 1, 10 Phenanthrolein spectrophotometric method

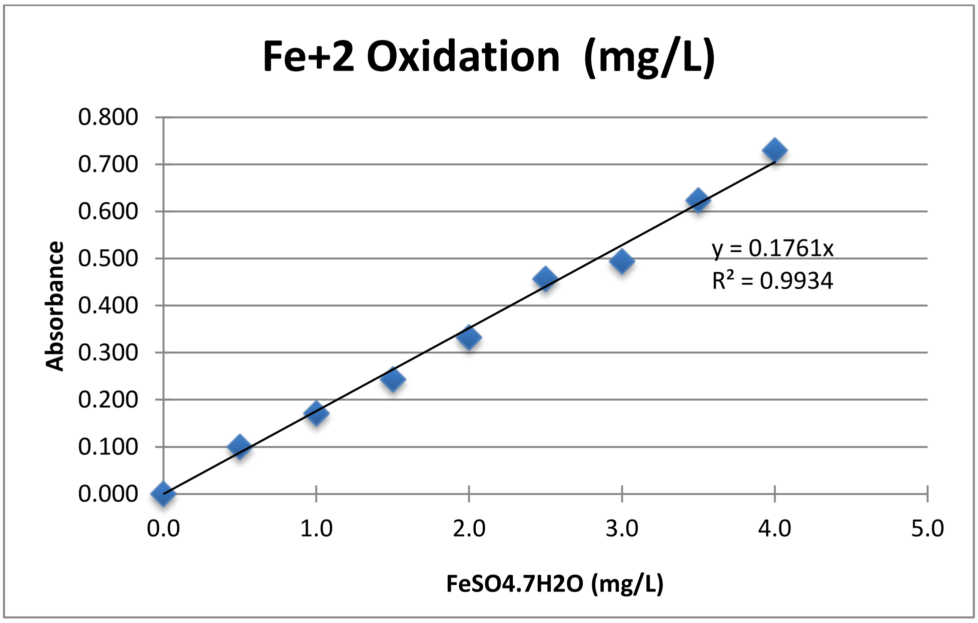

Figure A.1 Calibration curve of ferrous ion concentration versus absorbance at 515 nm.

A.2 Analysis of chloride ions concentration in water using Mercury (II) thiocyanate spectrophotometric method

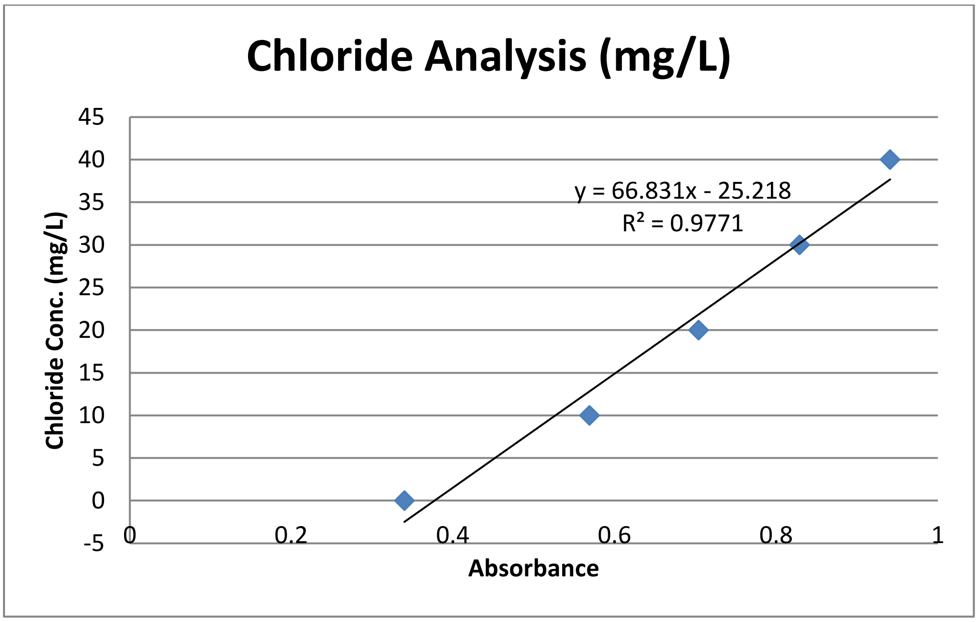

Figure A.2 Calibration curve of chloride ion concentration versus absorbance at 460nm.

Appendix B: Calculations

B.1 Chlorine Generation

Example: Find the concentration of chlorine generated by the PEFT cell from a solution containing 250 mg L^{-1} NaCl operating at 190ml min^{-1}. The end point of the titration was reached when 4ml of 0.0125M sodium thiosulphate solution was added to the effluent.

Solution

Sodium Thiosulphate = 0.0125mol L^{-1}

Volume = 0.5ml

Therefore, n = 6.25 X 10^{-6}mol

$$ClO^- + 2I^- + 2H^+ \rightleftharpoons Cl^- + I_2 + H_2O$$

$$I_2 + 2S_20_3^{2-} \rightleftharpoons 2I^- + S_4O_6^{3-}$$

$$ClO^- : S_2O_3^{2-}$$

$$1 : 2$$

$\therefore ClO^- = \frac{6.25\ x\ 10^{-6}}{2} = 3.125 \text{ x } 10^{-6}$

n = c x v

$c = \frac{n}{v} = \frac{3.125\ x\ 10^{-6}}{0.1L} = 3.125 \text{ x } 10^{-5}\text{mol } L^{-1}$

M.W. Cl_2 = 35.4 x 2 = 70.8g mol^{-1}

$\therefore Cl_2$ generated = 70.8 x 3.125 x 10^{-5}

= 2.31 x 10^{-3}g L^{-1} = **2.31mg L^{-1}**

B.2 Current Density

Example : Calculate the current density of the multiple PEFT system having 2 cells working at 5A DC.

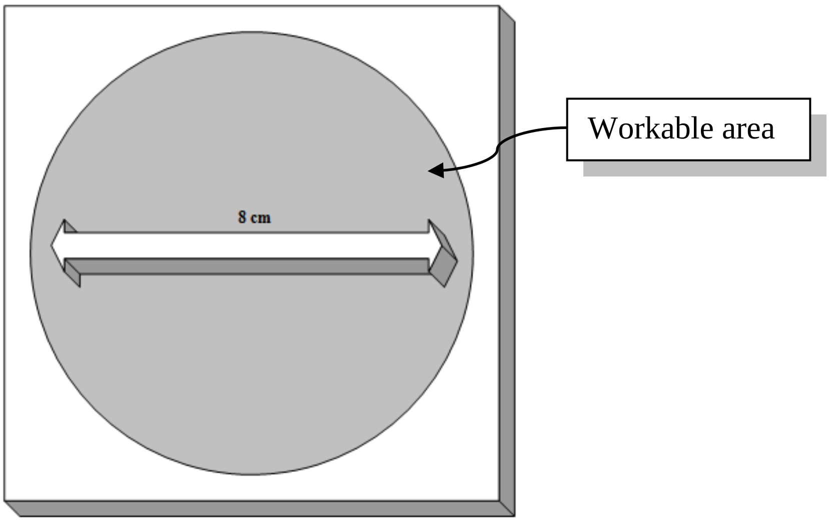

<u>Solution</u>

Area = πr^2

$= \pi \times 4 \times 4$

$= 50.265 \text{cm}^2$

Current Density = I/A

$= 5/50.265 = 0.0994 \text{A cm}^{-2}$

$= 99.47 \text{mA cm}^{-2}$ /2 (two cells connected in parallel)

= **49.85mAcm^{-2}**

B.3 Power Consumption

Example: Calculate the power consumption of a PEFT cell working at 1A and 5V, and flow rate of 35L hr^{-1}.

Solution

Power Consumption = V x I x t

= 5V x 1A x 1hr = 5Whr

Flow rate = 35L hr^{-1}

i.e. 35L → 5Whr

1L → 5/35

1000L ($1m^3$) → 5/ 35 x 1000 = **0.143kWhr m^{-3}**

B.4 Current efficiency

Example: Calculate the current efficiency of a PEFT cell which achieves75% oxidation of Fe(II) to Fe(III) at 1A and 5V. Flow rate = 35L hr^{-1}

Solution

$$1Fe^{+2} \rightarrow 1Fe^{+3} + 1e^{-}$$

$$20mg\ L^{-1}\ Fe(II) \rightarrow 15mg\ L^{-1}\ Fe(III)$$

M.W. Fe = 56mg L^{-1}

$$56g \rightarrow 1mole$$

$$15mg\ L\text{-}1 \rightarrow \frac{1mole}{56\ X\ 1000mg}\ X\ \frac{15mg}{L}$$

$$N = 2067 \text{ x } 10^{-4} mol\ L^{-1}$$

$Q = n \cdot N \cdot F$

$= 1 \cdot (2.67 \text{ x } 10mol\ L^{-1}) \cdot (96500C)$

$= 25.85C\ L^{-1}$

Flow Rate = 35L hr^{-1}

= 103sec

$$1L \rightarrow 25.85C$$

$$103sec \rightarrow 25.85C$$

$$1sec \rightarrow 25.85/103 = 0.25C\ sec^{-1} = 0.25A$$

∴ Current efficiency = $\frac{0.25A}{1A}$ X 100 = **2.5%**

Appendix C: Chlorine generation data (Section 5.3)

C.1 Chlorine generation using titanium ruthenium oxide and iridium oxide anode

Single Cell:

Table C. 1 Chlorine generation by TiO2/RuO2/IrO2 at 190ml min-1 (pH ≈ 5 at 20℃)

[NaCl] =20 ppm and Conductivity = 79.4 µS/cm @ 19.6℃

Current (A)	Voltage (V)	Cl_2 Production (ppm)
1	**5.96**	5.9
2	**9.00**	6.6
3	**11.67**	7.6

[NaCl] = 50ppm and Conductivity = 101.3 µS/cm @ 19.6℃

Current (A)	Voltage (V)	Cl_2 Production (ppm)
1	**5.64**	6.7
2	**7.97**	8.8
3	**10.20**	11.2

[NaCl] = 100 ppm and Conductivity = 172.7 µS/cm @ 20.7℃

Current (A)	Voltage (V)	Cl_2 Production (ppm)
1	**4.80**	11
2	**6.29**	13.6
3	**7.26**	17.2

Multiple Cells (2):

Table C. 2 Chlorine generation by TiO2/RuO2/IrO2 at 190ml min-1 (pH = 6.20 at 20℃)

[NaCl] = 20 ppm and Conductivity = 49.4 µS/cm @ 23.6℃

Current (A)	Voltage (V)	Cl_2 Production (ppm)
1	**5.75**	6.2
2	**9.52**	10.4
3	**13.85**	11.6

[NaCl] = 50 ppm and Conductivity = 92.0 µS/cm @ 28.9℃

Current (A)	Voltage (V)	Cl_2 Production (ppm)

1	**4.66**	8.8
2	**6.36**	12.4
3	**7.99**	16.0

[NaCl] = 100 ppm and Conductivity = 217 µS/cm @ 24.4℃

Current (A)	**Voltage (V)**	**Cl_2 Production (ppm)**
1	**3.95**	12.0
2	**4.80**	16.0
3	**5.56**	22.4